

This Page Is Inserted by IFW Operations
and is not a part of the Official Record

BEST AVAILABLE IMAGES

Defective images within this document are accurate representations of the original documents submitted by the applicant.

Defects in the images may include (but are not limited to):

- BLACK BORDERS
- TEXT CUT OFF AT TOP, BOTTOM OR SIDES
- FADED TEXT
- ILLEGIBLE TEXT
- SKEWED/SLANTED IMAGES
- COLORED PHOTOS
- BLACK OR VERY BLACK AND WHITE DARK PHOTOS
- GRAY SCALE DOCUMENTS

IMAGES ARE BEST AVAILABLE COPY.

**As rescanning documents *will not* correct images,
please do not report the images to the
Image Problem Mailbox.**

(12) INTERNATIONAL APPLICATION PUBLISHED UNDER THE PATENT COOPERATION TREATY (PCT)

(19) World Intellectual Property Organization
International Bureau



(43) International Publication Date
21 December 2000 (21.12.2000)

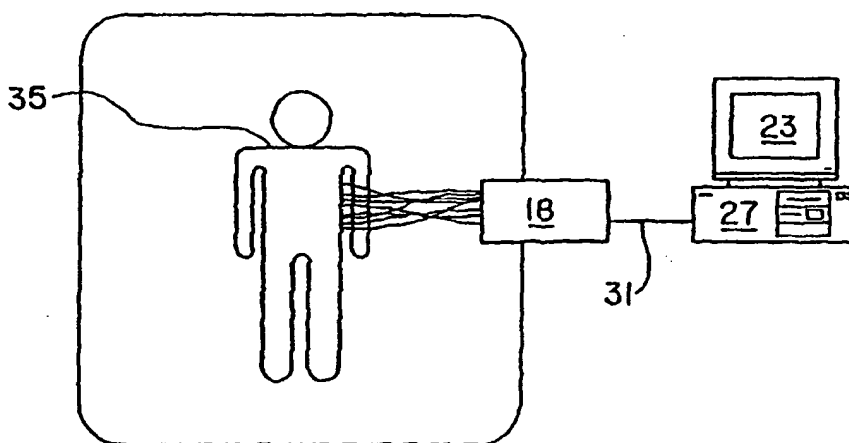
PCT

(10) International Publication Number
WO 00/76397 A1

- (51) International Patent Classification⁷: **A61B 5/0472**
- (21) International Application Number: **PCT/US00/15965**
- (22) International Filing Date: **9 June 2000 (09.06.2000)**
- (25) Filing Language: **English**
- (26) Publication Language: **English**
- (30) Priority Data:
60/138,497 10 June 1999 (10.06.1999) US
60/138,439 10 June 1999 (10.06.1999) US
60/191,029 21 March 2000 (21.03.2000) US
- (71) Applicant: **HARBINGER MEDICAL, INC.** [US/US];
12086 Oxbow Drive, Eden Prairie, MN 55347 (US).
- (71) Applicants and
(72) Inventors: **HOIUM, Harold, H.** [US/US]; 12086 Oxbow
Drive, Eden Prairie, MN 55347 (US). **MALIK, Marek**
[GB/GB]; 16 Verulam Avenue, Purley, Surrey CR8 3NQ
(GB). **RYAN, Stephen, J.** [US/US]; 1240 Wildwood Way,
Chaska, MN 55318 (US).
- (74) Agents: **DOLAN, John, F.** et al.; Patterson, Thunte &
Skaar, P.A., 4800 IDS Center, 80 South 8th Street, Min-
neapolis, MN 55402-2100 (US).
- (81) Designated States (*national*): AE, AG, AL, AM, AT, AU,
AZ, BA, BB, BG, BR, BY, CA, CH, CN, CR, CU, CZ, DE,
DK, DM, DZ, EE, ES, FI, GB, GD, GE, GH, GM, HR, HU,
ID, IL, IN, IS, JP, KE, KG, KP, KR, KZ, LC, LK, LR, LS,
LT, LU, LV, MA, MD, MG, MK, MN, MW, MX, MZ, NO,
NZ, PL, PT, RO, RU, SD, SE, SG, SI, SK, SL, TJ, TM, TR,
TT, TZ, UA, UG, UZ, VN, YU, ZA, ZW.
- (84) Designated States (*regional*): ARIPO patent (GH, GM,
KE, LS, MW, MZ, SD, SL, SZ, TZ, UG, ZW), Eurasian
patent (AM, AZ, BY, KG, KZ, MD, RU, TJ, TM), European
patent (AT, BE, CH, CY, DE, DK, ES, FI, FR, GB, GR, IE,
IT, LU, MC, NL, PT, SE), OAPI patent (BF, BJ, CF, CG,
CI, CM, GA, GN, GW, ML, MR, NE, SN, TD, TG).
- Published:
— *With international search report.*

[Continued on next page]

(54) Title: **DETERMINING A PATIENT'S SUSCEPTIBILITY TO ARRHYTHMIA**



(57) Abstract: A system and method for detecting a patient's susceptibility to arrhythmias and cardiac tissue abnormality is disclosed. The method consists of using a computer, a display, software loaded onto the computer that generates graphical user interfaces (GUIs), an electronic interface, and a plurality of electrodes. The electronics interface is in electronic communication with the computer, and further in electronic communication with the electrodes that are placed by self-adhesion at predetermined locations on a test subject. According to one aspect of the invention, the method enables a user, typically a medical professional, to initiate, with minimal input, certain diagnostic tests involving observing and analyzing a series of QRS complexes, some of which are biased with a subpacing current, and others of which are unbiased. The signals are then compared, and the differences are analyzed to detect a patient's susceptibility to arrhythmias and cardiac tissue abnormality.

WO 00/76397 A1



— Before the expiration of the time limit for amending the claims and to be republished in the event of receipt of amendments.

For two-letter codes and other abbreviations, refer to the "Guidance Notes on Codes and Abbreviations" appearing at the beginning of each regular issue of the PCT Gazette.

DETERMINING A PATIENT'S SUSCEPTIBILITY TO ARRHYTHMIA

FIELD OF INVENTION

5 The invention relates to the detection of patients' susceptibility to arrhythmias and, more particularly, to various techniques for improving the detection of signals to achieve this goal.

BACKGROUND OF THE INVENTION

10 There are various devices known in the art for monitoring heart function. Many of these devices typically function by analyzing signals such as an electrocardiogram signal, which can be representative of heart function.

 There is a need to identify patients at high risk for life-threatening arrhythmias.

15 Various means have been proposed for detecting patient susceptibility to arrhythmias. United States Patent No. 5,117,834 discloses one method by which pulses of electromagnetic energy are injected into a patient and the changes in the patient's electrocardiographic signals caused by the injection are recorded. U. S. Patent No. 5,351,687 is similar in concept to U.S. Patent No. 5,117,834, but it describes use of a magnetic sensor
20 for use in detecting the cardiographic signals. U. S Patent No. 5,555,888 discloses various means for adapting and automatically facilitating the assessment techniques and means similar to that shown in the above patents for determining patient susceptibility to arrhythmias.

 Other techniques which are used to analyze cardiac signals for somewhat
25 similar purposes include those known as t-wave alternans and signal-averaged

electrocardiograms. Each of these techniques is limited in its application and utility by various factors which are overcome through use of the below described inventions.

SUMMARY OF THE INVENTION

5 The present invention provides a system and method of determining, through noninvasive means, a patient's susceptibility to arrhythmia. More specifically, this invention comprises various improvements to known innovations for optimizing detection of a patient's susceptibility to arrhythmias. This invention embodies numerous software and sequence improvements for applying this basic technology.

10 Another purpose of this invention is to provide hardware and software analysis means for detecting and amplifying relevant signals.

 Another purpose of this invention is to provide for improved performance lead sets and the software to promote ease of attachment and removal from the patient and ease of connection of the lead system to the hardware.

15 A further object of this invention is to provide new combinations of electrode placement and use to promote better arrhythmia susceptibility diagnosis.

 A further object of this invention is to provide a reduction in the size of necessary components to allow for hand-held system dimensions.

 A further object of this invention is to provide a means for distinguishing
20 between the signals from the X, Y, and Z directions as well as previously unused directional components of very low-level signal data.

 Another object of this invention is to supply means for displaying of patient's waveforms and other data derived from the detected signals, as well as to provide various

interfaces to communicate the data between the patient and physician or health care professional.

It is a further object of this invention to provide signal artifact reduction, and to provide a single point connector for the set of leads.

5 Another object of this invention is to provide improved lead materials for improved performance, as well as an improved lead effect modeling (LEM).

It is yet another object of this invention to provide amplifier circuitry that minimizes amplifier saturation and optimizes fast recovery.

10 BRIEF DESCRIPTIONS OF THE DRAWINGS

Figure 1 depicts the broad overview of the invention, showing the patient electronic interface computer.

Figure 2 is an exemplary depiction of a patient showing possible electrode patient locations.

15 Figure 3 is a more close-up view of the lead system, showing the connector and attached electrodes.

Figure 4 depicts the principal graphical user interface (GUI) generated by the computer and the software portion of the invention.

20 Figure 5 is the principal GUI generated by the computer and software portion of the invention, with the testing menu engaged.

Figure 6 is the "New Subject" GUI.

Figure 7 is the "Acquisition" GUI.

Figure 8 is the "Perform All Standard Protocols" GUI.

Figure 9 is the "Ready to Verify Sensing" GUI.

Figure 10 is the "Acquisition Active" GUI generated by the computer and software portion of the invention.

Figure 11 is the "Sensing Problem" GUI generated by the computer and software portion of the invention.

5 Figure 12 is the "Repeat Sensing Verification" GUI generated by the computer and software portion of the invention.

Figure 13 is the principal GUI generated by the computer and software portion of the invention, depicting a pulse graph.

10 Figure 14 is the "Ready to Begin Testing Execution" GUI generated by the computer and software portion of the invention.

Figure 15 is the "Acquisition Active" GUI generated by the computer and software portion of the invention, depicting realtime R-wave acquisition.

Figure 16 is the "Halted Data Acquisition" GUI generated by the computer and software portion of the invention.

15 Figure 17 is the "Resume with Protocol" GUI generated by the computer and software portion of the invention.

Figure 18 is the principal GUI generated by the computer and software portion of the invention, depicting the "View" drop-down menu engaged.

20 Figure 19 is the "Options" GUI generated by the computer and software portion of the invention.

Figure 20 is the "Simulator" GUI generated by the computer and software portion of the invention.

Figure 21 is the "QRS Status" GUI generated by the computer and software portion of the invention.

Figure 22 is the "Simulator" GUI generated by the computer and software portion of the invention, depicting a further display option.

Figure 23 is the "Simulator" GUI generated by the computer and software portion of the invention, depicting a further display option.

5 Figure 24 is the "Simulator" GUI generated by the computer and software portion of the invention.

Figure 25 is the "Simulator" GUI generated by the computer and software portion of the invention.

Figure 26 is the principal GUI generated by the computer and software portion of the
10 invention, depicting the "Data" drop-down menu engaged.

Figure 27 is the "Accessing Stored Subject Data" GUI generated by the computer and software portion of the invention.

Figure 28 is the "Open" GUI generated by the computer and software portion of the invention.

15 Figure 29 is the "Protocol Steps" GUI generated by the computer and software portion of the invention.

Figure 30 is the "Select Protocol Step" GUI generated by the computer and software portion of the invention.

Figure 31 is an exemplary EKG signal.

20 Figure 32 is a block diagram of switching and planting circuit of the electronic interface.

Figure 33 is a flow chart showing the overall interaction of the invention.

Figure 34 is a more detailed view of the connector and attached leads, showing pin layout.

Figure 35 is a block diagram of the isolated driver and shunting switch, a portion of the electronics interface.

Figure 36 is an exemplary series of QRS complexes.

Figure 37 is a high-level block diagram of the electronics interface.

5 Figure 38 is a wire-level depiction of the electronics interface.

Figure 39 is a flow chart/block diagram of the isolated fast recovery EKG amplifier.

Figure 40 is a schematic of the fast-recovery EKG amplifier.

Figure 41 is a block diagram/flow chart of the isolated driver section of the electronics interface.

10 Figure 42 is a schematic of the isolated driver section of the electronics interface.

Figure 43 is a high-level flow chart of the operation of the software.

Figure 44 is a lower-level flow chart of the test control and acquisition portion of the software.

Figure 45 is a lower-level flow chart of the post-processing software operation.

15 Figure 46 is a lower-level flow chart of the realtime enter of controls implemented by the software.

Figure 47 is a data set of observed data.

Figure 48 is a data set of observed data.

Figure 49 is a data set of observed data.

20 Figure 50 is a data set of observed data.

Figure 51 is a data set of observed data.

Figure 52 is a data set of observed data.

Figure 53 is a data set of observed data.

Figure 54 is a data set of observed data.

Figure 55 is a data set of observed data.

Figure 56 is an exemplary depiction of a patient showing possible electrode patient locations combined with elements of existing ambulatory and/or implantable technology.

5

DETAILED DESCRIPTION OF THE INVENTION

The invention provided is an improved method and system for detecting patients' susceptibility to arrhythmia and cardiac tissue abnormality in a noninvasive fashion. In Figure 1, computer 27 is operably coupled to monitor 23, which is further closely coupled with electronic interface 18 via wire 31. Lead system 12 is connected between patient 35 and
10 electronic interface 18.

Figure 2 is a front and rear view of patient 35. In one preferred embodiment, lead system 12 consists of 9 lead wires. Advantageously, the lead system can be connected as shown in Figure 2 for efficient and consistent setup of the invention. Typically, the lead system is preassembled with a predetermined number of leads having predetermined lengths.
15 Although it is contemplated by this invention that the lead system can be preassembled with leads of different lengths to accommodate different room sizes and patient locations, among other factors, a general consideration is that the sensing leads and energy delivery leads are less than 9 feet in length to reduce possible induced noise. Further, the leads in lead system 12 are constructed from a low-impedance material, such as tin, sodium, silver, silver chloride,
20 or other low-impedance material recognized as such by those skilled in the art. This construction assists in efficient delivery of sub pacing energy for stimulation leads and increased sensitivity for sensing leads. The electrodes involved with energy delivery are advantageously shaped and sized for placement on the patient's body habitus to minimize signal quality reduction by avoiding muscle tissue.

Figure 3 shows a more detailed view of one preferred embodiment of single-point connector 15 with 9 lead wires electronically coupled thereto. In this embodiment, each of the 9 lead wires is connected to one of 9 self-adhesive electrodes. The adhesive used on any specific electrode can differ depending on various factors, including where on patient 35 the electrode or patch is to be affixed and whether the electrode is reusable or disposable. In one preferred embodiment, electrode 1 is to be connected in the correspondingly-numbered position indicated in Figure 2. Thus, for example, electrodes 1 and 2 are connected on patient 35 at the corresponding left and right mid-axillary lines, on a horizontal plane, at the level where the fifth intercostal space intersects the sternum. Electrode 3 is placed on the sternum. In this embodiment of the invention, electrode 4 is placed on patient 35 at the fifth intercostal space. Electrode 5 is a neck electrode and is attached generally at the back of the neck, as indicated on back view 2.2 of Figure 2. Lead 6 is a left leg lead that will attach generally in the location on patient 35, as shown on front view 2.1 of Figure 2. The larger, rectangular electrodes, electrodes 7 and 8, are attached in the pectoral area and back, respectively, as shown in Figure 2. In one preferred embodiment, the generally pectorally-placed electrode 7 or patch has a skin contact surface area of at least 20 cm², and typically less than about 70 cm². The patches of lead system 12 can be constructed with different electrical characteristics to facilitate energy transfer and sensing.

Single-point connector 15 is configured to electronically mate with electronic interface 18. A top-level block diagram of electronic interface 18 is shown in Figure 37. In one embodiment, single-point connector 15 advantageously couples 9 electroleads into one plug assembly. As can be seen in Figure 3, one preferred embodiment is a stacked lead receptacle having at least two rows of lead connections that are identified with respect to each lead (also see Figure 42). This advantageously provides for a more compact connector, and

provides for rapid and efficient coupling and decoupling to electronics interface 18. In one preferred embodiment, the connector 15 is designed to be easily and rapidly coupled and decoupled with the electronics interface 18 by the use of only one hand. Advantageously, this allows for efficient setup and takedown of the invention. Patches 1 through 9 are

5 premarked, as indicated on Figure 3, to provide for simpler and more convenient placement on patient 35. Further, the lead system 12 comprises a reference lead 9. It is anticipated that the lead system 12 can be a single-use system or a disposable system to provide for a safe and sterile means by which to perform the tests provided by this invention. Further, reusing the lead system may create a higher impedance in the system, which may make the lead system

10 12 more susceptible to noise. In one preferred embodiment of the invention, a means is provided for determining whether the lead system has been previously used. This can be done by using a single-use-type adhesive. Another means for detecting previous use is creating a deformable tab on connector 15 that deforms on its first mating with electronic interface 18, and thereafter is not usable. Creating fusible links or breakable tabs to indicate

15 the lead system has been previously used are an additional means, among others.

The electronics interface 18, by coupling with computer 27, allows for the injection of low-level electromagnetic energy into patient 35 to alter at least one cardiac signal. The energy is delivered at a sub pacing threshold and is typically introduced externally, through patient 35's chest and into cardiac tissue. The sub pacing energy is

20 delivered just before a QRS complex event, as determined by the data gathered by the hardware and electronic interface 18, and as analyzed by the software. Electronic interface 18 and attached computer 27 function to process received signals, among other functions. The energy delivery leads are typically leads 7 and 8; however, it is anticipated that circumstances may arise where more or less than two energy delivery leads may be needed.

In such cases, greater or fewer leads may be configured to delivery energy. Further, the number of sensing leads may be variable as well, depending on the needs and judgment of the medical professional administering the testing.

Figure 31 depicts an exemplary QRS complex and related signals. P-wave 153 is the signal that typically precedes the actual QRS complex 130. The interval between the start of the P-wave and the beginning of QRS complex 130 is known as the PR interval 150. QRS complex 130 is typically made up of three distinct components: Q 117, which is typically the first negative signal; R 113, which is typically the first positive signal; and S 121, which is the first negative signal subsequent to R 113 signal. T segment 133 is typically defined as the more-or-less flat signal, or absence of signal, subsequent to recovery of the S 121 portion of QRS complex 130, prior to commencement of t-wave 146. The QT interval is typically defined as the portion of the signals commencing at the beginning of QRS complex 130 and ending after t-wave 146. J Joint 137 is typically defined as the end of the QRS complex and the beginning of the ST segment 133. The T-P interval (not indicated) is the time period from the end of the T-wave to the beginning of the next P-Wave. The entire cardiac cycle is P-Q-R-S-T.

The slight transcutaneous biosync or subpacing current is typically introduced by the invention at odd numbers of QRS complex normal sinus beats. Resulting QRS complexes are then compared to the even-numbered unbiased beats. By computer-implemented software, the distinguishable signal differences can then be calculated and displayed. Generally, differences are found between the biased and unbiased QRS complexes in patients with ventricular tachycardia and other indices of arrhythmia or cardiac tissue abnormality. It is anticipated that these input potentials would be extremely small, for example, less than 100uV, and typically of a duration of less than about 100 mS. Such a

current might involve visualization of a possible analog of late potentials throughout the QRS complex. In similar fashion it is within the scope of this invention to apply the biased and unbiased signal analysis to various other types of test methods and signals. The application of external sub-threshold stimulation delivered through the skin surface affects the ECG signals which may be evaluated in a myriad of ways, including Heart Rate Variability (HRV), ST segment elevation, QRST Timing Changes, and T-wave alternans. These methods are currently in use today but have never been used in combination with the novel features of this invention. The combination of external sub-threshold stimulation delivered through the skin surface to change or modulate these measurements is further described herein.

10 Heart Rate Variability is commonly measured by taking a sampling of R-wave to R-wave intervals from a subject and computing the standard deviation of these intervals. Other methods include the evaluation of modes of distribution of these intervals. For the purposes of this description, HRV shall generally be defined as the evaluation of the intervals between re-occurring activity in the heart. When external sub-threshold stimulation is delivered through the skin surface, these intervals can change. The changes vary from individual to individual. These changes (or lack thereof) can be used to identify an individual's cardiovascular and autonomic condition.

20 QRST Timing Changes are commonly measured by assessing the variability in spacing between the Q-wave and T-wave of the heart. Other methods include the evaluation of variability between Q-R, Q-S and R-S waves. For the purposes of these claims, QRST Timing Changes may be generally defined as any evaluation of variability in relative timing of any combination of Q-wave, R-wave, S-wave, or T-wave. When external sub-threshold stimulation is delivered through the skin surface, these timings can change. The changes vary

from individual to individual. These changes (or lack thereof) can be used to identify an individual's cardiovascular and autonomic condition.

ST Segment Elevation is commonly measured by assessing the amplitude of the heart beat between the S-wave and the T-wave. Other methods include the evaluation of frequency content, amplitude variability and frequency variability. For the purposes of this description, ST Segment Elevation may be generally defined as any evaluation of signals occurring between the S-wave and T-wave. When external sub-threshold stimulation is delivered through the skin surface, these signals can change. The changes vary from individual to individual. These changes (or lack thereof) can be used to identify an individual's cardiovascular and autonomic condition.

T-Wave Changes are currently measured by evaluating sequential T-wave amplitudes for alternans behavior. Other methods include the evaluation of frequency content, and frequency variability. For the purposes of these claims, T-Wave Changes may be generally defined as any variation of signals occurring between the S-wave and the subsequent heart beat. When external sub-threshold stimulation is delivered through the skin surface, these signals can change. The changes vary from individual to individual. These changes (or lack thereof) can be used to identify an individual's cardiovascular and autonomic condition. Use of these techniques include, in one or more combinations:

- a. The use of HRV changes induced by sub-threshold (0ma-pacing threshold) stimulation delivered through the skin surface as an indicator of cardiovascular and autonomic condition;
- b. The use of QRST timing changes induced by sub-threshold (0ma-pacing threshold) stimulation delivered through the skin surface as an indicator of cardiovascular and autonomic condition;

- c. The use of ST segment changes induced by sub-threshold (0ma-pacing threshold) stimulation delivered through the skin surface as an indicator of cardiovascular and autonomic condition; and
- d. The use of T-wave changes induced by sub-threshold (0ma-pacing threshold) stimulation delivered through the skin surface as an indicator of cardiovascular and autonomic condition.

In summary, it is possible to use any of the above cardiac evaluation techniques with the induced signals of the invention to measure variability of the resulting signals. This variability can be compared to the variability of signals or intervals without stimulation. The relationships and mechanisms for the changes are discernible in these combinations, and provide considerable diagnostic value for the patient and the investigating caregiver.

Computer 27 operates a graphical user interface (GUI) based software, which generally includes a tool bar, a status bar, a display area, and various drop-down menus. The principal GUI is depicted in Figure 4. The GUI consists of display area 39, status bar 37, tool bar 42, and drop-down menus 46. Tool bar 42 contains button icons that represent shortcuts to many of the functions described below in association with drop-down means 46. Status bar 37 depicts the general status 13 of the software on the left-hand side, technical data 10 regarding the lead sensors and input current in the middle section, and frequency and protocol information 28 generally on the right-hand side. Figure 4 illustrates a GUI in Microsoft Corporation's Windows 95™ operating system format. The GUI is generated by computer 27, which typically consists of mouse 40, CPU 25, display 23, a keyboard (not shown) operably attached to computer 27, and peripheral input/output devices 26, as well as storage media 21.

Figure 5 depicts "Testing" drop-down menu 48 engaged. As revealed in Figure 5, "Testing" drop-down menu 48 provides a series of options to perform testing provided for by this invention. If the "Performed Test Sequence" 50 is selected, the GUI of Figure 6 is generated on display 23. Using mouse 40 or keyboard input, a preexisting patient 5 may be selected from display area 39 of this GUI, or "New Patient" button 52 may be selected. Mouse 40 or keyboard input may be used to select all operable functions of the GUIs involved in this invention. If "OK" 36 is selected from the GUI of Figure 36, subject information 41 is retrieved for the highlighted subject. "Cancel" 30 returns the operator to the view of the GUI of Figure 4.

10 Figure 7 depicts the informational GUI that appears if "New Patient" button 52 is selected. In the upper portion of the GUI represented in Figure 7, subject information may be entered in box 44 which includes identification number (ID) 55 to associate with the patient, patient's Name 58, patient's Birthdate 64, Gender 66 of the patient, Race 80 of the patient, and any miscellaneous notes 85 that might be helpful during or after the patient's
15 diagnostic sessions.

 The lower portion of the GUI depicted in Figure 7 includes six boxes where testing parameters are entered. The test duration box 90 is configured by the medical professional to indicate how many QRS complex signals will comprise the test. The options under the sensitivity input box 68 are low, medium, and high. This advantageously allows
20 the sensitivity to be adjusted to correct over- or under-sensing caused by subject-to-subject variation in QRS amplitude and morphology. The next variable parameter is the deviation limit 87, which is entered in milliseconds in the correspondingly marked box. Deviation limit 87 allows the operator to eliminate inaccurately-positioned stimulations from post-processing. This can happen due to the predictive nature of pre-R-wave stimulation and

the normal R-R interval variation (see Figure 36). The operator identifies the allowable tolerance. Any pulses that are greater than this tolerance are eliminated from further processing. Also in Figure 7 is pulse configuration box 33. In pulse configuration box 33, the low-current pulse can be configured to account for the different circumstances of the patient to be tested. The parameters or variables are current strength 72, width of the pulse 82 (in milliseconds), and temporal location 92 of the pulse with respect to the QRS complex. A one-millisecond Pulse Ramp Up 78 option is also available by checking the corresponding box on the GUI.

Figure 8 depicts a GUI option screen where a simplified selection can be made for all available testing standard protocols. There, selection of "Yes" 11 invokes all currently defined standard protocols. These protocols are set up initially and invoke from this screen. This option advantageously allows testing without requiring the operator to set the specific parameters for each subject being tested. "No" 17 returns the user to the previously displayed GUI.

Figure 9 is a GUI that appears on screen 23 to determine whether the professional is ready to verify the sensing of the electrodes attached to patient 35. "Yes" 36 will commence the sensor verification. "Cancel" 30 will return the operator to the previous screen. If default protocols are to be used on the patient, then the operator need not define the test parameters. The system will get these standard parameters from the internal disk (not shown) of computer 27.

If "Cancel" 30 is selected on the GUI of Figure 7, any changes will be discarded and the performed test function will cease. If "OK" 36 is selected on the GUI of Figure 7, the GUI of Figure 8 will appear. The medical professional will select "Yes" 11 if the system is to use the standard protocol stored internally.

In a particular embodiment of the subject invention, prior to acquiring test data for a particular test, the computer-implemented software will acquire data for a 10-second interval, displaying and indicating detected R-waves or QRS complexes (see Figure 31). This process allows the operator to confirm the placement of lead system 12, and the sensitivity settings that appear in the GUI of Figure 7. If the test data is not completely satisfactory to the operator, the steps represented in Figures 7, 8, 9, and 10 may be iterated to allow the medical professional to reposition the leads, if necessary, to provide for optimal sensing and signal amplitude. During data acquisition, a window depicting the data being acquired appears. An exemplary display of this graphical depiction of acquired signal 47 appears in Figure 10. After the typical 10-second acquisition time, the GUI of Figure 11 or Figure 12 may appear. The GUI of Figure 12 gives the operator the opportunity for another approximately 10-second data acquisition period. If software-detected problems occur during data acquisition, a GUI such as the one displayed in Figure 11 may appear, notifying the operator of potential problems. These features give the operator more control over the testing procedure, and advantageously provide for error control.

Typically, in one preferred embodiment of the invention, an auditory beeping occurs with R-wave acquisition. If no R-wave beeping occurs or if poor signal amplitude is noted, adjustments in the leads may again be required, and sensing verification should be repeated via the GUI of Figure 12.

In situations where the operator is not performing standard protocols, the system will allow the operator to interactively set the pulse position. Figure 13 is a graphical depiction of pulse 59 on display area 39. Under these circumstances, the operator may use the cursor keys on the keyboard (not shown), coupled to computer 27 (not shown in Figure

13), to position the pulse location using an average of the QRS complex signals received during sensing verification.

In one preferred embodiment, the final step in the performance of the test sequence function involves performing and recording the test. Prior to performing and
5 recording the test, the software will represent the GUI prompt of Figure 14. This will allow the operator to control the timing of the test to ensure that both patient 35 and the operator are ready to proceed.

When the "OK" 36 selection is made from the GUI of Figure 14, the GUI of Figure 15 is generated, graphically depicting the R-wave 34 in real time. If "Cancel" 30 is
10 selected, the operator is returned to the previous screen. The system is configured to emit an audible beep synchronously with each R-wave sensed. As indicated on the GUI of Figure 15, pressing any key of the computer keyboard will halt the performance test sequence. If a key is depressed during the test sequence, the GUI notification screen of Figure 16 appears, notifying the operator what has occurred.

15 This invention anticipates that several other events may occur that would halt acquisition, and similar GUIs to the GUI depicted in Figure 16 will report such termination of the test procedure. For example, if R-wave sensing is indicated at a rate greater than 180 beats per minute, the test will automatically be halted. Further, if the invention is having difficulty sensing the R-wave, or the R-wave is in any way irregular, the test will be halted.
20 If the test is interrupted during the execution of a test sequence, the sequence may be restarted at the beginning of the interrupted test by selecting "Yes" 11 from the GUI notification screen of Figure 17, which will be displayed after the test sequence is halted. Selecting "No" 17 from the GUI of Figure 17 causes the system to return to the main menu screen of Figure 4. If any of the remaining menu items in drop-down menu 48 are selected, a

shortcut to a previously-described procedure is executed. If "Quit" 19 (see Figure 5) from Testing drop-down menu 48 is selected, the software program is closed.

Figure 18 shows the View drop-down menu 55 engaged. View drop-down menu 55 provides access to functions required to select viewing options for data acquired or loaded from disk. Each test performed by the subject of the invention records 3 channels of data. The placement of electrodes (see Figure 2) allows these signals to record far-field ECG in roughly orthogonal directions. This advantageously provides for a data representation that defines the signal in three dimensions. Axes have been labeled X, Y, and Z. The X signal is recorded, for example, from left lead 1 to right lead 2, with left lead 1 being the positive direction. The Y signal may be recorded from neck lead 5 to leg lead 6, with neck lead 5 being the positive direction. The Z signal may be recorded from back lead 4 to sternum lead 3, with back lead 4 being the positive direction. Other configurations may be possible, depending upon the judgment and needs of the patient and operator. In addition to the three required signals, at least two additional signals are preferably calculated. The X, Y, and Z signals are combined to produce a magnitude and direction signal. A magnitude signal can be used to detect signal variation independent of direction. A direction signal can be used to detect signal variation independent of magnitude. The upper portion of View drop-down menu 55 contains selectable options for each of the signals X 100, Y 102, and Z 104. The options appear checked on the GUI when they are selected. These selections allow the medical professional to select which signals are displayed during certain viewing modes. The lower portion of the pull-down menu contains the viewing modes. Each mode allows the user to view the current data set in a different way. The viewing modes, as they appear on drop-down menu 55, are "View Full Resolution," 119, which displays the X, Y, and Z signals at high resolution on monitor 23; "View 2 Minute Screen" 123, which displays a selected

signal compressed into two minutes per screen; and "View QRS Change" 125, which displays the selected signals with normal average, biased average, and difference depictions.

Selection of "Vector Angle" 139 displays the angular velocity and direction change of the average signal. "Position Bias Pulse" 111 displays the average of the selected signals, along
5 with an indicator of pulse position. This advantageously allows interactive positioning of stimulation by the medical professional performing the diagnostics.

"Signal Averaged ECG" 135 displays signal-averaged ECG information for normal, biased, and difference signals. Typically, in the application of signal-averaged ECG 135, of primary importance to the medical professional is the flat area immediately following
10 the QRS complex, ST segment 133. ST Segment 133 is targeted because of its lack of signal in normal people (see Figure 31). This lack of signal allows the recognition of the presence of very small-amplitude signals that can occur in people with conduction problems indicative of a susceptibility to arrhythmia or other cardiac tissue abnormality. Further, abnormal signals may also exist within the QRS and be masked by the higher-amplitude signal present
15 there. Since this invention has the ability to perform comparative analysis between stimulated and non-stimulated beats, a much greater sensitivity may be achieved in areas where a higher natural signal is also present. Additionally, by examining various areas of the QRS complex, information regarding size and position of conduction alteration may also be evident.

20 If "Options" 128 menu selection is made from View drop-down menu 55, the GUI of Figure 19 is displayed. "Option" 128, which is selectable by the GUI, is represented in Figure 19. This function allows for better interpretation of the data accumulated. The "High-Pass Cutoff" option 60 of the GUI in Figure 19 can be set to use a fast-fourier transform (FFT), to filter out frequencies lower than those indicated prior to averaging. A

zero setting disables high-pass filtering altogether. Low-pass cutoff 94 uses an FFT to filter out frequencies higher than those indicated prior to averaging. A setting of 1,000 disables low-pass filtering. Advantageously, lead effective modeling (LEM) can be selected in the GUI represented in Figure 19. If LEM box 96 is checked, in a preferred embodiment, a

5 20-millisecond model of the impulse artifact is constructed, based on the first four simulations. This model is subtracted from subsequent simulations to reduce artifact in the displayed information. Any voltage shifts created during stimulation are also modeled and removed. LEM and this correction algorithm greatly reduce artifact created by stimulation. A muscle response correction algorithm may also be implemented by the invention to

10 advantageously correct for signal artifacts during stimulation and acquisition cycles. Using this technique stimulation is provided to the patient within an LEM time period between the T and P waves, at the beginning and periodically throughout the stimulation and acquisition process. Response to the stimulations is determined up to about 50 milliseconds for each stimulation. LEM is then created by combining the response of the stimulations during this

15 period to generate a response signal, whereafter the signal is used to mathematically attribute noise generated by electrical artifact and muscle activity. Also GUI selectable is a "60-Hz Notch FFT Filtering" 86 option, which advantageously filters out frequencies at the 60-Hz rate prior to averaging. Accumulation Start time 88 and End time 89 can also be input on the GUI indicated in Figure 19. Accumulation Start time 88 controls the starting range for the

20 accumulated difference measurement on the average screen. The Accumulation End setting 89 controls the ending range for the accumulated difference on the average screen. An exemplary result of selecting "View Full Resolution" mode 119 is depicted in Figure 20. Signal characteristics X 167, Y 173, and Z 177 are graphed independently. Again, status bar 37 indicates the various selected parameters previously discussed.

Individual QRS status may be determined from the GUI of Figure 21. The various options in the QRS Status window 97 are as follows: if the status indicated is "Biased," that means that the QRS complex has a stimulation associated with it. If it is "Normal," the QRS does not have an associated stimulation. The parameter "Valid" in status window 97 means that the QRS has past selection criteria which is included in the averaging. If the LEM stimulation is indicated (not shown), this means that the QRS complex is used for LEM. If "low correlation" is indicated (not shown) in status window 97, the QRS complex was too low and, therefore, was not used in the averaging. If there is a "Bad Interval" indication (not shown), then the preceding or following interval changed by greater than 300 milliseconds. If a "high-rate" status indication is indicated (not shown), the pulse rate exceeded 180 beats per minute and the QRS complex was not used in the averaging. If "manual exclusion" is indicated (not shown), that means that the QRS complex was manually excluded by the operator. If "Bad pulse Positioning" is indicated (not shown), the pulse position exceeded the tolerance set by the medical professional or the default tolerance. Further, it is possible to manually include or exclude a particular QRS from the averaging statistics by using the "Include" 162 and "Exclude" 168 selection buttons on the GUI of Figure 21. A previous QRS complex may be viewed by selecting the "prior QRS" button 142. The next QRS complex can be viewed by the selection of the "Next QRS" button 143.

An exemplary result of selecting "View 2 Minute Screen" 123 is depicted in Figure 22. The 2 Minute Screen mode allows the medical professional to view a selected channel in an overview mode. In this mode, a two-minute portion of the selected channel 138 is displayed on display area 39. R-wave correlation points and stimulation points are indicated on the display area of Figure 20. R-wave correlation points are longer, white indications (not shown) above the waveform. Stimulation points are red indications (now

shown) below the waveform. Note that both Full Resolution 119 and View 2 Minute Screen 123 modes display the current start and end time for the displayed portion of the test on status bar 37 at the bottom of the relevant GUI. Advantageously, as the operator scrolls through the data, these values change to indicate the portion of data currently being displayed.

5 An exemplary result of selecting "View QRS Change" 125 mode is depicted in Figure 23. In Figure 23, the upper graph 61 shows the average of all nonbiased QRS complexes. The middle graph 65 shows the average of all biased or stimulated QRS complexes. The lower graph 67 is the difference graph that shows the difference between the normal and biased waveforms. Statistics identifying the accumulated area under each curve
10 are displayed on the right. A double-end arrow 33 on the lower graph indicates the range over which the statistics were generated. The end points can be adjusted in the view options window. The Difference graph contains cumulative Difference results along the bottom of each 10-millisecond region, based on the magnitude signal. Figure 24 depicts the Vector Angle GUI. Vector Angle mode displays angular information 151 not reflected in the
15 magnitude signal. The Vector angle mode displays changes in the direction of the electrical signal, whereas the Magnitude mode displays changes in the amount of electrical signal.

When the Signal Averaged ECG menu selection is made from View drop-down menu 55, the GUI of Figure 25 is displayed on computer screen 23. The various graphs represent the Signal Averaged information for the Normal 43 and Biased 44 QRS
20 complexes, along with the Difference 45 between the two. Standard QRS, LAS 40 and RMS 40 calculations can be made. Noise threshold is displayed along with the standard deviation of the noise, as can be seen on the GUI of Figure 25.

Another drop-down menu 46 is the Data drop-down menu 58. Data drop-down menu 58 provides access to functions required for loading previously acquired

data from storage, such as a hard disk located in computer 27, or from removable storage, such as a Zip™ disk or other removable storage media. Configuration of protocol steps is also supported here, along with typical backup and restore functions.

Figure 27 is a GUI depiction of an exemplary menu for stored data. The date 16 and time 20 of acquisition, the identification 38, name 32, age 53, gender 54, bias information 63, R-wave sensitivity, and valid count 71 are all identified for reference, as can be noted in the upper area 14 as depicted in Figure 27. Selecting "Load From Internal Disk" option 126 from drop-down menu 58 reveals the GUI depicted in Figure 28. The GUI of Figure 28 depicts a variety of test data 57 that can be selected.

If "Load Protocol Step" 131 is selected from the drop-down menu, the GUI of Figure 29 is displayed. This function loads an identified protocol step 69 into the current test configuration. The GUI dialog box allows the operator to identify the protocol step to load. Current patient information is not changed. To select a test configuration as a protocol step, the GUI of Figure 30 is used. The protocol step is entered into "Select Protocol Step" window 158 of the GUI, and "OK" 36 is selected to save the step.

Selection of "Restore" 114 from Data drop-down menu 58 restores data from an external media, such as a Zip™ disk, back to the internal hard drive of computer 27. Further, using the "Export" 195 command, data can be exported to certain spreadsheet software programs.

20

The "Append To Stats" option 163 can be selected to append the statistics of the current configuration parameters to the file. Advantageously, this option allows all test data sets in the current drive and directory to be processed using the current processing

parameters and appended to the selected text, or .TXT, file. This useful option allows for batch processing and results based on altered settings.

Another menu 46 is Help drop-down menu 60. Full index and search capabilities of Help information is available. Further, on-line help, such as information gatherable through the Internet, is also anticipated.

A high-level operator flow chart for the software described above appears in Figure 43. A typical embodiment of the method of using the software begins at the Attach Leads To Patient stage 280. As described above, the operator will then Invoke Testing 282 and Input Patient Information 284. If only a single test is desired, path 287 is taken, wherein the operator has a chance to Define Test Parameters 291. Otherwise, the operator has the choice of selecting All Tests Desired 289 and proceeding directly to Verify Sensing 293. If Verify Sensing 293 is Bad 295, then the lead positioning can be adjusted 297, and the verified sensing retried 294. Once the sensing is Good 198, the test parameters are loaded and the test is performed 288. Once the test is completed 292, there is a chance for the operator to see if more tests need to be performed 296. If "Yes" 290, then the next predefined tests are loaded 286, and the operator is returned to Test Parameters Loaded and Test

is Performed 288. If no further tests are to be formed at the 296 state, the "No" path 299 is selected and the test is completed and leads are disconnected 300.

Figure 44 is a depiction of the test control and data acquisition software flow chart. Raw data received from lead system 12 is received at the Realtime Test Control and Monitor Software 310, along with Realtime R-Wave Indicators 306. Realtime Test Control and Monitor Software 310 then controls and relays this information to generate GUIs to make a realtime display 312 on monitor 23. Inputs from the control system can control other test

features, as well, such as User Abort Control 304 and the user's ability to perform Test Configuration 308. Realtime Test Control and Monitor Software 310 can also send the Raw Data 303 to storage 313, and save Subject & Test Information 315.

Figure 45 depicts the software flow charts of the post-processing software.

- 5 Annotation and post-processing control 332 controls View Options 325 as described above, and subject and test information retrieval from storage 320. Raw data from storage 326 is retrieved and analyzed for R-wave detection 332. If LEM generation 330 is requested, then LEM Correction 334 will be performed, and Correlated QRS Alignment 336 performed. Then, one to typically four processing options may be selected. Average Processing 340 can
10 be selected for the data to be analyzed after being filtered through filtering process 338. Then the options of displaying 350 or saving 355 the data are available. If variance processing 342 is selected, the results may be displayed 350 or saved 355. Similarly, if Power Spectrum Processing 344 is selected, the results may be displayed 350 and/or saved 355. Also, Direction Vector Processing 346 may be selected and, again, the resulting
15 information can be displayed 350 and/or saved 355.

- Figure 46 displays the lower-level flow diagram, more particularly, the stimulation timing software and the switch, shunt, relay, and stimulation control features that allow for efficient subspacing stimulation signals to be timely and efficiently administered, as well as to facilitate the ability of the invention to make fast recovery to prepare for the next
20 QRS complex event. Raw Data Stream 370 is filtered by Filters 368 and is sent to Realtime LEM Generator 360, and any realtime LEM correction is made at 366. Realtime R-wave detection is determined at step 364; and, if detected, the realtime r-wave indications are passed on at 362. Realtime R-Wave Detection 364 is also linked with the Stimulation Timing Software 352 that determines the timing of the subspacing electrical pulse. Stimulation

Timing Software 352 interacts with the switch on the relay and the stimulation control portion of the software 358. The computer interconnects to the electronic interface as shown at 372.

Figure 36 depicts an exemplary series of QRS complexes 130, or R-wave events. As can be seen, interval 144 is defined by that interval from the beginning of one QRS complex to the beginning of the next QRS complex. During the testing provided by this invention, a Pulse-Delivery Point 110 is determined by the invention, and a subpacing current is delivered, typically as shown in Figure 36. There is then the anticipated R-wave 115, based upon two previous R-waves. In one preferred embodiment, the response to the stimulation is determined for a period of up to about 50 ms after the stimulation. Any change in the characteristics of the QRS complex 130 following delivery of the subpacing pulse at delivery point 110 can be used in the diagnosis of a patient's susceptibility for arrhythmia and cardiac tissue abnormality. A desired pulse position with respect to a detected R-wave is configured by the operator. When the intended position and time with respect to a detected R-wave is at or following the R-wave, then the device delivers a pulse after an appropriate-length delay following the most recently detected R-wave. When the intended position and time with respect to a detected R-wave are before the R-wave, then the device uses the previous R-interval 144 to determine an estimated time for delay by subtracting the desired amount from the R to R interval 144. The device then delivers the pulse after the determined delay following the most recently detected R-wave. The computer software is controlled with simulation and data acquisition during testing. During each test, the software delivers stimulation to alternating QRS complexes, based on realtime R-wave detection. Signals are recorded from lead system 12, along with the stimulation and R-wave detection

locations. This is monitored and is terminated when the appropriate number of pulses have been delivered in the region identified in the test parameters.

Another process for arrhythmia detection is that of t-wave alternan analysis.

This process involves looking for alternations from beat to beat in the signal produced during the t-wave portion of the heart signal. The t-wave is the portion of the heart signal that follows the QRS "contraction" (see Figure 31) of the heart. The QRS area is called depolarization. The t-wave is called repolarization because the cells are electrically preparing for the next depolarization. T-wave analysis involves computing the 'power' of each t-wave and looking for alternations in this power from beat to beat. This phenomenon tends to increase in people prone to arrhythmia. The use of t-wave alternan analysis with the previously-described technique of subthreshold stimulation is anticipated by this invention.

An overview of the operation of this invention can be seen in Figure 33.

Sensing Leads 202 pass received Signals 248 to the fast-recovery amplifier, at which time the Signals 248 are passed to the Analog to Digital converter 208. Thereafter, Data 250 is used to determine R-wave Detection 237 and for LEM modeling 215. Data 250 is also capable of going to Storage 218, and is further used for Post-Processing 240, where data 250 is eventually displayed to computer monitor 23. During the fast-recovery amplifier stage 254, Blanking Control 212, through Control 253, is used to compensate for blanking. This blanking control is initiated through the Software and Hardware Control Logic 234 via Control 253. Control 259 controls the R-wave detection 235 as it is passed to the Software and Hardware Control Logic 234. Software and Hardware Control Logic 234 further controls a Shunt Control 225 via Control 254; and Control 257 controls Current Controlled Driver 221. Hardware and Software Control Logic 234 passes Data 250 to the Digital to

Analog Conversion 228, thereafter passing those Signals 255 to the Current Controlled Driver 221. At the appropriate time, Signal 255 is delivered to Stimulation Leads 206. Post-Processing 240 also performs LEM modeling 215, Digital Filtering 243, and Statistical Calculations 246, described in more detail below.

5 A significant part of the subject invention is the amplifier and driver circuitry located in electronic interface 18. Electronic interface 18 provides amplification of signals received from lead system 12 and amplifies those signals to a level of impedance readable by the computerized data acquisition/control system, such as computer 27. Electronic interface 18 also takes control signals from the computerized data acquisition/control system, such as
10 computer 27, and provides stimulation into lead system 12, as described above. The amplifier circuitry is designed to record lead signals that occur immediately following the injection of energy into the lead system. The recording typically occurs within only several milliseconds of the injection of energy. Fast recovery is important to the system because of the need to sense electrical information very shortly after a stimulation. In one preferred
15 embodiment shown in Figure 37, each vector X, Y, and Z has its own amplifier, X amplifier 155, Y amplifier 165, and Z amplifier 175. Stimulator 180 controls subpacing pulse delivery in conjunction with computer 27; and the software Power Conditioning Circuit 182 powers amplifiers 155, 165, and 175 supplying Stimulator 180 with subpacing current. Figure 38 is a wire-level diagram of Figure 37, illustrating this advantageous design.

20 To provide for such fast recovery, several methods are employed. The sensing leads are comprised of fast-recovery material, such as tin, sodium, silver and silver chloride, or other such material known to those skilled in the art, to facilitate rapid dissipation of any energy induced by the system. Further, electronics interface 18 uses a multistage amplification scheme as known to those persons skilled in the implementation of amplifiers,

with improvements for fast recovery. Figure 38 shows a wire-level block diagram of this embodiment of electronic interface 18. In one preferred embodiment, electronic switches are placed between amplification stages, which are used to decouple stages within the amplifier. The amplifier must be switched into its high-impedance mode, with appropriate time

5 allowances for all electrical switching to be completed prior to the application of any energy to the stimulation leads. Similarly when switching back to normal impedance mode, appropriate timings must be used to ensure that all stimulation energy is completely terminated prior to lowering the amplifier impedance. This timing must account for any engaging or disengaging delay in both the amplifier and energy delivery circuits. When the

10 amplifier is in its normal- or low-impedance mode, it has a capacity to store up charge in a very short period of time. Therefore, application of stimulation energy, however short, in this mode will greatly increase undesirable artifact. Therefore, timing is critical in decoupling the amplifier to reduce artifact. Advantageously, switch timing is software-controlled in one preferred embodiment of this invention. Other timing means are known to those skilled in

15 the art. Filtering is implemented by this invention to filter the acquired signal to eliminate possible high frequency, switch-related artifacts.

An additional clamping circuit is also employed to aid in the reduced recovery time during stimulation. As can be seen in Figure 39, an electronic track and hold switch 160 is placed between two stages of the amplifier. Track and hold switch 160 remains closed

20 during stimulation, and in a preferred embodiment, a blanking period following stimulation. Figure 39 is a block diagram/flow chart of the operation of the isolated fast-recovery EKG amplifier. Differential input signal 261 enters the Differential First Stage Amplifier Circuitry 264. Thereafter, it is controlled by Clamping Circuit 117. The signal is thereafter controlled by Clamping Circuit 117. The signal is then conditioned by Bandpass Gain Stage 267 and is

regulated by Impedance Switching Track and Hold Circuitry 160. As depicted in Figure 39, Switch Control 277 and Switch Isolation circuitry 275 control the timing of the signal. At the appropriate time, signals pass to Low Pass circuitry 269 and then to Final Gain Stage 271 and Isolation Stage 273. Finally, the amplified signal leaves the fast-recovery EKG amplifier as

5 Amplified Signal 278.

Figure 40 is a schematic of the fast-recovery EKG amplifier. Figure 40 depicts the circuitry implementing the flow chart of Figure 39. As can be seen, differential inputs 183 connect to the differential first-stage amplifier circuitry 187. The next stage is clamping circuitry 184, which is in electrical communication with the bandpass gain stage

10 185. Next are the switch-and-hold circuitry 181, low-pass filter stage 189, and final gain stage 188. Isolated circuitry 186 and switching circuitry 181 are also depicted in Figure 40.

Figure 32 is a block diagram of the switching circuit. A clamping circuit is also added within the preswitch stages. The clamping circuit is designed to engage when the input signal is greater than about plus or minus 5 mV. When switch 70 is closed, the circuit

15 behaves as a typical amplifier, using the reference lead as a body surface reference point for amplification of the differential signal between the positive and negative leads.

Advantageously, this reference point is utilized during periods of blanking of the input signals. The clamping circuit remains inactive for input signals of plus or minus 5 mV. This allows amplification of normal skin surface ECG signals. During stimulation, the switch

20 electronically disengages the amplification stages from each other. While open, switch 70 itself provides a hold function that holds constant the signal level for all postswitch stages 74. Switch 70 also decouples the reference signal from the preswitch stage 77. This decoupling advantageously prevents the preswitch stage from accepting any transient energy present during stimulation. In addition to switch 70, clamping circuit 62 engages when the input

signal of greater than plus or minus 5 mV occurs. This clamping circuit 62 uses reference lead 9 to measure a baseline. A baseline shift is caused by the remnant charge left in the patient's body following the stimulation, shunting and modeling cycles performed by a preferred embodiment of the invention. This remnant charge equalizes over time at an exponential rate referred to as baseline decay. Compensation for baseline effects can be done by subtracting a non-stimulated waveform from a stimulated wave form. Further, a baseline shift with a time constant decay may also be utilized. The decay rate may be modeled by sampling the decay rate over a predetermined interval, for example, about 10 ms. The decaying baseline shift can then be mathematically removed from the acquired data.

Advantageously, the decaying baseline shift may be removed for predetermined intervals, for example, intervals up to about 300 ms. Baseline noise can advantageously be reduced by filtering and statistical noise reduction by this invention, Whenever the input signal deviates from this baseline by more than 5 mV, the internal amplification stage is held at that level. This further reduces the effect of transient voltages generated during stimulation. These two features work together to keep the amplifier stages as close as possible to their prestimulation values, advantageously providing a very fast recovery time. An additional circuit in postswitch stage 74 provides a filter that eliminates any possible high-frequency, switch-related artifact that may occur. This is required because of the nature of the switch employed. This recovery technique is incorporated within the amplifier in one preferred embodiment of this invention.

Figure 41 is a flow chart/block diagram of the isolated driver section of the subject invention. This is additional circuitry located within electronic interface 18. This driver section depicted in Figure 41 has the characteristics to shape the energy delivery pulse to reduce rise-and-fall slopes, thereby reducing induced artifact signals. Further, the isolated

driver depicted in Figure 41 provides for shunting of any charges built up as a result of energy delivery. Shunting means may include switching from a high-impedance path to a low-impedance path for a short period of time to dissipate unwanted voltage that is present. The switching between high and low impedances is designed to occur within a time of less than 1 ms. Typically, high impedance is greater than about 5,000 Ohms, and low impedance is less than about 500 Ohms. This shunting means can be connected between more than one energy delivery lead. Further, the driver employs a constant current circuit, thereby allowing control over energy delivery and varying lead or physiological impedances. As can be seen from Figure 41, the Current Control 197 communicates with Isolated Driver Circuitry 193.

Advantageously, there is also safety circuitry, which includes Safety Fuse 199 and Isolated Safety Relay 198, controlled by Safety Relay Control 192. Shunt Control 196 then controls the Isolated Shunt Circuitry 170, which timely delivers the subpacing current output 194 to the subject.

Figure 42 is a schematic level of an exemplary isolated driver section.

Blocked off on the schematic are Isolated Driver section 193, Safety Fuse 172, safety switch 174, and shunting circuitry 170.

Additional techniques and means for improving sensing and analysis of cardiac signals will now be discussed, including both stimulated as well as non-stimulated signals. Such techniques and means include: wavelet decomposition, alternative or passive shunting, detection of ECG alternans, stimulation of alternans behavior, detection of differences between natural and stimulation induced alternans behavior, cardiomyopathy detection techniques, body surface shunting synchronous with the R-Wave on Signal Averaged Electrocardiogram, subthreshold stimulation without capture to reduce the stimulation threshold causing changes to the action potential of a subsequent suprathreshold stimulation with capture, Wedensky transthoracic

stimulation, Wedensky phenomenon within the late potential region, wavelet analysis of subthreshold stimulated and control Signal Averaged Electrocardiograms in healthy subjects and ventricular tachycardia patients, QRS complex alternans detected by wavelet decomposition of Signal Averaged Electrocardiograms, and QRS background noise
5 differentiation. Each such means will now be discussed, including reference to Figures 47-57.

Wavelet Decomposition is a mathematical analysis allowing the study of a particular signal of interest in the presence of other signals. The analysis allows itself to be tuned towards higher sensitivity to one or more particular type(s) of waveforms while reducing sensitivity towards another. This type of analysis is particularly useful when used on ECG
10 data. ECG data can contain specific environmentally present electrical noise, for example 50 Hz or 60 Hz. ECG data may also contain broadband constant or intermittent noise produced by local sources of electromagnetic interference. The dynamics of the ECG waveform itself (as it is produced by the heart) can be defined in both frequency and amplitude. Research has defined such an analyzing waveform for use with Wavelet Decomposition in studying ECG
15 data. This application includes the use of such wavelet decomposition to analyze either the natural ECG or stimulated ECG data produced by an ECG device, including the devices disclosed herein. Also included is the use of wavelet decomposition to analyze combinations of natural ECG or stimulated ECG data produced by an ECG device, including the devices disclosed herein.

20 This application discloses, inter alia, the methods and apparatus of using the stimulation electrodes (or any large area surface electrodes) in an ECG device, including the devices disclosed herein, as a method of enhancing sensing of cardiac condition. First, these electrodes can act as a shielding mechanism to enhance the sensing of ECG signal. The

presence of a large area electrode acts as an electrical shield allowing better sensing of cardiac signal. The use of such an electrode is identified and claimed here.

Embodiments of the present invention also include an optimum electrode configuration to induce non-invasive Wedensky phenomenon in organisms. Wedensky phenomenon is the effect of subthreshold stimulation on the subsequent suprathreshold excitation. Recently, it has been shown that external transthoracic subthreshold stimulation synchronous with the R wave produces Wedensky phenomenon which differs in normal subjects and ventricular tachycardia patients. To produce non-invasive Wedensky phenomenon optimally, sufficient myocardial current density (MCD) has to be combined with minimum MCD variance. A computer model of transthoracic currents was used to study the effects of different electrode systems on mean MCD and its variance. Three 2D horizontal thorax cross-sections were considered with high, middle, and lower sections of ventricular myocardium. Tissue characteristics were taken from an anatomical atlas and represented by conductivities within a rectangular grid of 460 x 700 nodes. Finite difference model of current flow investigated 30 different frontal electrodes used in 13 different positions against 5 different positions of a dorsal patch (1950 experiments with each cross-section). The current densities within the modeled myocardium of all three cross-sections were considered together (79956 nodes) and for each experiment, the mean MCD and its standard deviation were computed. Independent of the position, there is a positive relationship between the area of the frontal electrode with mean MCD (3.78, 4.29, 4.68, 4.98, 5.18, 5.32, 5.39 [in technical units] for linearly increasing length of the frontal electrode of simulated sizes from 15 to 120 mm) while the coefficient of variance of MCD decreases with the increasing area of the frontal electrode (0.52, 0.49, 0.46, 0.43, 0.41, 0.38, 0.36). The coefficient of variance of MCD was further improved when introducing perforations into the

largest size electrodes. However, this improvement was only marginal (lowest coefficient of variance of 0.31 and 0.29 was achieved with un-perforated and perforated electrode, respectively – 7% reduction). Embodiments of the present invention provide that non-invasive induction of Wedensky phenomenon involves a large precordial electrode.

- 5 Furthermore, embodiments of the present invention demonstrate that the variance of myocardial current density is slightly reduced by using perforated electrodes.

Shunting is a technique of dissipating unwanted voltage. Use of the devices and methods disclosed herein involve the delivery of energy followed by the shunting of the stimulation leads as a means of reducing the artifact caused by charge remaining on the lead
10 system. This shunting process also has application when no energy is delivered through the leads, and is interchangeably referred to herein as alternative or passive shunting.

By passively changing (shunting) the potential of a large area of the body, an impedance modulation in the body can be realized. The generation of the surface ECG from the heart involves the current flow from cell to cell as depolarization recruitment progresses.
15 This current vector multiplied times the local resistivity gives the local electrical field. The components of that on the skin are what is called the ECG. By pulsing the shunt across the chest it is possible to modulate that resistance (i.e. "impedance modulation"). This is similar to changing the angle of view of the cardiac signal. This altered measurement can also be compared against the non-shifted measurement.

20 Also disclosed here is the process of shunting these or any larger area surface electrodes together to effectively provide an isopotential at the skin surface. This action can be viewed as "passive stimulation." It can shift the body potentials and possibly alter conduction pathways to allow better sensing of the cardiac condition. This altered measurement can also be compared against the non-shifted measurement. The use of either

"impedance modulation" or "passive stimulation" and its effect on the QRS signal is thus disclosed herein.

Alternan behavior consists of the changing of cardiac signal in a modal fashion. That is, one beat will have certain characteristics, the next will have different characteristics, and the following will have characteristics like the first. The process of averaging together alternate beats used in an ECG device, including the devices disclosed herein, allows the measurement of the natural ECG alternan behavior. The extent and change of this measurement can be a measure of cardiac condition. The use of this measurement as an indication of cardiac condition is disclosed and included in this application.

By averaging together alternate beats, the systems and methods disclosed herein allows the measurement of alternan behavior. This method can be useful in the determination of cardiac condition. Thus, this application discloses use of the systems and methods to achieve stimulation-related changes in alternan behavior, or shunting/impedance shifting-related changes (passive stimulation in alternan behavior as a method for detecting cardiac condition). Furthermore, the differences between natural alternan behavior and stimulated alternan behavior can also be useful in determining cardiac condition. This application discloses and includes the use of the differences between these behaviors as an indicator of cardiac condition.

A further use of the devices and methods disclosed herein is to assess conduction pathway changes within the heart by examining the changes in ECG while stimulating and not stimulating the myocardium. Another use disclosed herein is to detect non-conduction related abnormalities of the heart including, but not limited to, cardiomyopathy. The changes invoked by the process of stimulating, shunting, or examining alternate beats could also be used to determine the extent of physical myocardial abnormality. Stimulation related

changes, shunting and impedance shifting related changes (passive stimulation), or changes due to average of alternate beats as a method of detecting non-conduction related abnormalities are disclosed and included herein.

Applicants have further discovered improved means for signal analysis by analyzing the effect of body surface shunting synchronous with the R-wave on Signal Averaged Electrocardiograms by comparing the differences between normal subjects and patients with ventricular tachycardia. This study investigated the effects of creating a body surface short circuit synchronous with the R-wave on the spectral profile of signal averaged electrocardiograms.

In 35 patients with EP inducible ventricular tachycardia and in 30 healthy volunteers, 60 to 200 QRS complexes were digitally recorded using orthogonal leads. Synchronous with on-line R-wave detection, two surface patches corresponding to the orthogonal Z lead (a precordial patch and a left dorsal subscapular patch) were electrically connected with negligible impedance for 2 ms. The QRS complexes recorded in this way were averaged and compared with the same number of averaged QRS complexes recorded without surface shunting. Both high-gain signals were decomposed with 53 scales of Morlet wavelets of central frequencies 40 to 250 Hz and vector magnitudes of wavelet decompositions were constructed. The differences between these decompositions were characterized by their surface areas in windows of 0 to 10 ms, 10 to 20 ms, and 20 to 30 ms, etc., after surface shunting.

The area difference was substantially greater in healthy volunteers, as shown by the light bars in Figure 47, than in VT patients (dark bars) both immediately, i.e. 0-10 ms after surface shunting ($p < 0.04$) and 10 ms later ($p < 0.03$) but not later ($p = 0.4$ at 20 ms later, and $p = 0.5$ at 30 ms later). From this research data it may be concluded that short circuiting the body surface produces both recording artifact and physiological stimulus affecting the depolarization

sequence. This stimulus is very short lived and is more marked in healthy hearts than in VT patients who are probably less susceptible to minor electrical provocations.

Applicants further compared high-gain electrocardiographic evidence of Wedensky Phenomenon in healthy subjects and ventricular tachycardia patients. Of course it is known
5 that Wedensky Phenomenon is the effect of a subthreshold stimulation without capture that reduces the stimulation threshold and changes the action potential of a subsequent suprathereshold stimulation with capture.

To investigate whether this phenomenon can be documented after transthoracic subthreshold stimulation (2 ms. pulse of 5 to 40 MA between surface precordial and subscapular
10 patches delivered synchronous with R-wave detection), 60 to 200 subthreshold stimulated QRS complexes were signal averaged and compared with the same number of average non-stimulated complexes recorded during the same experimental session. The electrocardiographic recordings were obtained with standard orthogonal leads. In order to detect even minor changes within the QRS complex, each lead of both stimulated and control averaged complexes were wavelet
15 decomposed (53 scales of the Morlet wavelet with central frequencies of 40 to 250 Hz). The wavelet residuum corresponding to the Wedensky Phenomenon was obtained by subtracting the vector magnitude wavelet decomposition of the control QRS from the vector magnitude decomposition of the subthreshold stimulated QRS. The surface of the residuum was investigated in windows of 1 to 25 ms following the stimulation. The test was performed in 35
20 patients with EP inducible ventricular tachycardia and in 30 healthy controls.

The wavelet residuum showed sharp increase in the spectral power of the stimulated complex that was significantly more marked in healthy volunteers ($p < 0.01$) than in VT patients. This is shown in Figure 48 in which there is 20 ms stimulation, and in which full circles are VT patients, and empty circles are control patients. This shows that Wedensky phenomenon

induced by an external transthoracic subthreshold stimulation can be documented in man and differentiates VT patients from controls.

In further investigation, patients with electrophysiologic documented ventricular tachycardia (n=35) and healthy controls (n=30) were subjected to a subthreshold external stimulation between precordial and left subscapular patches. Stimuli of 5, 10, 20, and 40 ma were delivered for 2 ms synchronous with R-wave detection. 60 to 200 subthreshold stimulated QRS complexes were averaged and compared with the same number of non-stimulated complexes. Vector magnitude wavelet decompositions (53 scales of central frequencies 40 to 250 Hz) were obtained for both stimulated and non-stimulated complexes and their difference characterized the Wedensky Phenomenon numerically. The surface area of the 3D envelope of the wavelet residuum was measured in a window ± 5 ms from the R peak (stimulation moment) and in surrounding 10 ms windows.

The wavelet residuum showed a sharp increase of the surface of the 3D spectral envelope at and after the stimulation that was more marked in healthy volunteers than in VT patients, as shown in Figure 49 in which 40 ma experiments were conducted, and full circles are VT patients, and open circles are control patients. The maximum changes in wavelet residuum increased with stimulation subthreshold energy: 5 ma: control 1993 ± 181 technical units, VT patients 1488 ± 159 ; 10 ma: control 2151 ± 200 , VT patients 1543 ± 154 ; 40 ma: control 2746 ± 332 , VT patients 1842 ± 177 , i.e. all were statistically significant. Thus, externally induced Wedensky phenomenon shows a dose response that is more marked in healthy volunteers than in VT patients.

Wedensky Phenomenon within the late potential region was analyzed utilizing dose-related separation of patients with ventricular tachycardia from healthy controls. Patients with EP documented ventricular tachycardia (n=35) and healthy controls (n=30) were subjected

to a subthreshold external stimulation between precordial and left subscapular patches. Stimuli of 5, 10, 20, and 40 ma were delivered by 2 ms after a 20 ms delay following a real-time R-wave detection. 60 to 200 subthreshold stimulated QRS complexes were averaged and compared with the same number of non-stimulated complexes. Vector magnitude wavelet decompositions (53
5 scales of central frequencies 40 to 250 Hz were obtained for both stimulated and non-stimulated complexes and their difference characterized the Wedensky Phenomenon numerically. The surface area of the 3D envelope of the wavelet residuum was measured in a window 20 ± 5 ms after the R peak (a window centered around the stimulation moment) and the subsequent 10 ms windows (30 ± 5 ms after the R peak). The areas of the residuum spectral 3D envelope in these
10 windows were statistically compared in the VT patients and healthy controls.

All differences were highly statistically significant, as shown in Figure 50 (up to $p < 0.00005$), with the manifestation being more pronounced in the control group. The separation of the groups was more significant in the window around the stimulation moment than in the subsequent window and the significance decreased with increasing subthreshold stimulation
15 energy. Accordingly, a Wedensky phenomenon in the late QRS part is brief, and VT patients are less sensitive to the phenomenon, especially at very low subthreshold energies.

In yet another assessment, patients with EP documented ventricular tachycardia ($n=35$) and healthy controls ($n=30$) were subjected to a subthreshold external stimulation between precordial and left subscapular patches. Stimuli of 5, 10, 20 and 40 ma were delivered for 2 ms
20 either simultaneously with the R-wave or 20 ms after the R-wave. 60 to 200 subthreshold stimulated QRS complexes were averaged and compared with the same number of non-stimulated complexes (reference). Vector magnitude wavelet decompositions (53 scales of Morlet wavelet with central frequencies 40 to 250 Hz) were obtained for both stimulated and non-stimulated complexes. Local maxima of the 3D spectral envelopes were counted in 50 ms

windows following the subthreshold stimulation and compared in VT patients and healthy controls.

In reference recordings, Figure 51, there were no statistical differences between VT patients (shown as closed dots) and controls (open dots). In subthreshold stimulated recordings, the local maxima decreased (3D spectral envelopes became more smooth). This decrease was greater in healthy controls and with stimulation after the R wave, Figure 52, wherein all the differences except in experiment 10/00 were significant up to $p < 0.001$. Accordingly, subthreshold external stimulation makes the depolarization wave more uniform, mainly when delivered in the terminal QRS part in healthy volunteers.

Although the electrical alternans of the ST segment and T-wave has been extensively researched, the alternans of the QRS complex has generally not been investigated-mainly because of difficulties in detecting it. Applicants' innovations overcome such previous limitations, and allowed further assessment as follows.

In 35 patients with EP inducible ventricular tachycardia and in 30 healthy volunteers, 120 to 400 QRS complexes were digitally recorded using orthogonal leads. From these sequences of beats, the complexes with even and odd order numbers were separately aligned and averaged. The resulting high gain signals were processed with wavelet decomposition (53 scales of Morlet wavelets with central frequencies of 40 to 250 Hz) and the differences between the resulting 3D spectral envelopes were computed. These created alternans-related 3D spectral envelopes and were characterized by surface areas in subsequent 10 ms windows.

The surfaces of the alternans-related 3D spectral envelopes were substantially larger, as shown in Figure 53, in VT patients (full circles) compared to healthy controls (open circles). The differences between the groups were particularly marked within the initial and terminal portions of the QRS complex ($p < 0.00005$ in the 10 ms window preceding the R wave by 40 ms). Thus,

a wavelet decomposition of alternating signal averaged ECG is capable of detecting electrical alternans within the QRS complex, and the QRS complex alternans is significantly more expressed in VT patients compared to healthy controls. Also, the QRS complex alternans differs between VT patients and controls mainly at the beginning and at the end of the QRS complex.

5 Of the many improvements discussed above, it is worth noting that wavelet analysis is particularly significant. Indeed wavelet analysis is a highly reproducible method for SAECG processing which is as powerful as the time-domain analysis for the identification of ischemic VT patients. As compared to the time-domain analysis, wavelet analysis is not dependent on infarct site, and is able to distinguish post myocardial infarction patients without VT from
10 healthy subjects. As compared to known applications of wavelet representations, Applicants utilized much finer distinctions of scales (7 vs. 54) with a different range of middle frequencies (70-200 Hz vs. 40-250 Hz). Applicants also determined that wavelet analysis of signal-averaged ECGs is superior to the standard time-domain analysis in predicting post myocardial infarction events. In particular, this analysis identifies not only those post MI patients who are at risk of
15 non-fatal sustained ventricular tachycardia, but also those who are at risk of sudden cardiac death. Thus, this is the first discovery of using wavelet analysis for categorical risk analysis with prospectively collected signal-averaged ECG data in an almost consecutive population of MI survivors. As such, a significant advantage of this technology is that compared with standard time-domain analysis, the wavelet decomposition of signal-averaged ECGs provides a more
20 powerful distinction between survivors of an acute MI who are and are not at high risk of further complications. Figure 54 shows sample data of the interdependence of time-domain and wavelet decomposition indices, in which is presented the correlation coefficient between the two techniques. The value of correlation coefficient is shown above the diagonal, and the corresponding p-values are displayed below. Figure 55 is data representing a comparison of

signal-averaged ECG indices in patients with and without follow-up events. For each category of follow-up events and for each time-domain and wavelet decomposition parameters, the table lists the averaged value in patients with and without the event. The last column ($p =$) shows the significance of statistical comparison of values in patients with and without events

5 (nonparametric Mann-Whitney test). Figure 56 shows the association of positive SAECG findings with follow-up events. For each category of two year followup events and for each of four diagnostic criteria, the table shows the number of true positive (tp) and true negative (tn) patients as well as the statistical significance (p -) of the association of events with findings of a positive signal averaged ECG analysis (Fishers exact test). Herein, CM represents cardiac

10 mortality, PAD represents potentially arrhythmic death, SCD represents sudden cardiac death, VT represents sustained ventricular tachycardia, PAE represents potentially arrhythmic events, and ARF represents sudden cardiac death and/or ventricular fibrillation. Figure 57 is a comparison of positive predictive accuracy of predicting follow-up events. In this Figure, for each category of follow-up events and for six selected levels of sensitivity (Sen), the table shows

15 maximum positive predictive accuracy (PPA) achieved at that level of sensitivity with time-domain indices (TD) and wavelet decomposition indices (WD) of signal averaged ECGs. The table also shows the numbers of patients for which the diagnostic criteria of both techniques adjusted for the given level of sensitivity did not agree (Discordance) divided into the number of those for which the time-domain diagnosis was correct (TD+) and those for which the wavelet

20 decomposition diagnosis (WD+). The last column shows the statistical significance ($p=$) of the comparison of values of TD+ and WD+ (sign test).

One additional signal improvement technique involves improved noise management in the QRS realm. When sensing signals from electrodes, a certain amount of environmental background noise is unavoidable. This noise may vary in frequency and direction, causing

certain electrode placements to be more sensitive to receiving it than others. The following software-based approach addresses an implementation to reduce sensitivity to this background environmental noise during the processing of data recorded from electrodes.

When sensing signals from electrodes, a certain amount of environmental background noise is unavoidable. This noise can vary in frequency and direction causing certain electrode placements to be more sensitive to receiving it than others. To improve alignment of QRS complexes of multiple channel ECG data (XYZ, multi-lead intercardiac, 2 lead, etc.,) a mechanism which reduces sensitivity to background noise may be applied. The mechanism involves the determination of the signal level of the background noise and the signal level of the desirable signal (in the case of ECG data, the QRS). These parameters are determined for each data channel. The parameters are combined into ratios of Desirable/Background signals (hereby called D/B ratio). Channels with low D/B ratios are excluded from use during QRS alignment. Since it is possible for background noise to vary over time, an alternate implementation of this mechanism could be to assess the signal around each QRS complex for D/B ratio and exclude QRS's based on their individual ratios.

One embodiment of software source code to implement the above wavelet processing for SAEKG data may include one or more of the following functionality features:

- a. the software shall accept two orthogonal XYZ SAEKG signals for analysis along with any parameters required to perform the remaining analysis;
- b. the software shall process the region of interest of the two signals into individual wavelet surfaces using the Morlet wavelet;
- c. the software shall mathematically combine the two wavelet surfaces to form a wavelet residuum;

- d. the software shall calculate the surface area for the region of interest within the wavelet residuum;
- e. the software shall return the surface area calculation along with any other pertinent results of the calculation; and
- 5 f. the software shall calculate the count of local maxima of the two wavelet surfaces in the region of interest and return these counts.

Although many of the above embodiments have been described in the context of a system and method having non-invasive elements only, it is not necessarily a limitation of this invention. Indeed, in other embodiments it is preferred to combine the above technically
10 advantageous stimulation features and controls with elements of existing ambulatory and/or implantable technology. For example, one embodiment is shown schematically in Figure 58 in which select portions of electronic interface 18, computer 27, monitor 23, and lead system 12 may be incorporated into an external ambulatory or implantable module 401. As shown, module 401, or sub-components of module 401, may be positioned as a permanent or
15 temporary component within or on the body of the patient 35. One embodiment locates module 401 as a pectoral region implant, while another embodiment comprises locating the module as an abdominal region implant. It is of course possible to locate such implant(s) or in on other sites of the body, as appropriate.

Accordingly, it is possible to combine the sensing means of the above
20 described invention as a component and feature of an implantable pacemaker, defibrillator, cardioverter, or similar device. Other elements may also be combined as an implanted component or feature, such as, for example, fast recovery means, timing or synchronization means, processing means, or other features shown in the embodiments of Figures 1-46 as external of the patient's body. In this manner, the system and method allows for an external

or internal stimulation using the unique stimulation techniques disclosed herein along with implanted signal sensing and processing means. This combination provides for greatly expanded features having considerable value to patients and medical providers by allowing virtual on-demand in-situ monitoring and analysis of cardiac susceptibility and change

5 without the drawbacks normally associated with full electrophysiologic studies or Holter monitoring. Alternatively, it is also of substantial benefit to combine features of the above invention to portable external monitoring systems to afford non-permanent ambulatory analysis having extraordinary accuracy and predictive value without substantial encumbrance of the patient. Indeed such a systems will likely prove more efficacious than existing

10 ambulatory monitoring systems in establishing baseline recordings which will provide well-defined intervention criteria and lead to demonstrably improved therapy, both prophylactically as well as reactive to cardiac events.

Thus, it is possible to stimulate externally while sensing and processing the above described signals with permanent or temporary internal system components; or it is

15 possible to stimulate internally and detect and process internally; or in other embodiments it is possible to stimulate internally or externally and detect externally using mobile units such as a mobile pack or the like. In various embodiments of these systems and methods it may be necessary to stimulate so as to capture the ventricle, or be synchronous with the R-wave, in order to avoid patient compromise and to optimize performance. Overall, however, these are

20 techniques that differ in the context of this use from normal threshold testing or mapping techniques.

These embodiments also allow for use of this technology in ways not envisioned or even perceived possible before. For example, in one embodiment, an implanted defibrillator or pacemaker can also periodically establish cardiac baseline analyses using the

sub-threshold stimulation and sensing techniques described above but installed in the implanted unit. Moreover, with proper placement, it may be possible to locate the requisite sensing means for this invention at various depths beneath the surface of the patient's external anatomy. Baselines or other analyses may also be performed with the external

5 portable systems described above, or with a partially implanted system component such as a lead configured with stimulation or energy delivery means placed in or near the heart. The further advantage of these new systems is the relatively small amount of energy consumed by such baseline tests and analyses of this invention, a fact of particular relevance to implanted systems. Another advantage of this system is the ability to conduct sub-threshold baseline

10 testing both before and after supra-threshold stimulation, e.g. a defibrillation shock, to consistently and accurately monitor cardiac risk factors, tissue rate of change indicia, heart rate variability, memory effect, or other phenomenon.

Analysis was performed regarding Wavelet decomposition of Wedensky modulated signal averaged electrocardiograms. Investigations were performed utilizing

15 electrocardiographic recordings supplied by Harbinger Medical.

The recordings analysed originated from Wedensky modulated signal averaged electrocardiograms and were supplied in pairs for each investigated subject. These pairs contained both signal averaged modulated electrocardiograms and control electrocardiograms obtained from unmodulated alternating cardiac cycles. Each recording was given in three

20 orthogonal leads both unfiltered and digitally filtered. The analysis performed utilized the unfiltered recordings.

As with the previous set of electrocardiograms that were processed at the end of 1998, each triplet of orthogonal signal average leads was subjected to the wavelet analysis using 53 scales of Morlet wavelet and from the resulting orthogonal wavelet decompositions, wavelet

vector magnitude was calculated. The data of the wavelet vector magnitudes were stored digitally on a dedicated personal workstation and used for a extraction of characteristic parameters. All the data is available and if any further analysis is needed, the computation of the wavelet decomposition does not need to be repeated.

5 For the purposes of the analysis of this data set, a new version of the wavelet decomposition software package has been programmed. The original implementation which utilized Borland Pascal was transferred into C++ and implemented using a 32 bit compiler by Watcom. A substantial gain in processing time was achieved in this way. With the present version, processing of one set of three orthogonal electrocardiograms including the
10 computation of the wavelet vector magnitude takes approximately four to five minutes on a personal computer equipped with a 450 MHz Pentium II processor. While programming this new implementation of the decomposition system, further experience has been gained and further reprogramming concepts developed that should potentially allow the processing of one recording to be achieved within less than one minute on a suitable fast personal
15 computer.

 The parameters extracted from the vector magnitudes of wavelet decompositions were firstly related to the individual decompositions and secondly taken from the differences of the Wedensky modulated and reference recordings that were obtained within the same experiment.

20 The parameters extracted from the individual recording were related to the localized maxima of the wavelet decomposition envelope. Within each wavelet scale, local maxima were counted in a pre-specified interval relative to the R wave of the analysed electrocardiogram. These counts, taken within the same time segment, were subsequently summed over the whole spectrum of scales. The numerical parameters obtained in this way

represented the general smoothness of the wavelet decomposition and was hence likely to differentiate between subjects with and without disturbed intra-cardiac conduction.

The parameters related to the wavelet decomposition residuum, i.e. to the difference between the vector magnitude of wavelet decomposition of the Wedensky modulated and reference electrocardiograms, were based on calculating the surface area of the residuum. For this purpose the residuum was represented also by a 3-D envelope along individual scales of the original wavelet decompositions and the time synchronised in individual scales. Four different segments relative to the R wave as well as relative to the stimulation moment the surface area of the residuum was calculated. For this purpose, the spatial distance between the individual scales was considered negligible and the surface area of the residuum was represented by the sum of the distances along the 2-D graphs corresponding to individual scales within the specified time segment.

Graphical images of both the original wavelet decompositions of the Wedensky modulated and reference electrocardiograms as well as of the wavelet decomposition residua were produced and visually checked on the computer screen. The images did not substantially differ from the images produced with the previous set of recordings at the end of 1998 and were therefore not printed on paper because of the complexity of the technical work involved. Selected images were converted into transportable bitmaps and used for presentation purposes such as selected slides and poster presentations. Generally, the images suggested that the noise level achieved in the present recordings was slightly lower than compared to that observed previously.

Together with the original electrocardiographic data set, a database of individual subjects was received from Harbinger Medical in which the general clinical distinction between the normal subjects and patients with EP documented ventricular tachycardia was

made. From this database, all subjects recorded within the new data set were considered with the exception of 136 recordings that were excluded and that are listed in Figures 59A-C. The Figures 59A-C list the time stamp of the individual excluded recordings, the identification of the subject as taken from the database, and a code for the reason for exclusion. Four codes
5 have been introduced and their explanation is as follows: 1 = exclusion of a subject from the normal volunteers because of a potential clinical abnormality, 2 = exclusion of a subject from the ventricular tachycardia patients group because of reasons that were listed in the comments of the database, 3 = duplicate recording, and 4 = recording without any signal.

As previously observed, the count of wavelet maxima in 50 msec segments
10 distinguishes statistically normal subjects from VT patients.

In the present data set, this distinction was observed in both sub-threshold stimulated and reference recordings. The distinction was namely achieved when analyzing the segments shifted by 20 msec from the R wave as seen in the graphs of Figures 60A-B. In these graphs, the lines with open circles correspond to healthy volunteers and the lines with the closed
15 circles correspond to patients with EP documented ventricular tachycardia. The same layout of the graphs is maintained throughout the whole of this report.

Contrary to the observations made in the analysis made on the previous set of recordings, the distinction based on the maxima count does not differ between the reference and sub-threshold stimulated recordings. This is in line of our present understanding of the
20 differences caused by Wedensky stimulation in the 3-D wavelet decomposition envelopes which seem to produce a rather smooth additional activation pattern.

Despite this present understanding of the pattern produced by Wedensky stimulation in the 3-D wavelet envelopes, a more systematic study investigating the difference in the wavelet maxima was attempted. For this purpose, the whole 3-D wavelet envelope was

divided into non-overlapping 10 msec segments. Within mutually corresponding segments, the wavelet envelope maxima were counted and compared in the reference and sub-threshold stimulated recordings. The differences of these maxima count and the bottom being the reciprocal of statistical significance when comparing the data of individual segments of the wavelet envelopes between normal subjects and VT patients. As can be seen in the graphs, statistical significance seems to be rather disorganized and is not generally convincing.

Similar to the analysis performed with the previous data set, the surfaces of the wavelet residua were calculated in three different modes.

Firstly, the whole envelope of the residuum was divided into non-overlapping segments of 10 msec and comparisons were made between the individual patients and volunteers group (i.e. the groups of subject for whom corresponding experiments were available) for these individual segments. A number of the graphs of the analysis are shown in Figures 61A-F. Again, one page is shown for each experimental setting. In the top graph, the original data is shown and in the bottom graph, the reciprocal of statistical significances corresponding to the top graph are listed. The 10 msec segments in which the comparisons were made centred around the times that are shown in the graphs.

Generally, the same observation that was previously made, can be seen in these figures. Healthy volunteers tend to produce higher responses to the sub-threshold stimulations compared to the VT patients. Because of the leakage of the signal in calculating the original wavelet envelopes and their residual difference, the change produced by the sub-threshold stimulation is seen both after and before the sub-threshold stimulus. The separation of the groups, however, tends to be more prominent in segments following the stimulation moment.

The only exception of this general rule is the graph showing the stimulation of 20 mA at the position of 30 msec after the R wave detect. In this situation, the inverse relation between the normal subjects and VT patients was noticed, which is probably due to the small number of individuals involved in this test. All other results are consistent with the
5 previously made observations.

The evaluation of the dose response to the separation of the clinical groups in respect of the stimulation analogy was attempted for the stimulation synchronous with the R wave and for the stimulation delivered 20 msec after the R wave because only in these cases, a sufficient number of individuals were available for a comparative study. The graphs of the
10 dose response evaluation are shown in Figures 62A-B. For both positions, reciprocal of statistical significance are shown for three different segments following the R wave and difference stimulation energies.

Both graphs are highly suggestive of a dose response effect which is different for the stimulation synchronous with the R wave and delayed by 20 msec. However, these
15 observations are to some extent at odds with the observations of the dose response affect made in the analysis of the previous data set. Consequently, the issue of the dose response effect and, likewise, of the optimum stimulation energy should be further investigated.

To guide further investigations in respect of the optimum analytical window positioning and width, a comprehensive analysis was performed comparing the residuum
20 surfaces in windows related to the R wave of different duration. Graphs showing to comparisons in windows symmetric around the R wave are shown in Figures 63A-F while graphs showing the corresponding analysis in segments following the R wave are shown in Figures 64A-F.

Generally, it can be concluded that an optimum window should be centred around the sub-threshold stimulation moment and that it should last for at least 10 to 20 msec to achieve a suitable separation of the clinically relevant responders and non-responders to the Wedensky phenomenon.

5 The observations previously made, especially those that the wavelet residuum surface distinguishes normal subjects from patients with EP documented ventricular tachycardia were not artifactual and seem to be firmly established by these observations. A further study is needed to establish whether these differences are related to the presence of ventricular tachycardia or whether they are merely related to the presence of the underlying cardiac
10 condition such as the ischaemic heart disease. For this purpose, a group of patients with a post-infarction ischaemic heart disease and uncomplicated follow-up after myocardial infarction should be performed. By comparing the Wedensky phenomenon related parameters recorded in such patients to the corresponding parameters recorded in patients with ventricular tachycardia, it will be possible to elucidate whether the observations of the
15 different characteristics of the noninvasively induced Wedensky phenomenon are related to ventricular tachycardia and whether they carry potential prognostic significance.

Because of the small number of subjects involved in the individual studies and because of the difference of the protocol in individual subjects, the data presently available does not allow a firm conclusion on the optimum stimulation moment or on the optimum
20 stimulation energy to be made. Because of the substantial differences in the phenomenon induced synchronously with the R wave and delayed after the R wave, the possibility of stimulating prior to the R wave should be carefully considered. It is also not obvious whether grouping the individual subjects according to the stimulating energy in milliamperes is the optimum procedure. It might be more appropriate to consider the true energy delivered

during the stimulation since the same current might have different effects in different individuals with different trans-thoracic impedance.

If the appropriateness of the present setting of computing the wavelet residuum surface is confirmed in the study of uncomplicated ischaemic heart disease patients, search
5 for additional data analytical procedures will probably not be necessary. Once such a confirmation is available, the development of a standard version of the data analytical procedures should be organized so that an analytical system can be distributed to different centers which will allow to compare results obtained in a truly multi-site manner.

Embodiments of the present invention also included analysis of computer simulations
10 of optimum electrode configuration for the induction of noninvasive Wedensky Phenomenon in man. A technical study was conducted that used a 2-D computer model of trans-thoracic cross-sections to simulate current density within ventricular myocardium with a special aim of investigating the optimum properties of an electrode system that might be used for the noninvasive induction of Wedensky phenomenon in man.

15 An anatomical atlas has been used to select three representative cross-sections of the human thorax within the lower mediastinum that corresponded approximately to the upper, middle and lower cross sections of ventricular myocardium.

The cross sections were scanned digitally and converted into colour bit map images that were manually edited in order to achieve suitable distinction of different morphologies.
20 Colour images of the bit maps that were obtained in this way are shown in Figures 65A-E. In these images of the cross-sections, ventricular myocardium is shown in brown, atrial myocardium is shown in dark violet, lungs in blue, bones in black, cartilage in dark yellow, muscle layers in violet, fat and cutaneous tissue in yellow, oesophagus in green, liver in dark blue and blood in red. It should be noted that the cross sections were taken from the

orientation used in the original atlas and hence correspond to the view caudo-cranial rather than cranio-caudal.

The images of the cross sections shown in Figures 65A-E also show the possible positioning of electrodes considered in individual modeling studies. These are shown in cyan
5 line on the frontal and dorsal part of each cross section.

The individual tissue types were assigned electrical resistances that are listed in the table in Figure 66. The table contains values in technical units and their absolute numbers are meaningless. Nevertheless, the relationship between these individual resistance characteristics corresponds to the relationship between electrical resistance of true tissue
10 types. Individual tissue structures were considered homogenous. In particular, no difference between the electrical resistance of the myocardium in respect of fibre orientation was introduced.

The model was implemented on an advanced model of a personal work-station that was equipped with a 450 MHz Pentium II processor. The resolution of the bit map images
15 shown in Figures 65A-E was not compromised and each pixel in these images was considered as a separate nod of three individual 2-D conduction models. The total sheet used in each model was 704 X 464 nodes and correspondingly the resolution of the model was approximately in 0.5 mm steps. Taking all the three cross sections together, the tissue of ventricular myocardium was modeled by more than 79, 000 individual nodes.

20 The model was implemented as a grid of electrically conductive rectangular mesh with individual resistance values assigned to individual nodes rather than connectors. These corresponded to the resistance constants as introduced for each tissue type considered.

When introducing simulated electrodes on the frontal and dorsal part of the model, electrical current passing through the structures of individual sheets was computed according

to the Kirkhoff laws by the standard finite difference method. In more detail, the Kirkhoff laws were used to describe each of the 2-D models by a set of linear equations with as many variables as non-empty nodes in each sheet. The set of such equations was solved by Gauss-Jordan elimination method and the distribution of potential was obtained for each
5 computational experiment.

In each experiment, the potential of the front electrode introduced into the computational experiment was considered to equal to zero while the potential of the electrode simulating the dorsal part was considered to equal to one on a hypothetical voltage distribution scale. From these two potentials, the voltage distribution across each whole sheet
10 of the model was computed and the voltage differences between neighbouring nodes were, together with their resistance constants, used to calculate the current density for each node of the model.

The values of the current densities obtained for the ventricular myocardium were considered and statistically evaluated for each electrode combination.

15 Compared to the defibrillation models which aim at achieving a minimum current density in a pre-specified percentage of myocardial tissue, the concepts involved in simulating the optimum electrode positioning for the induction of Wedensky phenomenon is different. The phenomenon relies of sub-threshold stimulation and should therefore be ideally introduced with the same level of sub-threshold current density in the whole
20 myocardium. Since the level of the current density can be made variable by introducing different voltage gradient between the frontal and dorsal electrodes, the optimum position of the electrodes will be such that the variance of the myocardial current density is the lowest. In practice, this means trying to identify such a combination of frontal and dorsal electrodes

which will lead to the lowest coefficient of a variance (i.e. the standard deviation divided the mean) of myocardial current densities. This approach was used in this modeling study.

Since the dorsal patch is unlikely to have a very significant effect of the efficacy of the system, a simple 15 cm continuous patch was considered in five different positions starting at the very right edge of the dorsal electrode area as shown in the image in Appendix B. (Note that the area for electrode placement of the three sheets of the model correspond fairly each to the other.) This position at the very right edge was termed "Position 0" and was further shifted in steps of simulated 2cm. Positions 1 to 4 (shifted by 2 to 8 simulated centimeters) were obtained in this way.

In a similar manner, the positioning of the frontal electrode was introduced. Thirteen different positions of an electrode were considered. Position 0 again corresponded to the very right edge of the frontal electrode areas as shown in images in Figures 63A-E and further 12 positions were introduced by shifting the original position by simulated $7\frac{1}{2}$ mm. The frontal positions of the electrode were combined with 30 different shapes of the electrodes. The shapes of the electrodes introduced in the computation experiments are shown in Figure 65. The sizes of the electrodes in this appendix are listed in bitmap pixels of the model which approximately correspond to 0.5 mm. Thus, the largest electrode considered was the electrode 7 which corresponded to a 12 cm long continuous patch.

As it can be seen in Figure 67, electrodes 1 to 7 were composed of one solid segment and modeled differently only single patches. Electrodes 8 to 21 were composed of two segments and thus corresponded to a patch with one perforation (the sizes of the segment of the patch as well as the sizes of the perforation differed in these electrodes). Similarly, electrodes 22 to 26 were composed of three different segments, electrodes 27 to 29 of four

difference segments and finally the electrode 30 of five different segments (that is a model of a patch with four individual perforations).

All the different possibilities of the dorsal patch in positions 0 to 4 were combined with all different electrode shapes 1 to 30 in frontal electrode positions 0 to 12 and were considered for each sheet of the model. That is, for each sheet of the model, 1,950 individual computational experiments were performed and for each of these experiments, the mean and standard deviation of the myocardial current density was obtained both for the individual sheets as well as for the composition of the myocardial tissue combining all the three sheets together.

Graphical summaries of the individual results obtained in the whole set of 1,950 experiments are shown in Figures 68A-H. It is obvious that there are remarkable differences not only between individual electrodes positioning but also between the three sheets of the model. Therefore, the composite values which consider all three sheets of the model together are most representative and will be further relied on in the subsequent analyses.

Figures 69A-G shows the individual values of the coefficient of variance of myocardial current density obtained for individual electrode configuration and positioning. The individual sheets of the Appendix correspond to the individual shapes of the frontal electrode while the variability in their positioning is depicted in the 3-D graphs. Rather than showing the values of the coefficient of variance, the graphs of the Appendix show their reciprocal values. This the higher values, the better for the performance of a Wedensky induction system.

It can be clearly seen that the larger the area occupied by the electrode, the better its performance. The best results were obtained with the shapes of the electrode 19 and 24, followed by the shape 28 and finally followed by the shape 7. The differences are not very

large but it should also be noted that the stability of the electrodes modeling a very large patch with perforations (e.g. shapes 19 and 24) are more stable in terms of achieving very low coefficient of variance of the myocardial current density for different frontal positionings. Electrode 7 which models the large single patch is without any perforation is less efficient in
5 this respect.

It should be also noted that the coefficient of variance of the myocardial current decreases from electrode shape 1 to electrode shape 7 dramatically which suggests that for achieving a low coefficient of variance of the myocardial current density, one should use a rather large precordial patch.

10 It should also be noted that the variability in both mean and standard deviation of the myocardial current density introduced by varying either the frontal electrode position or the frontal electrode shape and different dorsal position is considerable.

The model is of course very restricted since it is based only on the three individual sheets and does not include the true 3-D structure of the heart and thorax which would be
15 needed for a more accurate prediction of the effects of different electrode positionings. Nevertheless, even from this restricted set of experiments, significant conclusions may be drawn.

For the optimum induction of Wedensky phenomenon in man, a rather large frontal electrode
20 should be used. The electrodes presently available of the experiments performed by Harbinger Medical seem to be appropriate for this purpose.

Since the differences between the solid patch front electrodes and perforated path front electrodes seen in the model were rather negligible, current experimenting performed by Harbinger Medical should be continued with the presently available electrode design. The

observation of the model should be tested that a more pronounced induction of the Wedensky phenomenon will be achieved when placing the frontal electrode more medially than laterally.

Additional embodiments of the invention also consider perforated frontal electrodes. The
5 model suggests that a large electrode composed of two segments with a larger center opening was the optimum in this two 2-D study. Probably, electrodes composed of several large squares with openings of about 2 cm in-between would correspond most to the model prediction.

As previously discussed, various means of optimizing the noninvasive detection and
10 localization of potential or actual sites of arrhythmias are possible and hereby enabled. In addition to the embodiments disclosed previously, it is possible to enhance this invention by careful electrode design, location, configuration, size, and current delivery means. For example, one or more energy delivery electrodes of any shape having one or more holes of various similar sizes and positions may be employed. Holes or apertures in the electrode may
15 be empty or have an electrically (or magnetically) nonconducting material in them. If these holes are material filled, this material may also have one or more holes as described above which are filled with energy delivery electrode material. Any energy delivery material can be connected to a dedicated energy delivery wire, or, some or all of the energy delivery material within an electrode can be electrically connected with other material within the same
20 electrode. This pattern of holes--nonconducting material--holes--nonconducting material, etc., and various connections described above may be repeated either symmetrically or asymmetrically according to the application.

In yet another embodiment, a plurality of small electrodes may be substituted instead of a singular large electrode in order to properly and more accurately deliver energy. Such

small electrodes may deliver energy simultaneously or separately under hardware and/or software control. Figures 70-73 illustrate various embodiments of the above disclosures. For example, in these figures element 12 represents a stimulation lead or electrode having one or more holes or apertures 16 consisting of nonconducting material, and energy delivery wires
5 or similar energy delivery means 22.

These embodiments of the invention, utilizing portions of nonconducting material within the normal periphery of stimulation leads or electrodes, may actually result in substantial increases in energy performance of these materials. This optimizes field shaping and current delivery to the subject. This technique may also facilitate the staging of current
10 among leads in sequential, seriatim or another pattern of energy delivery not normally used or associated with this diagnostic procedure. In one example, this staging of current may facilitate optimization in some form of synchronization with the cardiac sinus rhythm or other bodily rhythm.

While the invention has been described in conjunction with specific embodiments
15 thereof, it is evident that many alternatives, modifications, and variations will be apparent to those skilled in the art in light of the foregoing description. Accordingly, it is intended to embrace all such alternatives, modifications, and variations which fall within the spirit and broad scope of the invention.

WHAT IS CLAIMED IS:

1. A method for detecting patient susceptibility to arrhythmias comprising the steps of:
 - providing means for injecting low level electromagnetic energy stimulations into
 - 5 a patient's body suitable to alter at least one cardiac signal to allow a comparison of
 - acquired distinguishable signal differences with at least one other cardiac signal which
 - has not been affected by said injected energy;
 - connecting a lead system for both sensing the cardiac signals and delivering the
 - injected energy to said means for injecting low level electromagnetic energy into the
 - 10 patient's body, said lead system, comprising a plurality of energy sensing and energy
 - delivery leads; and
 - utilizing sensing improvement means for improving the quality of the sensed
 - electromagnetic energy during the stimulation and acquisition process.
- 15 2. A method for assessing heart characteristics comprising the steps of:
 - providing means for injecting low level electromagnetic energy stimulations
 - into a patient's body suitable to alter at least one cardiac signal to allow a comparison
 - of acquired distinguishable signal differences with at least one other cardiac signal
 - which has not been affected by said injected energy;
 - 20 connecting a lead system for both sensing the cardiac signals and delivering
 - the injected energy to said means for injecting low level electromagnetic energy into
 - the patient's body, said lead system, comprising a plurality of energy sensing and
 - energy delivery leads; and
 - utilizing sensing improvement means for improving the quality of the sensed
 - 25 electromagnetic energy during the stimulation and acquisition process.

3. The method of claim 2 wherein the sensing improvement means further comprises analysis of the cardiac signals with an algorithm comprising Wavelet Decomposition of the cardiac signal(s).

5

4. The method of claim 3 wherein the cardiac signals are natural.

5. The method of claim 3 wherein the cardiac signals are stimulated.

10 6. The method of claim 3 wherein the cardiac signals are a combination of natural and stimulated cardiac signals.

7. The method of claim 2 wherein the sensing improvement means comprises the step of providing the energy delivery leads with shunting means.

15

8. The method of claim 7 comprising the step of providing switch means configured to sense termination of an output current in the energy delivery leads and switch from a high impedance to a low impedance for a short period of time to allow dissipation of any voltage present.

20

9. The method of claim 7 wherein at least two of the leads are shunted together, whereby an isopotential at the surface of the skin may be provided.

10. The method of claim 7 comprising a large area electrode.

11. The method of claim 10 wherein the large area electrode is used for energy delivery.
12. The method of claim 11 comprising a means of controlling the potential of the large
5 area electrode, whereby the large area electrode is used to passively change the potential of a
large area of the body so that the impedance of the body may be modulated whereby
impedance modulation is achieved.
13. The method of claim 12 wherein the step of impedance modulation is used to affect
10 the QRS signal.
14. The method of claim 10 comprising the step of controlling the surface potential of the
large area electrode so that the potential of the body may be shifted, whereby passive
stimulation is achieved.
- 15
15. The method of claim 14 wherein the step of passive stimulation is used to affect the
QRS signal.
16. The method of claim 2 in which the sensing improvement means comprises the steps
20 of:
- stimulating at least one heartbeat, and
- comparing the stimulated heartbeat(s) to unstimulated heartbeats.

17. The method of claim 16 wherein the heart is stimulated on every other beat, whereby ECG alternans may be measured.

18. The method of claim 17 comprising the step of averaging heartbeat ECG data so that
5 an improved comparison may be made.

19. The method of claim 17 wherein the step of stimulating of the heart comprises a shunting step.

10 20. The method of claim 17 wherein the step of stimulating of the heart comprises passive stimulation.

21. The method of claim 17 wherein the step of stimulating of the heart comprises impedance modulation.

15

22. The method of claim 17 wherein the differences in every other heart beat are compared so that indicator(s) of cardiac condition may be measured.

23. The method of claim 22 wherein every other heart beat is stimulated.

20

24. A device for detection of a patient's susceptibility to arrhythmias, the device comprising,

means for injecting low level electromagnetic energy stimulations into a patient's body, the stimulations being suitable to alter at least one cardiac signal;

means for comparing a cardiac signal affected by the injected energy stimulations to at least one other cardiac signal which has not been affected by said injected energy;

5 a lead system for both sensing the cardiac signals and delivering the injected energy to said means for injecting low level electromagnetic energy into the patient's body, said lead system comprising at least one energy sensing and at least one energy delivery lead; and

at least one sensing improvement means, for improving the quality of the sensed electromagnetic energy during the stimulation and acquisition process.

10

25. The device of claim 24 wherein the sensing improvement means comprises means for executing an algorithm comprising Wavelet Decomposition analysis of the cardiac signal(s).

26. The device of claim 25 wherein the cardiac signals are natural.

15

27. The device of claim 25 wherein the cardiac signals are stimulated.

28. The device of claim 25 wherein the cardiac signals are a combination of natural and stimulated cardiac signals.

20 29. A method for assessing cardiac condition comprising the steps of:

providing means for injecting low level electromagnetic energy stimulations into a patient's body suitable to alter at least two cardiac signals to allow a comparison of acquired distinguishable signal differences between said at least two cardiac signals which are affected by said injected energy;

connecting a lead system for both sensing the cardiac signals and delivering the injected energy to said means for injecting low level electromagnetic energy into the patient's body, said lead system comprising a plurality of energy sensing and energy delivery leads which are selectively functionally connectible at different positions, for delivery of optionally different energies for optionally different durations; and

utilizing sensing improvement means for improving the quality of the sensed electromagnetic energy during the stimulation and acquisition process and comparing differences or similarities to determine cardiac condition.

10

30. The method of claim 41, further comprising the final steps of:

saving the acquired data to an internal disk by selecting features available from the computer-generated GUI;

saving the acquired data to an external disk by selecting features available from the computer-generated GUI;

15

retrieving data from an external disk by selecting features available from the computer-generated GUI;

saving protocol steps for future use by selecting features available from the computer-generated GUI; and

retrieving selected protocols from past use by selecting features available from the computer-generated GUI.

20

31. A system for detecting patient susceptibility to arrhythmias comprising:

means for injecting low level electromagnetic energy into a patient's body suitable to alter at least one cardiac signal to allow a comparison of distinguishable signal differences with at least one other cardiac signal which has not been affected by said injected energy; and

5 sensing improvement means for improving the quality of the sensed electromagnetic energy.

32. The system of claim 31 in which the means for injecting low level electromagnetic energy is configured for external placement on the patient.

10

33. The system of claim 31 in which the means for injecting low level electromagnetic energy is configured for placement internal to the patient.

34. The system of claim 31 in which the sensing improvement means is configured for
15 external placement on the patient.

35. The system of claim 31 in which the sensing improvement means is configured for placement internal to the patient.

20 36. A method for assessing heart characteristics comprising the steps of:
 providing means for injecting low level electrode magnetic energy stimulations into a patient's body suitable to alter at least one cardiac signal to allow a comparison of acquired distinguishable signal differences with at least one other cardiac signal which has not been affected by said injected energy;

connecting a lead system for both sensing the cardiac signals and delivering the injected energy to said means for injecting low level electromagnetic energy into the patient's body, said lead system comprising a plurality of energy sensing and energy delivery leads; and

5 at least of one of said energy delivery leads comprising perforation means for optimizing the current delivery of said at least one energy delivery lead.

37. A method for assessing heart characteristics comprising the steps of:

 providing means for injecting low level electrode magnetic energy
10 stimulations into a patient's body suitable to alter at least one cardiac signal to allow a comparison of acquired distinguishable signal differences with at least one other cardiac signal which has not been affected by said injected energy;

 connecting a lead system for both sensing the cardiac signals and delivering the injected energy to said means for injecting low level electromagnetic energy into
15 the patient's body, said lead system comprising a plurality of energy sensing and energy delivery leads; and

 wherein at least one of said energy delivery leads comprises a plurality of small electrode leads instead of one larger electrode lead.

20 38. The method of claim 36 in which the method is used for conducting cardiac pacing of the patient's body.

39. The method of claim 37 in which the method is used for conducting cardiac pacing of the patient's body

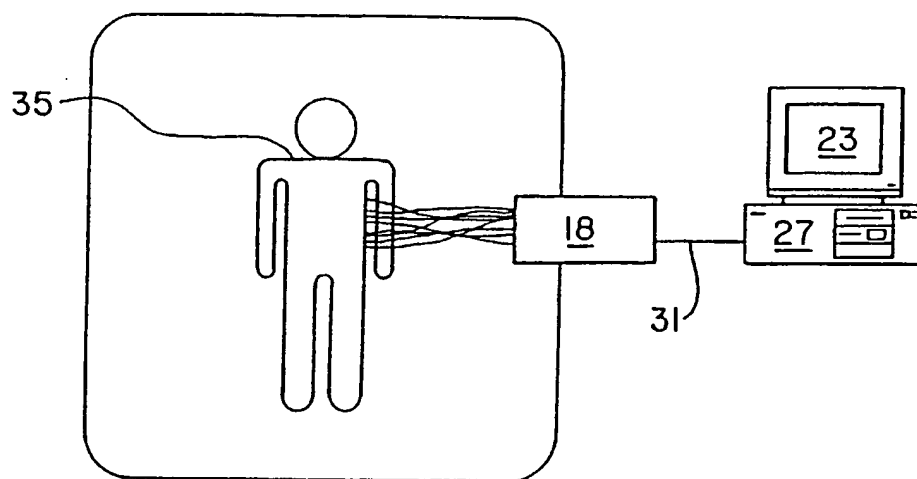
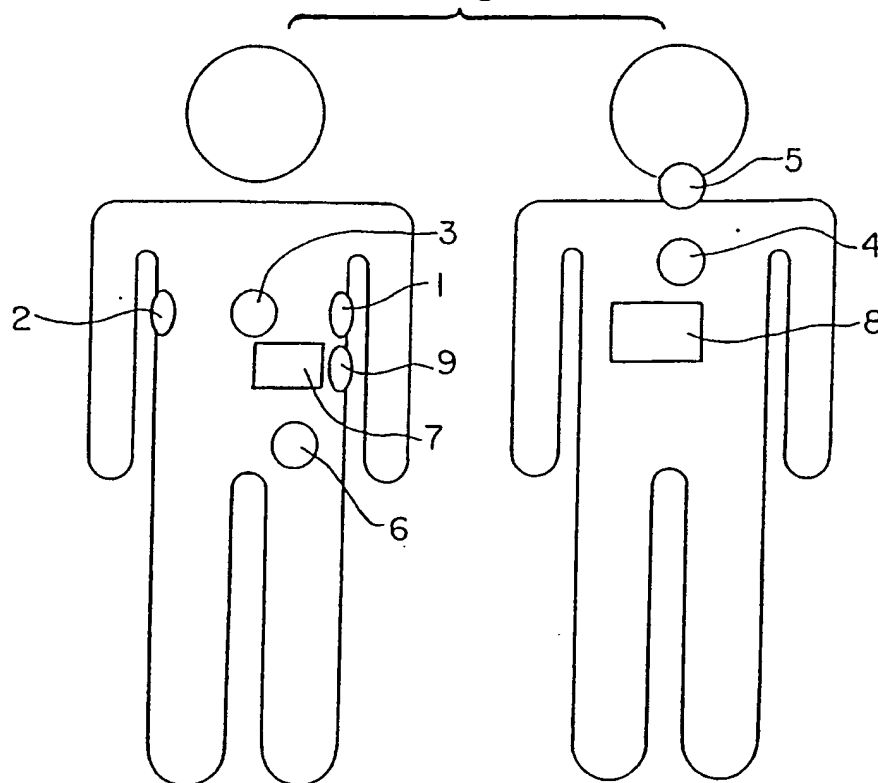
Fig. 1**Fig. 2**

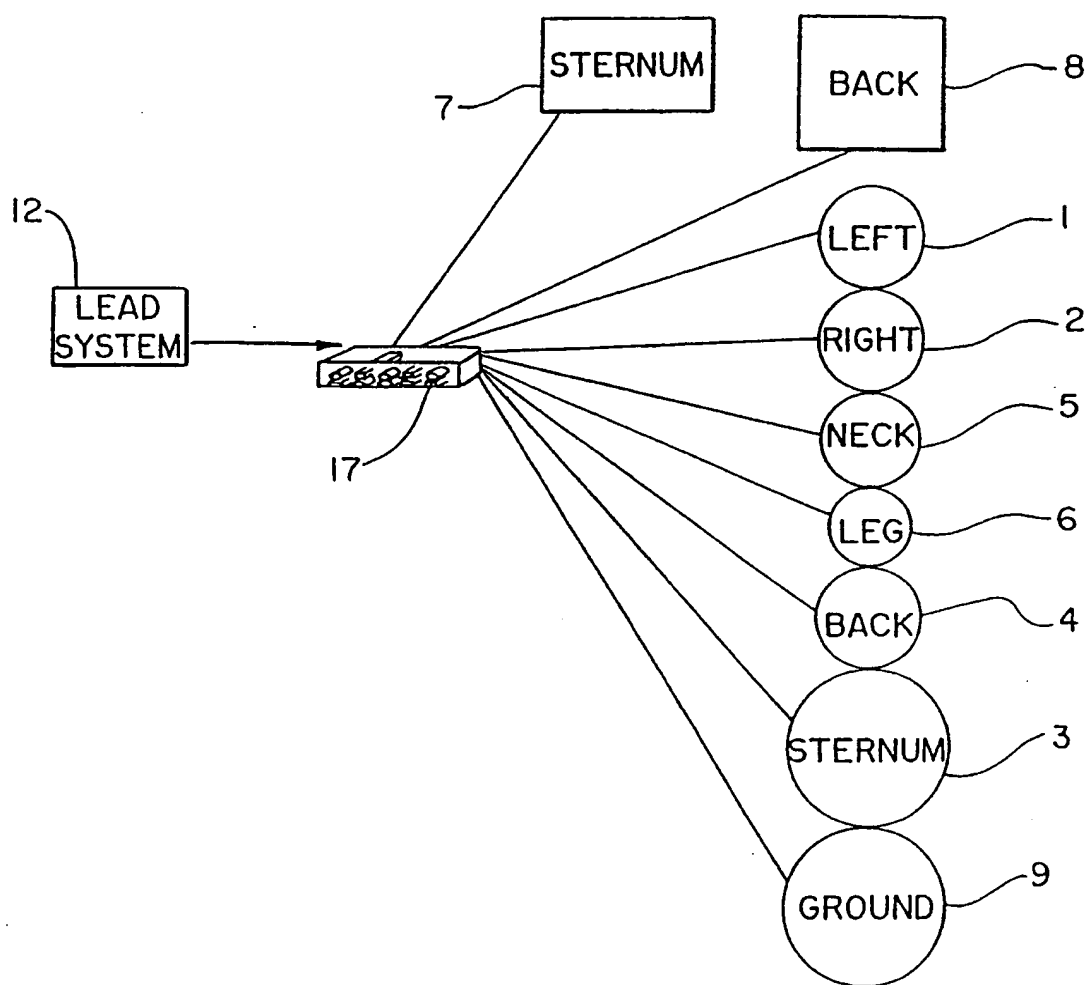
Fig. 3

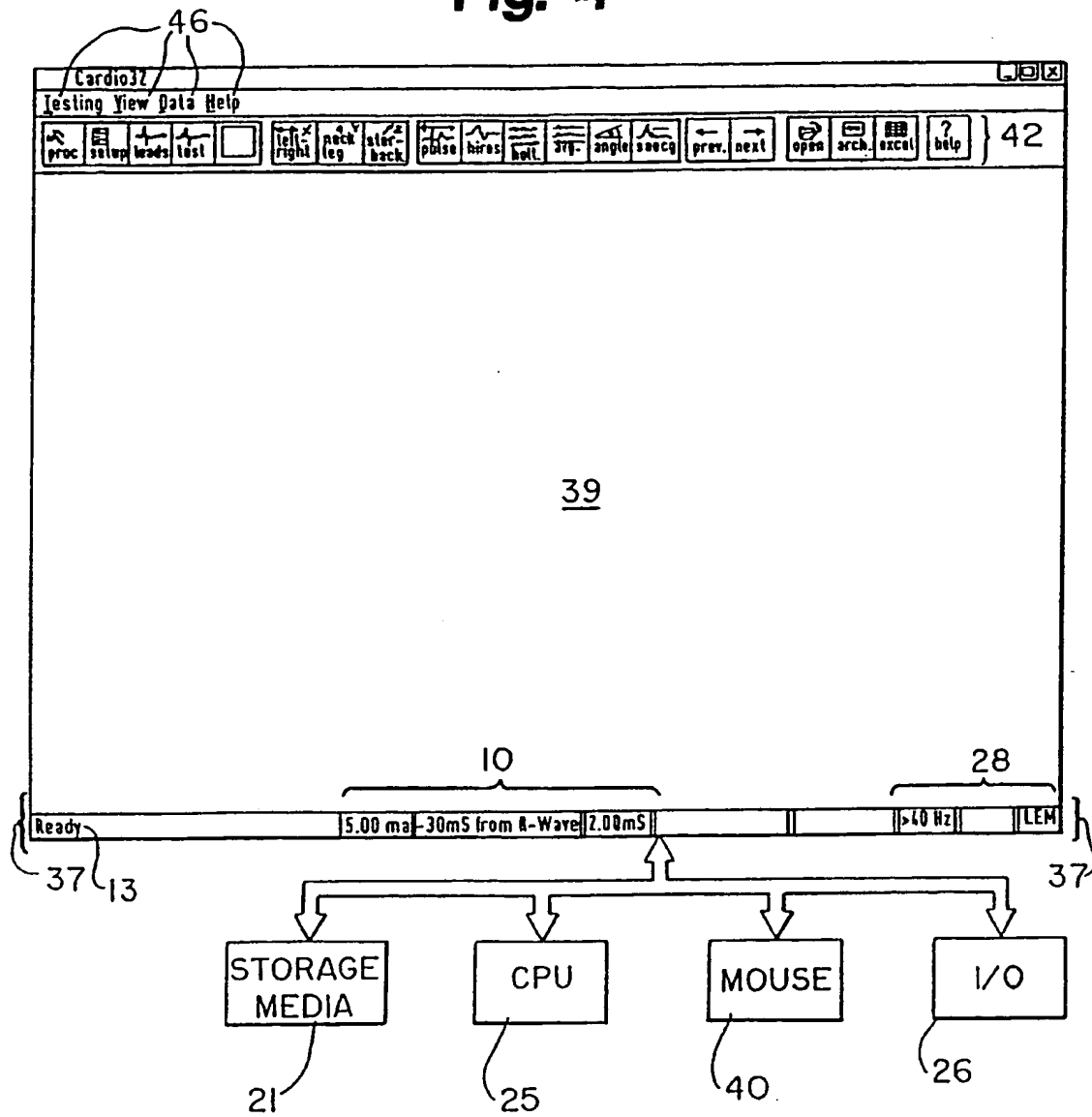
Fig. 4

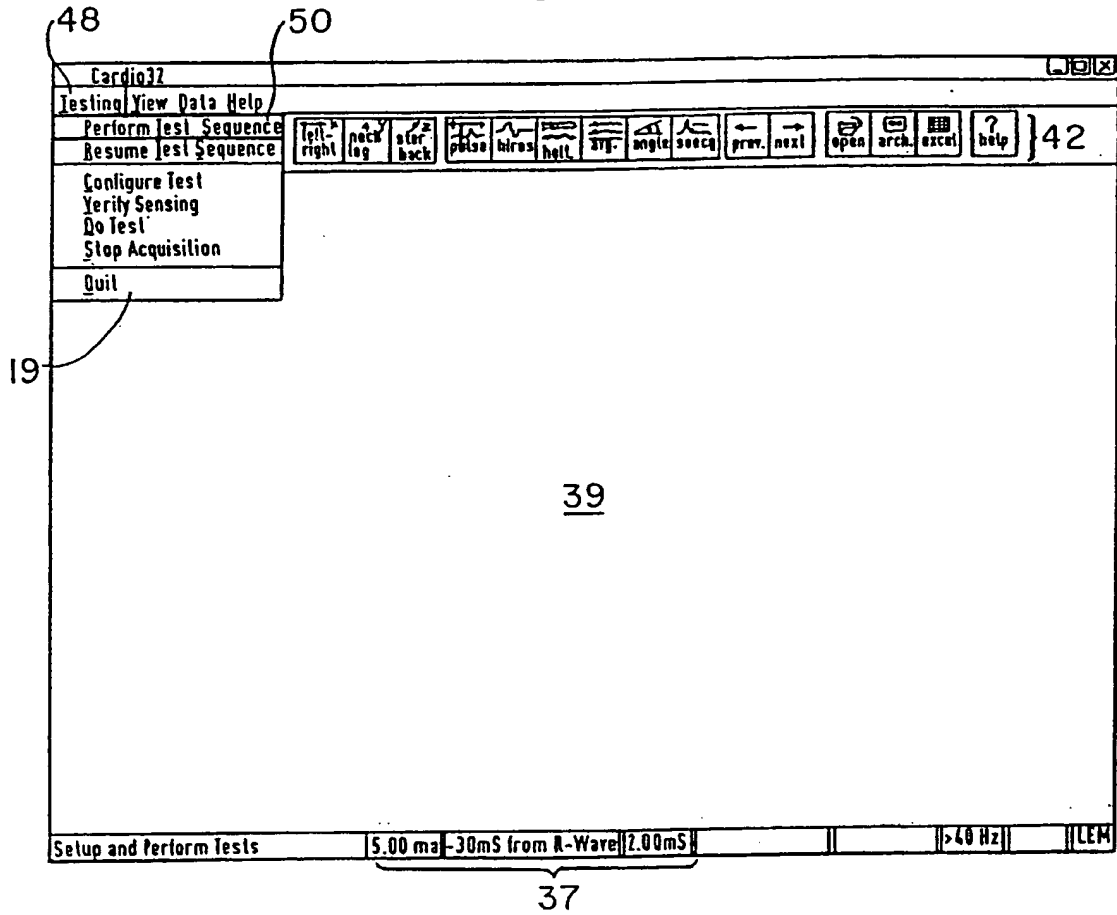
Fig. 5

Fig. 6

Identify Existing or New Subject

Subject Information
ID - Name - Age - Gender - Race

135XYZ - David Harris - 62 - Male - Caucasian
997ABC - William Baker - 38 - Male - Caucasian
123ABC - John Andrew - 46 - Male - Caucasian

OK Cancel New Patient

Fig. 7

The 'Acquisition: new' dialog box contains the following fields and controls:

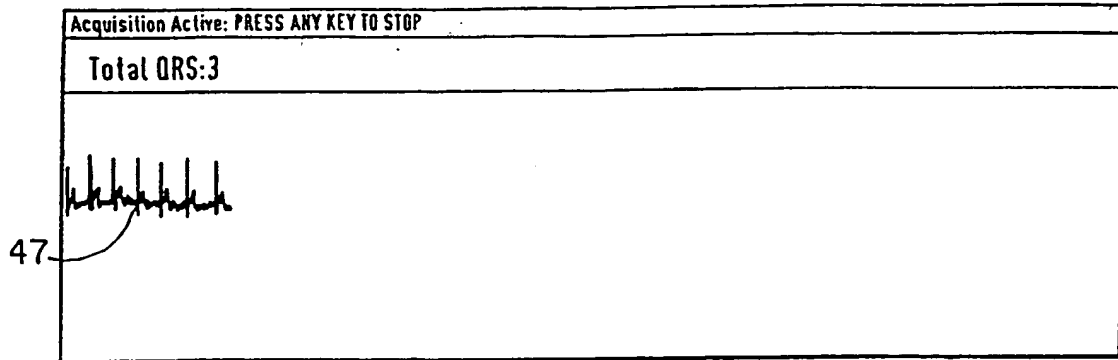
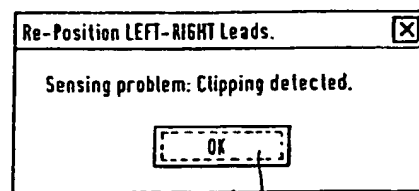
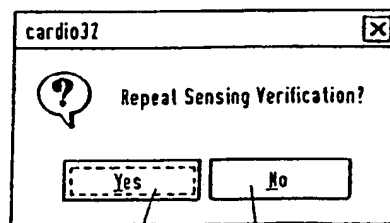
- Subject Information:**
 - ID: 1234321 (55)
 - Name: sr (58)
 - Birthdate: 8/1/58 (66)
 - Gender: ☒ MALE ☐ FEMALE (64)
 - Race: Caucasian (80)
 - Misc: (85)
- Test Parameters:**
 - Test Duration: 15 pulses (68)
 - Sensitivity: Low (87)
 - Deviation Limit: 15 mS.
- Pulse Configuration:**
 - Current: 5.00 mA (72)
 - Width: 2.00 mS. (82)
 - Location: -30 mS. (36)
 - ☒ 1 mS. Pulse Ramp Up (78)
- Buttons:** OK (90), Cancel (30)

Fig. 8

The 'cardio32' dialog box displays a question mark icon and the text 'Perform All Standard Protocols?'. It includes two buttons: 'Yes' (11) and 'No' (17).

Fig. 9

The 'cardio32' dialog box displays an exclamation mark icon and the text 'Ready to Verify Sensing.'. It includes two buttons: 'OK' (36) and 'Cancel' (30).

Fig. 10**Fig. 11****Fig. 12**

8/85

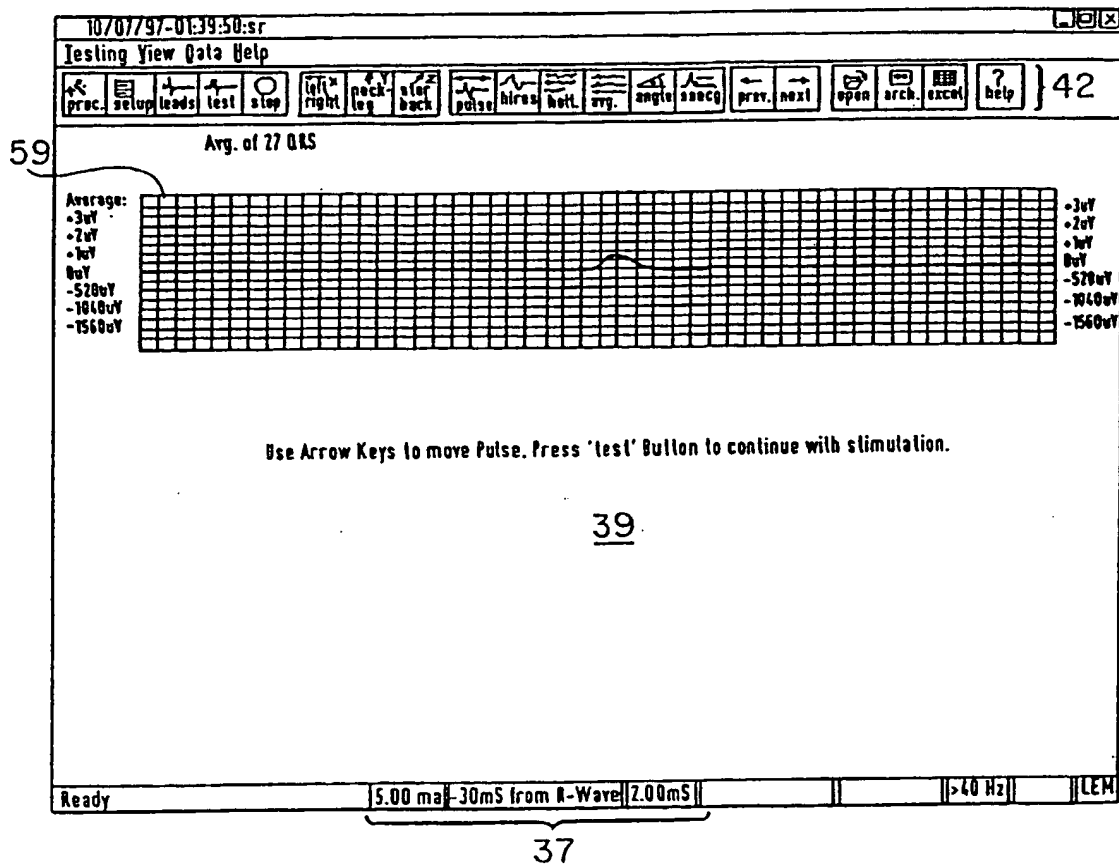
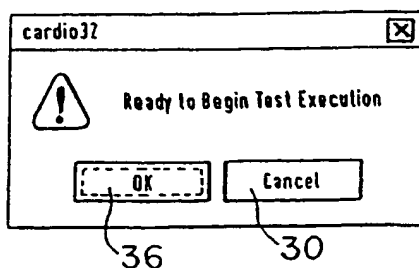
Fig. 13**Fig. 14**

Fig. 15

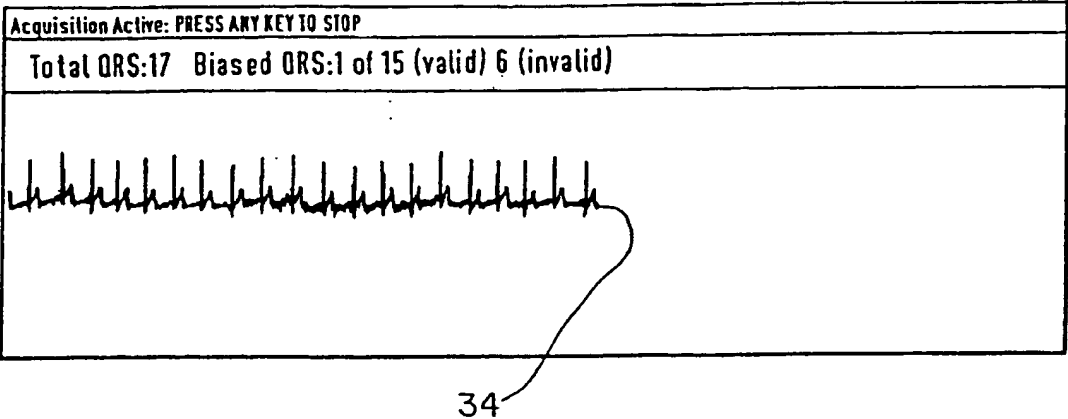


Fig. 16

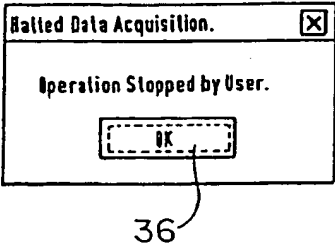
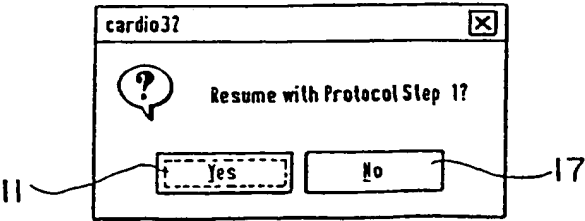
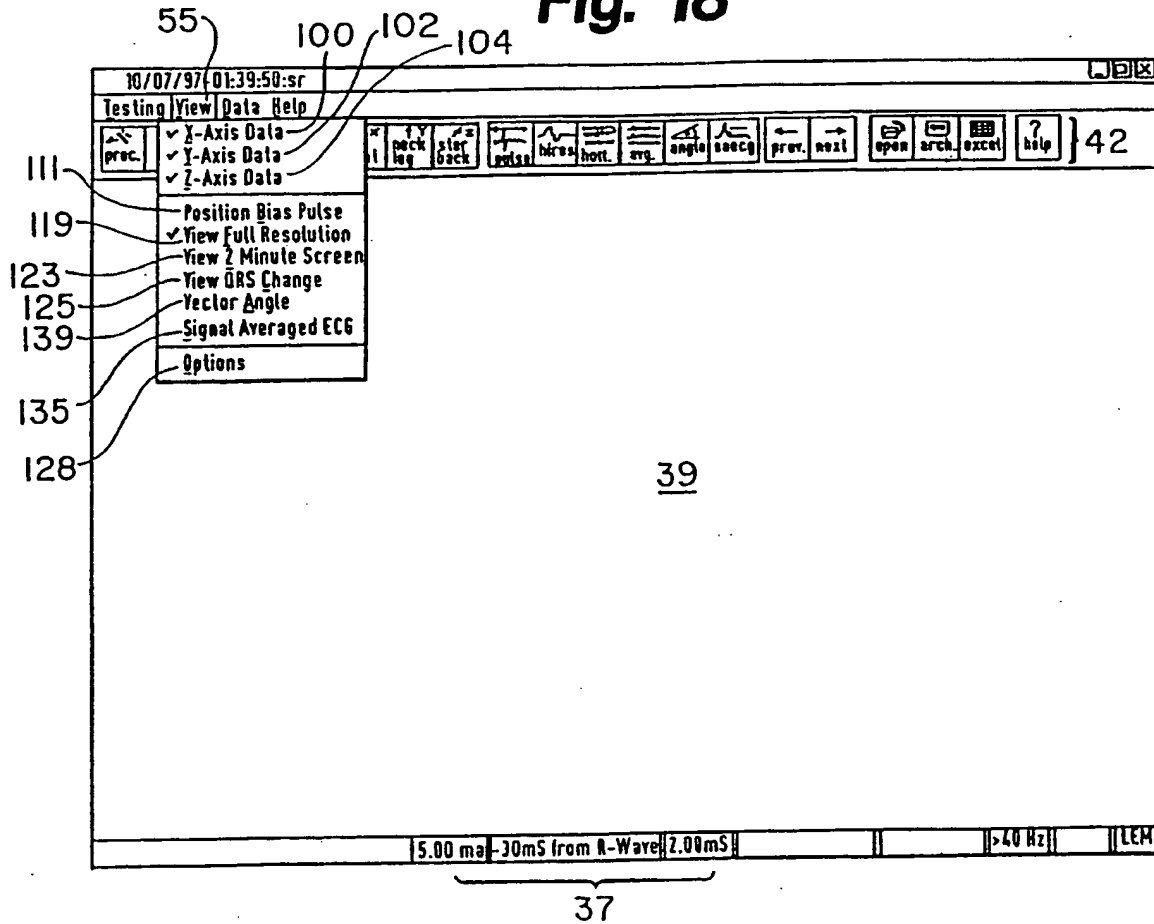
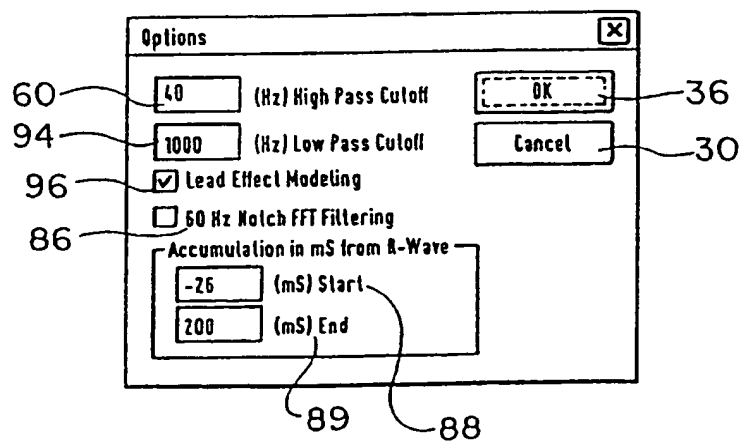


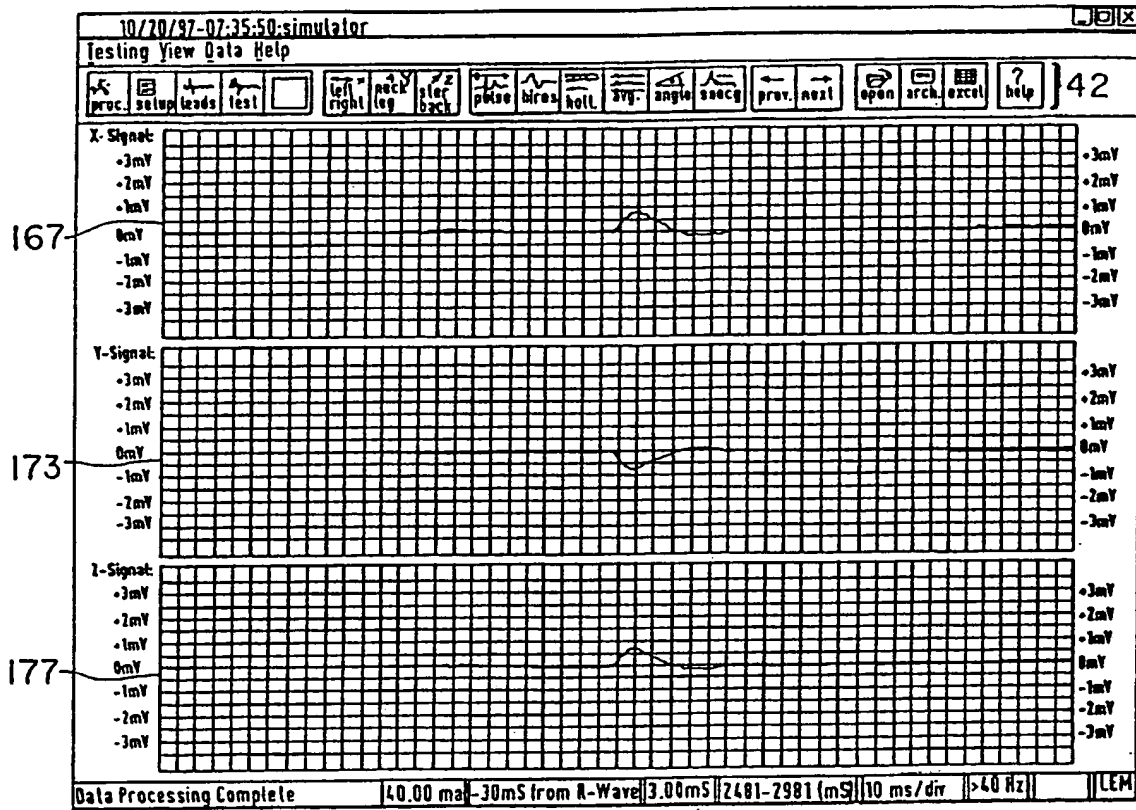
Fig. 17



10/85

Fig. 18**Fig. 19**

11/85

Fig. 20

37

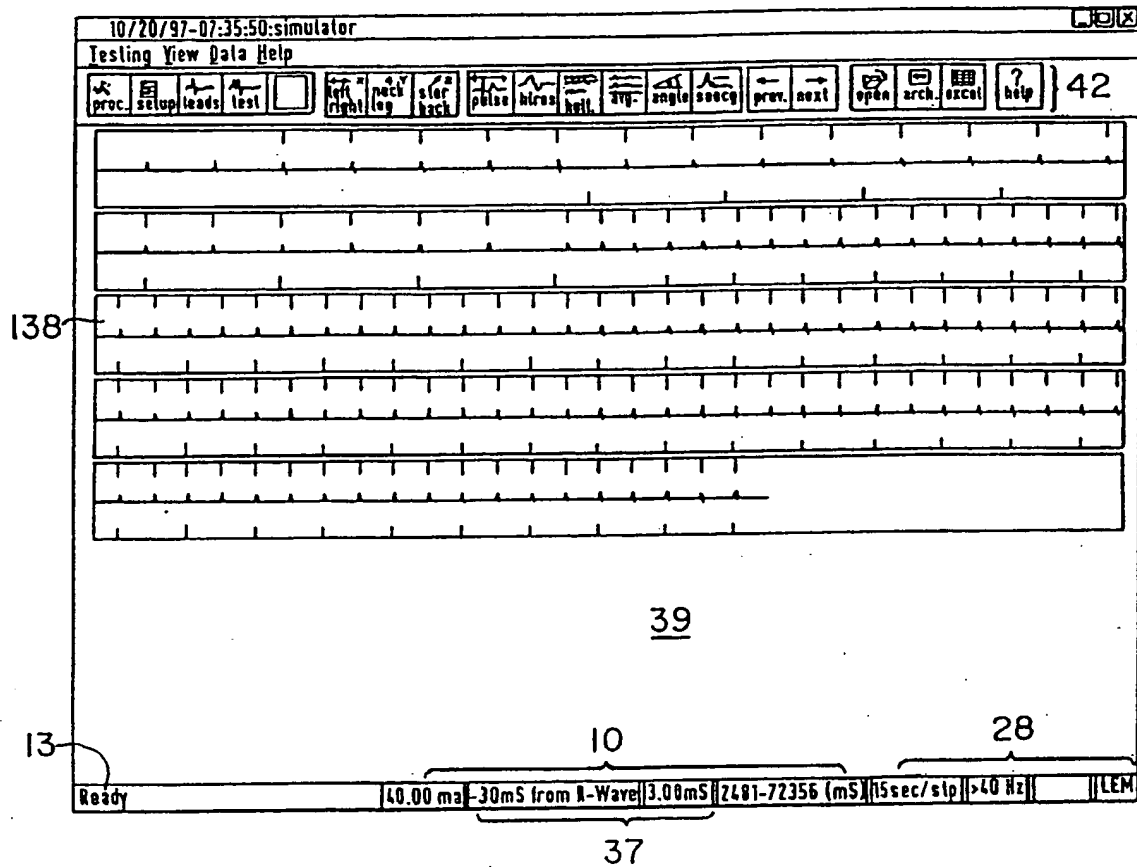
Fig. 21

The figure shows a dialog box titled "QRS Status". It contains the following fields and buttons:

- Initial Location:** 23581
- Correlated Location:** 23585
- Impulse Offset:** 16
- Correlation Value:** 0.9557631692
- Status:** Biased:Valid
- Buttons:** Include, Exclude, <-Prior QRS, Next QRS->

Labels 97, 162, and 168 point to the "Biased:Valid" status field, the "Include" button, and the "Exclude" button, respectively. Label 142 points to the "<-Prior QRS" button, and label 143 points to the "Next QRS->" button.

12/85

Fig. 22

13/85

Fig. 23

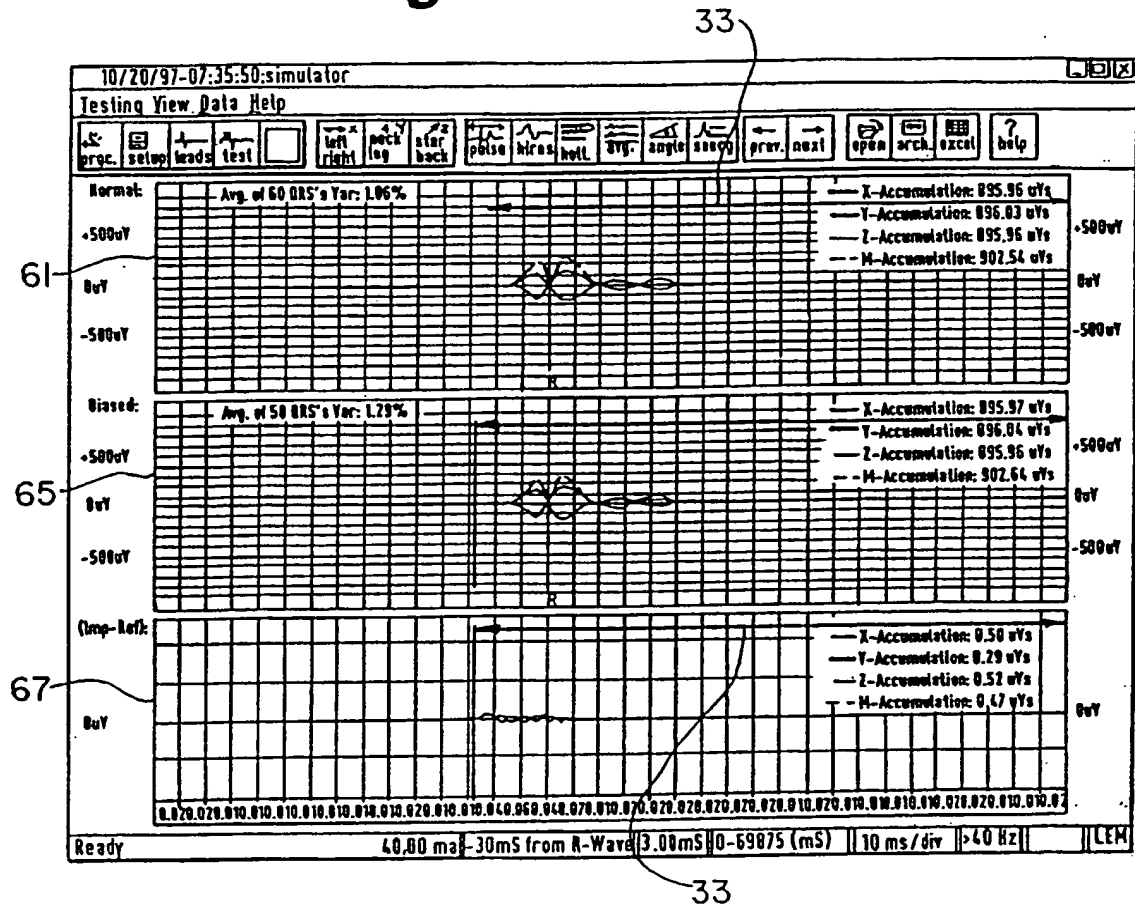
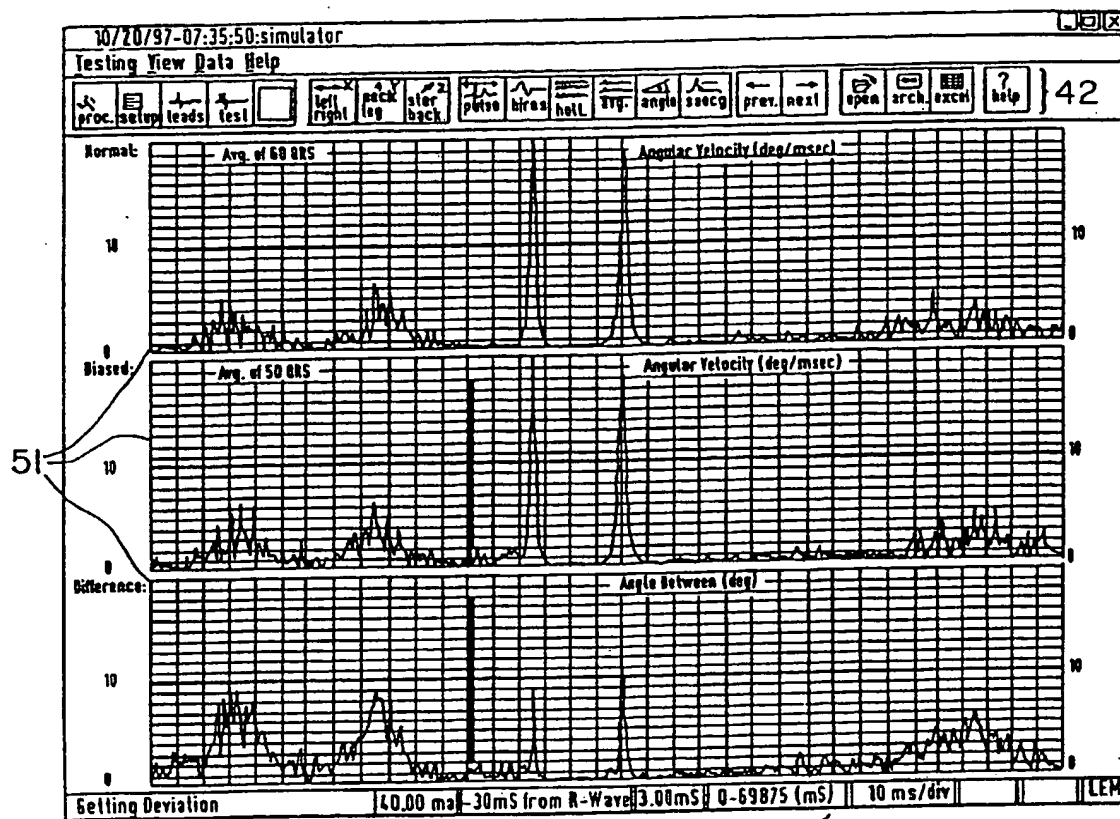
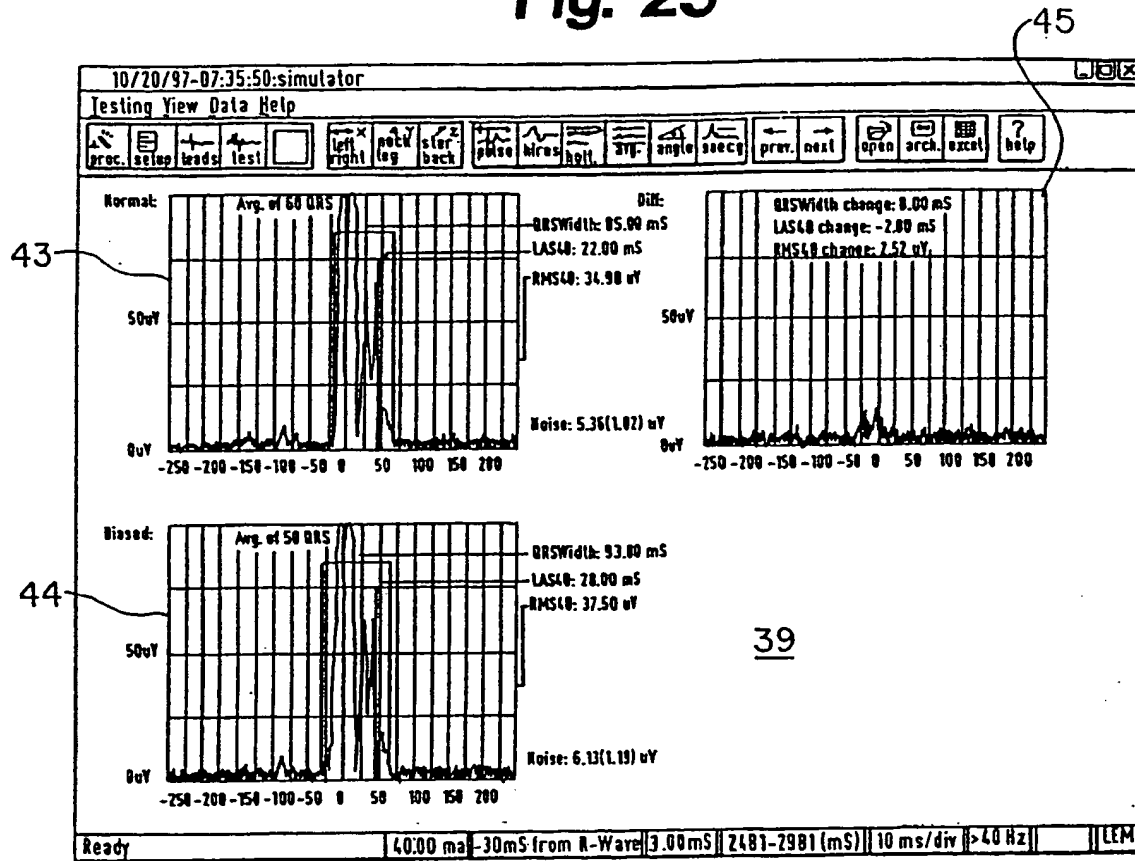


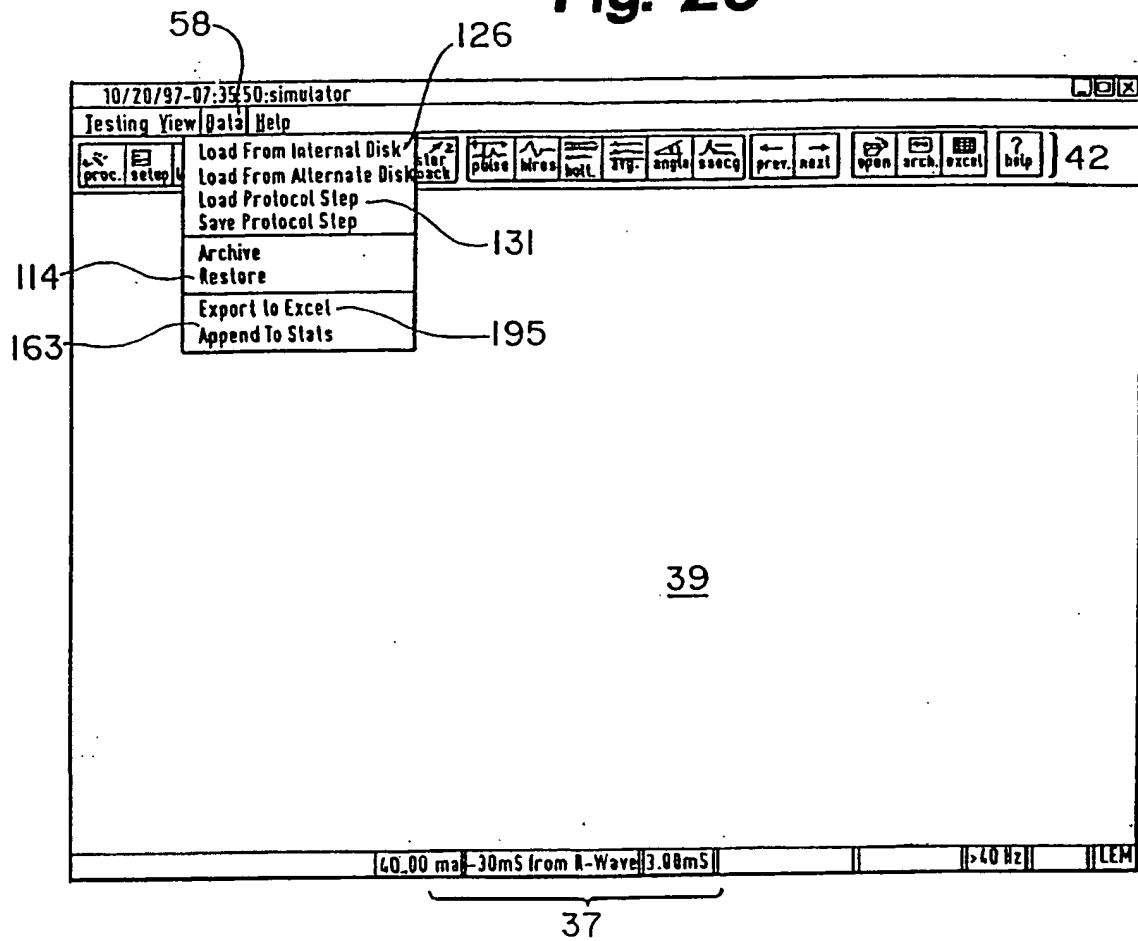
Fig. 24

15/85

Fig. 25



16/85

Fig. 26

17/85

Fig. 27

14

Accessing Stored Subject Data

Test Information		Bias Information		Subject Information	
Timestamp	Valid Bias Count	μ A	mS	Position	ID Name (age/gend)
03/12/97-14:41	15 (+/-10mS.)	5.00mA	2.00mS.	-30mS.	123456789AB Samuel Jones(52/m)
03/12/97-14:26	15 (+/-10mS.)	5.00mA	2.00mS.	-30mS.	123456789AB Samuel Jones(52/m)
03/12/97-13:41	15 (+/-15mS.)	5.00mA	2.00mS.	-30mS.	123456789AB Samuel Jones(52/m)

16 20 71 63 38 32 53 54

OK Cancel

Fig. 28

Open

Look in: data

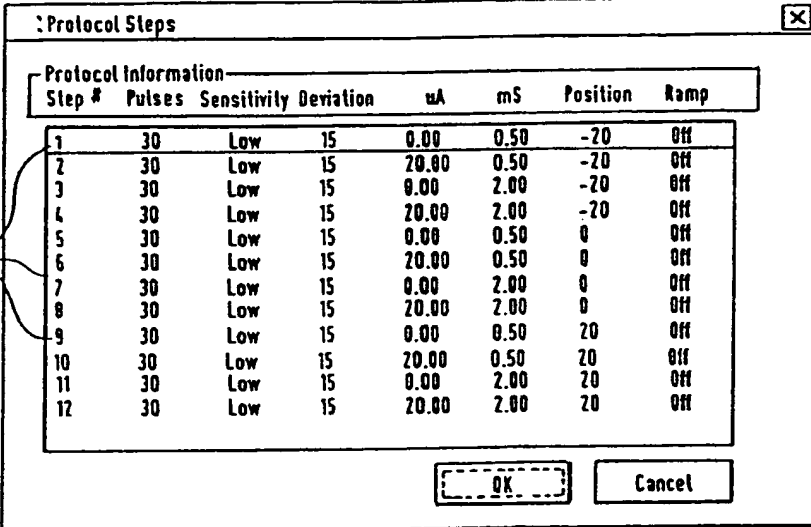
66H004R	66H0142	66H0236	66HC045
66H006S	66H0162	66H0501	66HC059
66H0089	66H017F	66H059A	66HC06R
66H0091	66H018P	66HC00F	66HC081
66H011E	66H0204	66HC011	66HC095
66H012N	66H0210	66HC031	66HC108

57

File name: 66H004R Open

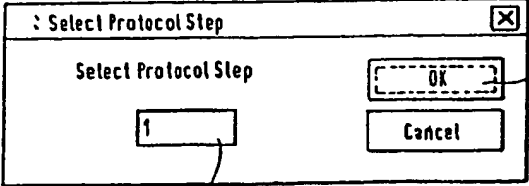
Files of type: Harbinger Tests Cancel

18/85

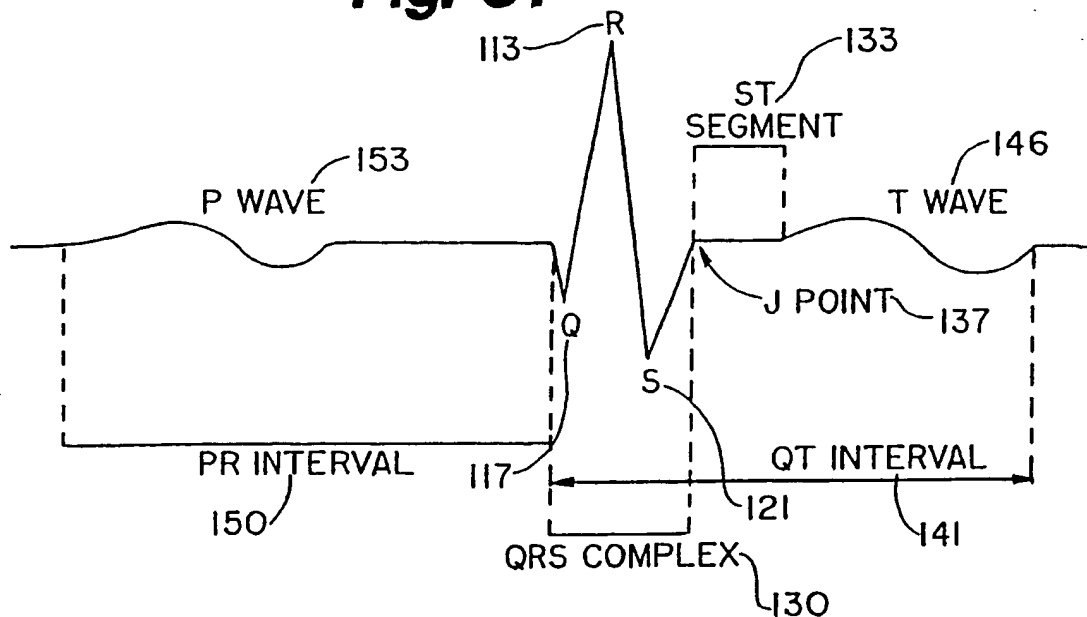
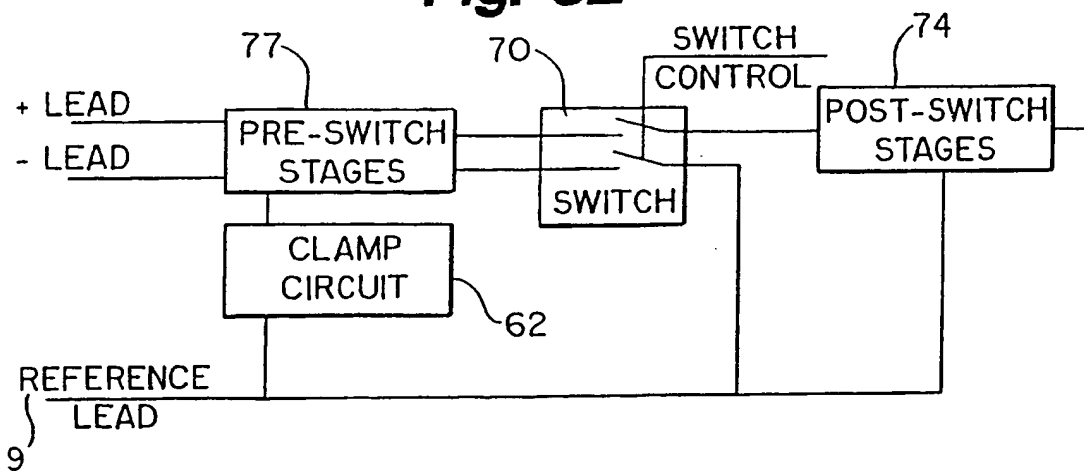
Fig. 29

A dialog box titled "Protocol Steps" with a close button in the top right corner. It contains a "Protocol Information" section with a table of 12 steps. A bracket labeled "69" points to the first six rows of the table. At the bottom are "OK" and "Cancel" buttons.

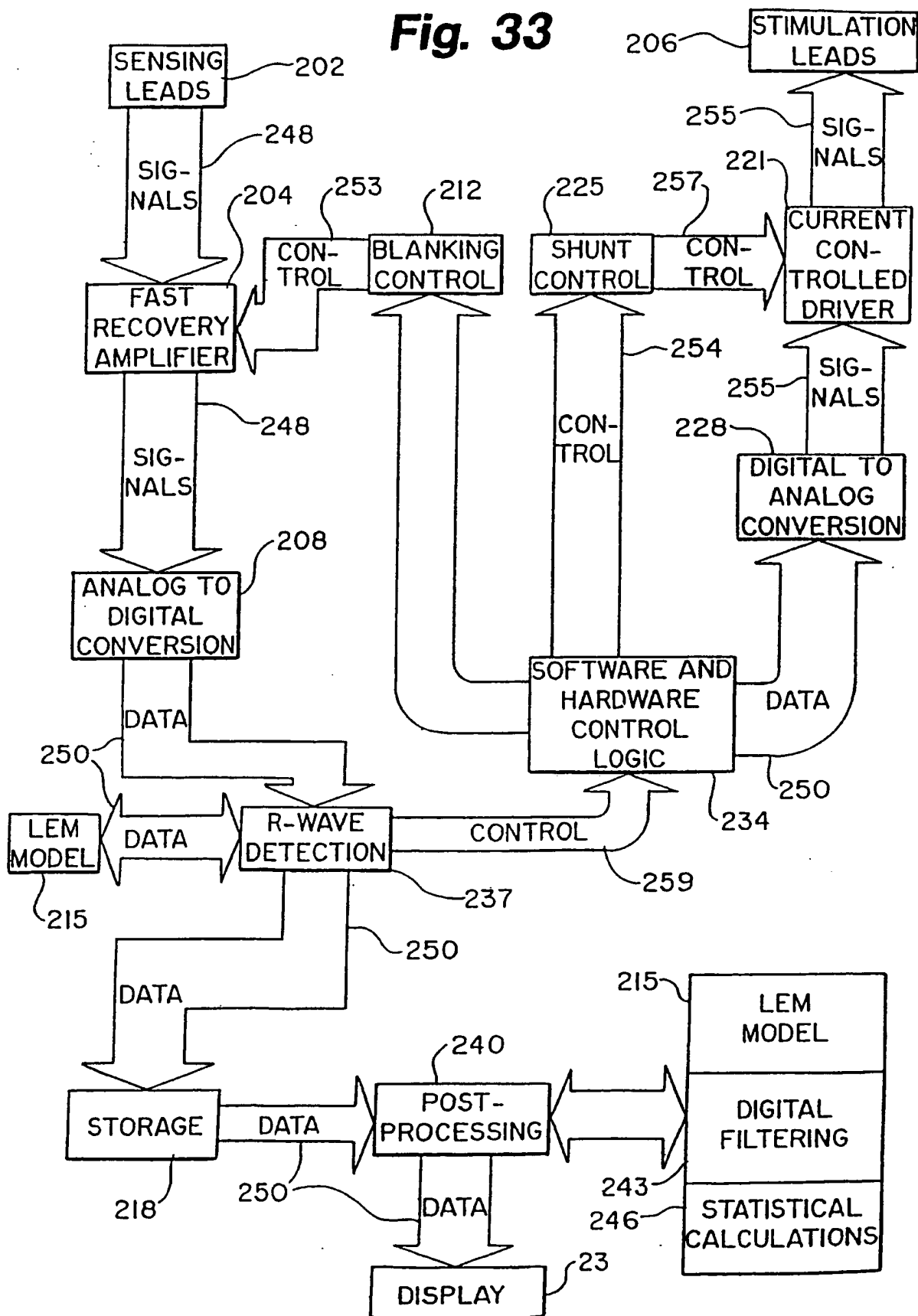
Step #	Pulses	Sensitivity	Deviation	uA	mS	Position	Ramp
1	30	Low	15	0.00	0.50	-20	Off
2	30	Low	15	20.00	0.50	-20	Off
3	30	Low	15	0.00	2.00	-20	Off
4	30	Low	15	20.00	2.00	-20	Off
5	30	Low	15	0.00	0.50	0	Off
6	30	Low	15	20.00	0.50	0	Off
7	30	Low	15	0.00	2.00	0	Off
8	30	Low	15	20.00	2.00	0	Off
9	30	Low	15	0.00	0.50	20	Off
10	30	Low	15	20.00	0.50	20	Off
11	30	Low	15	0.00	2.00	20	Off
12	30	Low	15	20.00	2.00	20	Off

Fig. 30

A dialog box titled "Select Protocol Step" with a close button in the top right corner. It contains a text input field with the number "1" inside, a bracket labeled "158" pointing to it, and "OK" and "Cancel" buttons. A bracket labeled "36" points to the "OK" button.

Fig. 31**Fig. 32**

20/85

Fig. 33

21/85

Fig. 34PIN LAYOUT FROM
CONNECTION END

1	3	5	7	9	
2	4	6	8		

29

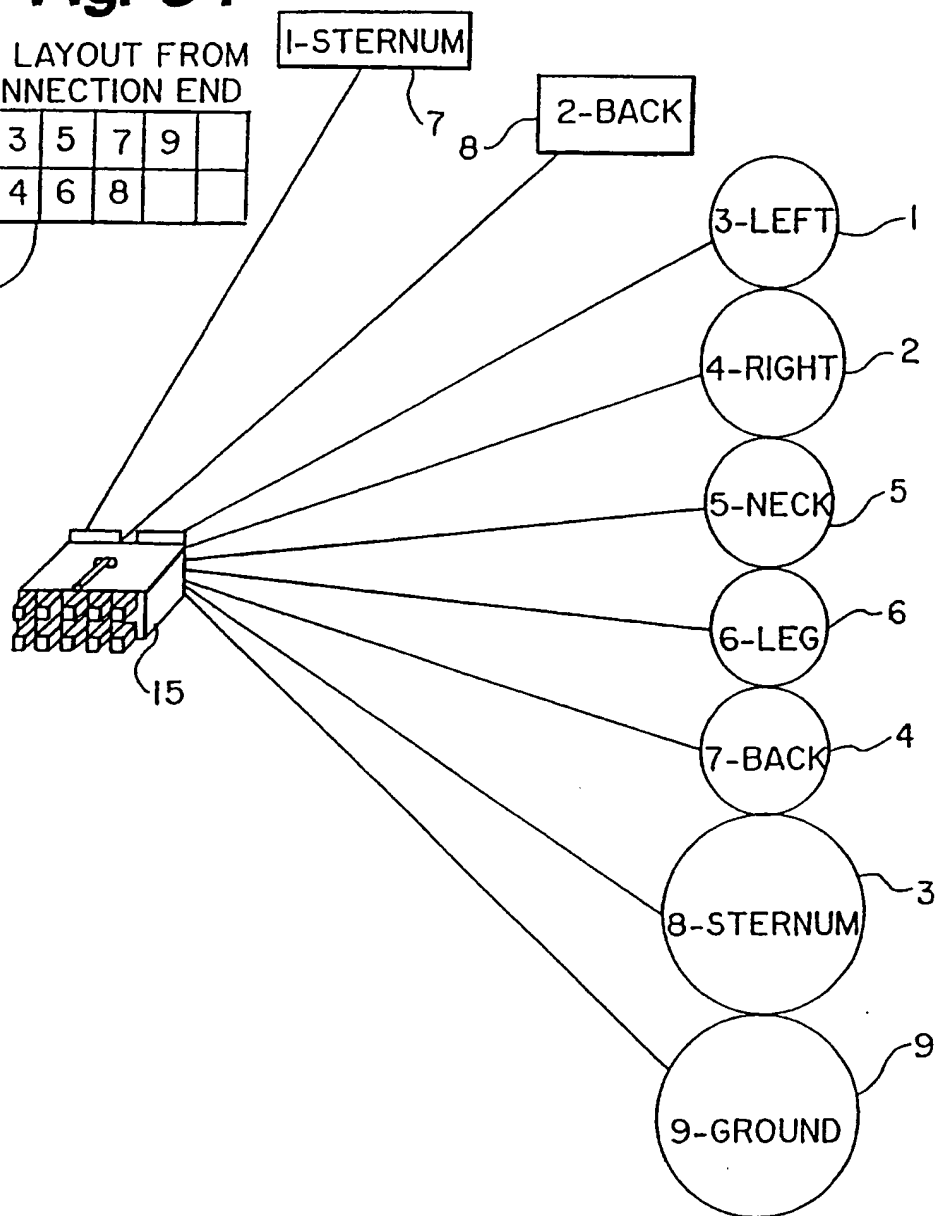


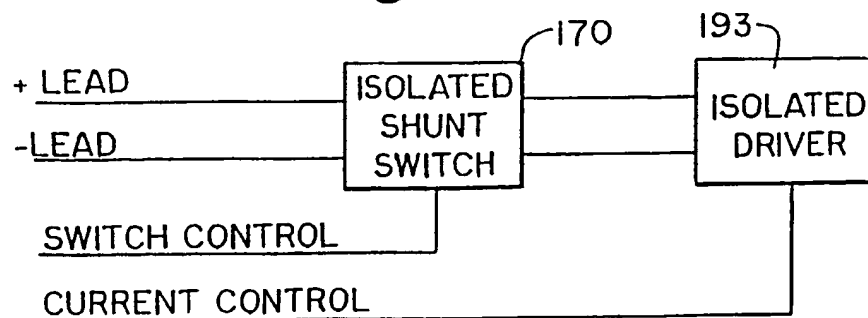
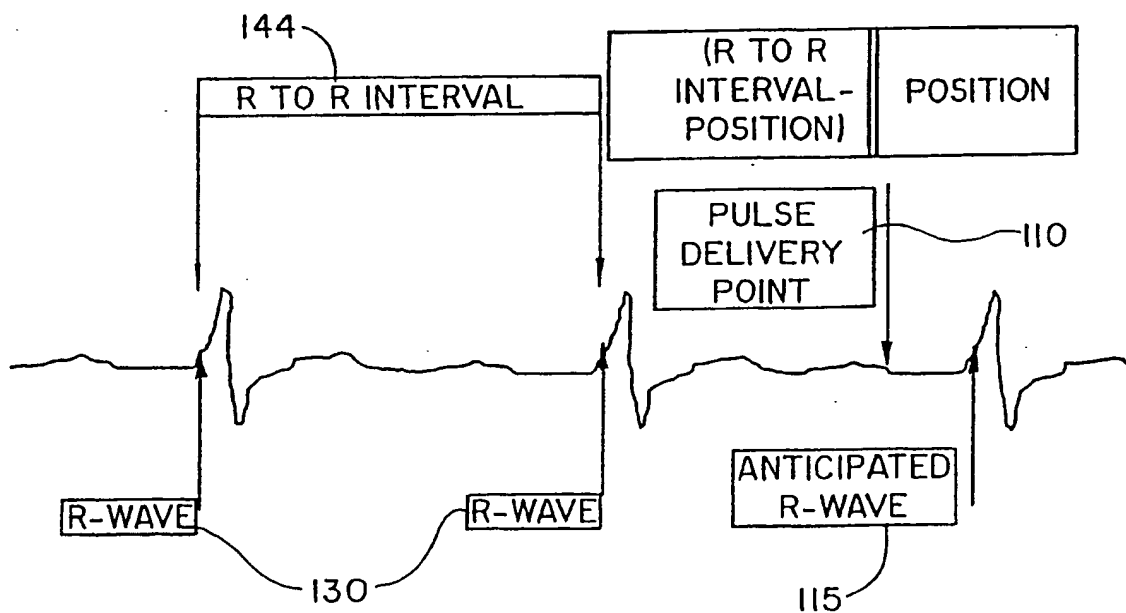
Fig. 35**Fig. 36**

Fig. 37

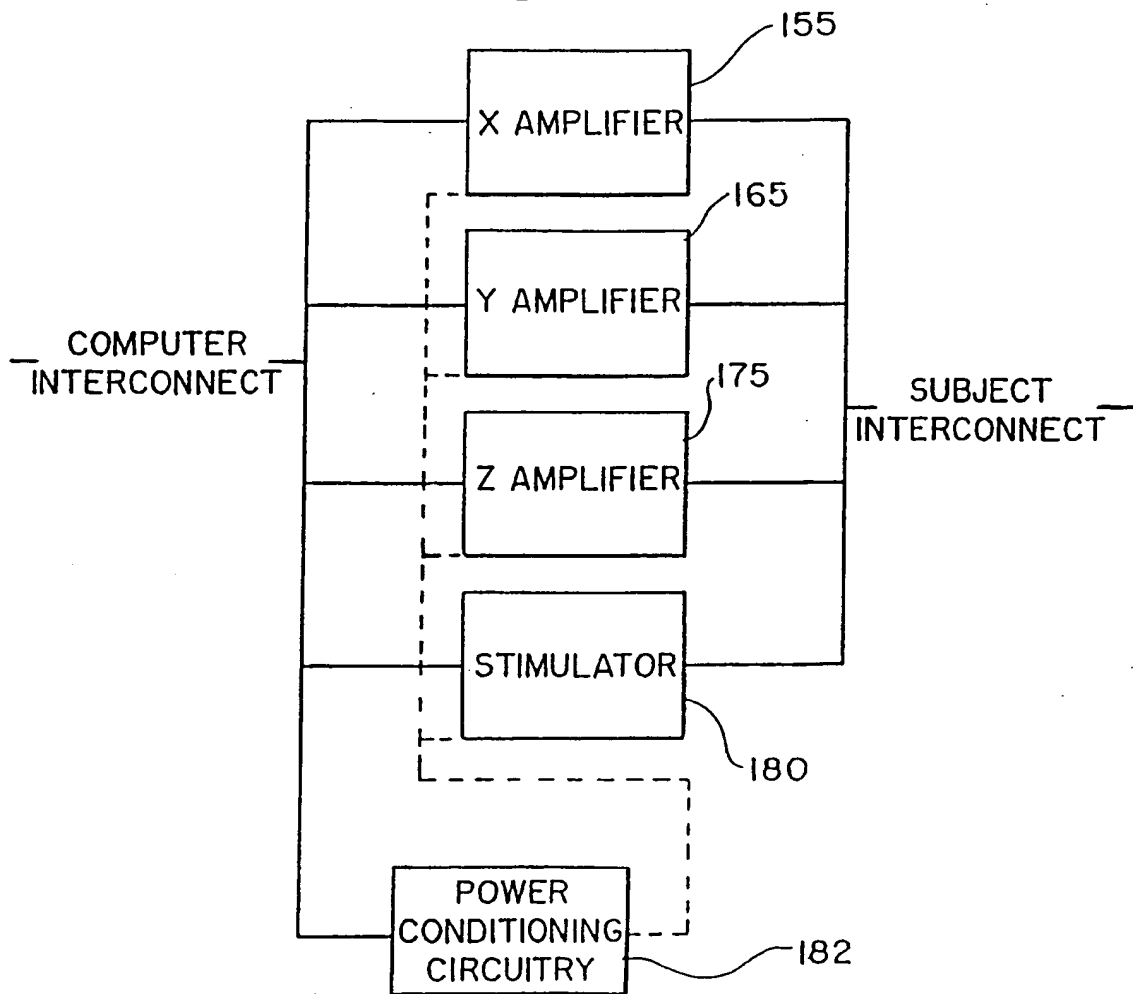
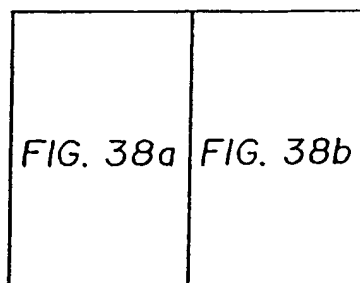
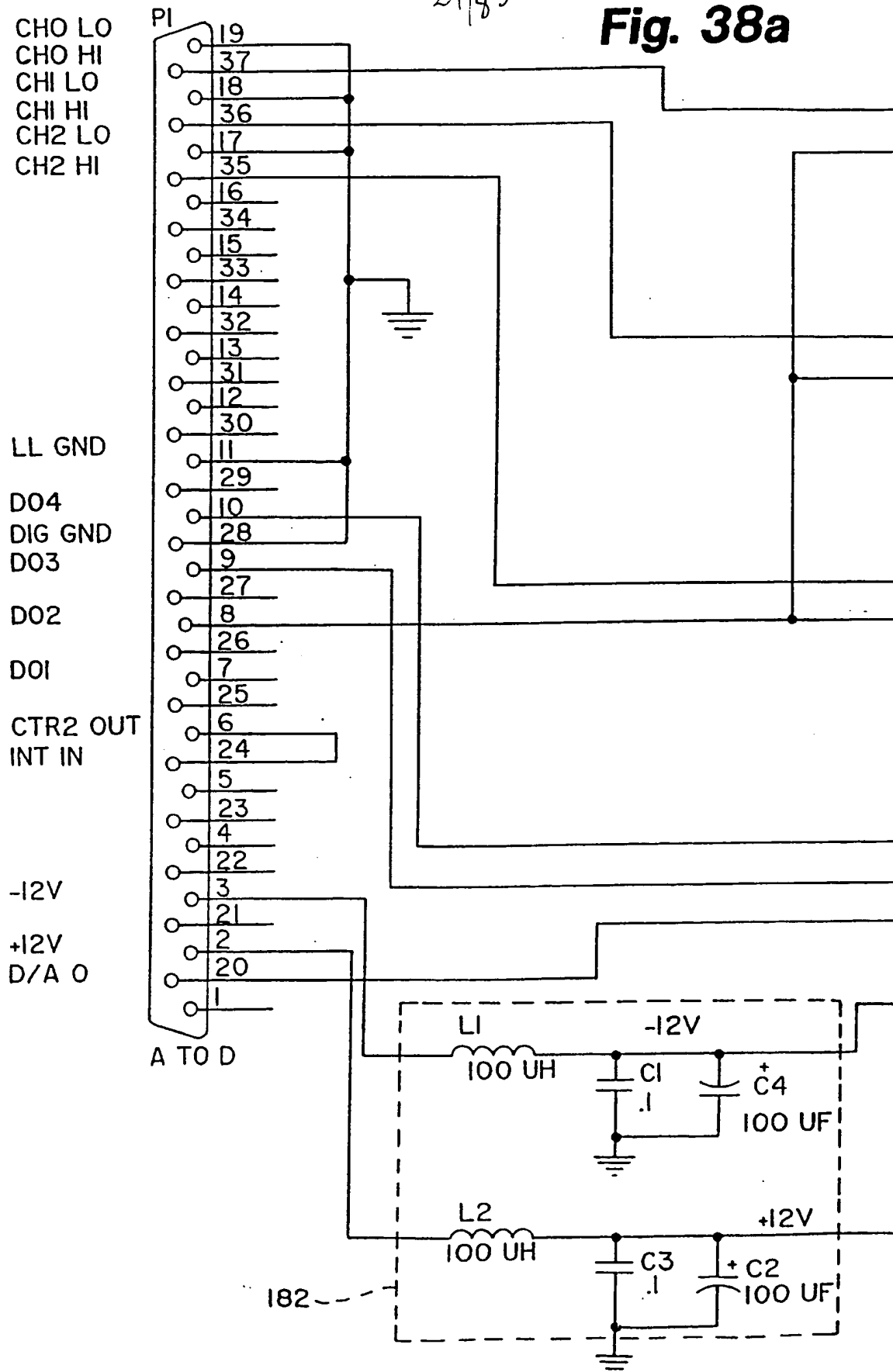


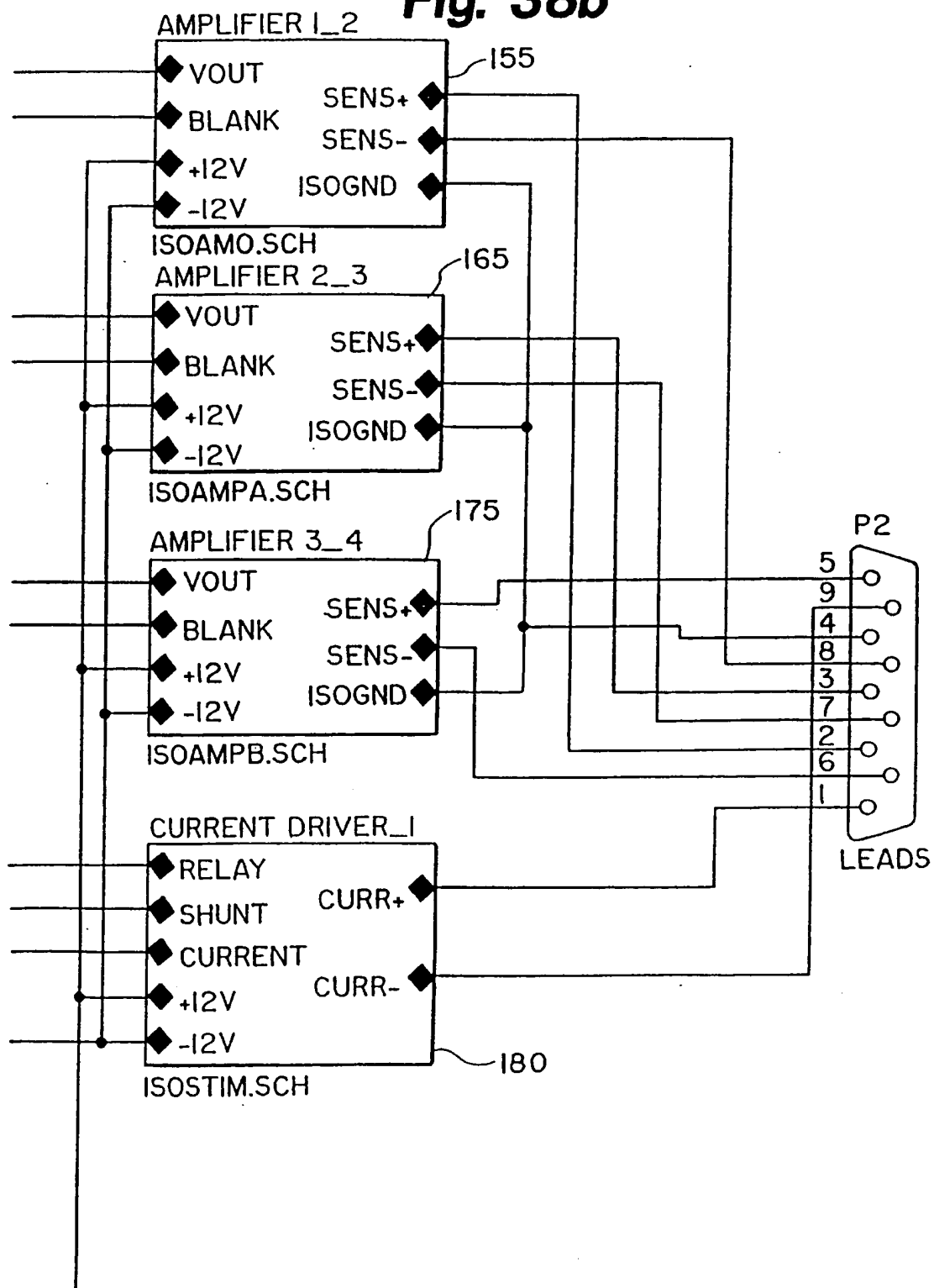
Fig. 38



24/95

Fig. 38a

95/85

Fig. 38b

26/85

Fig. 39

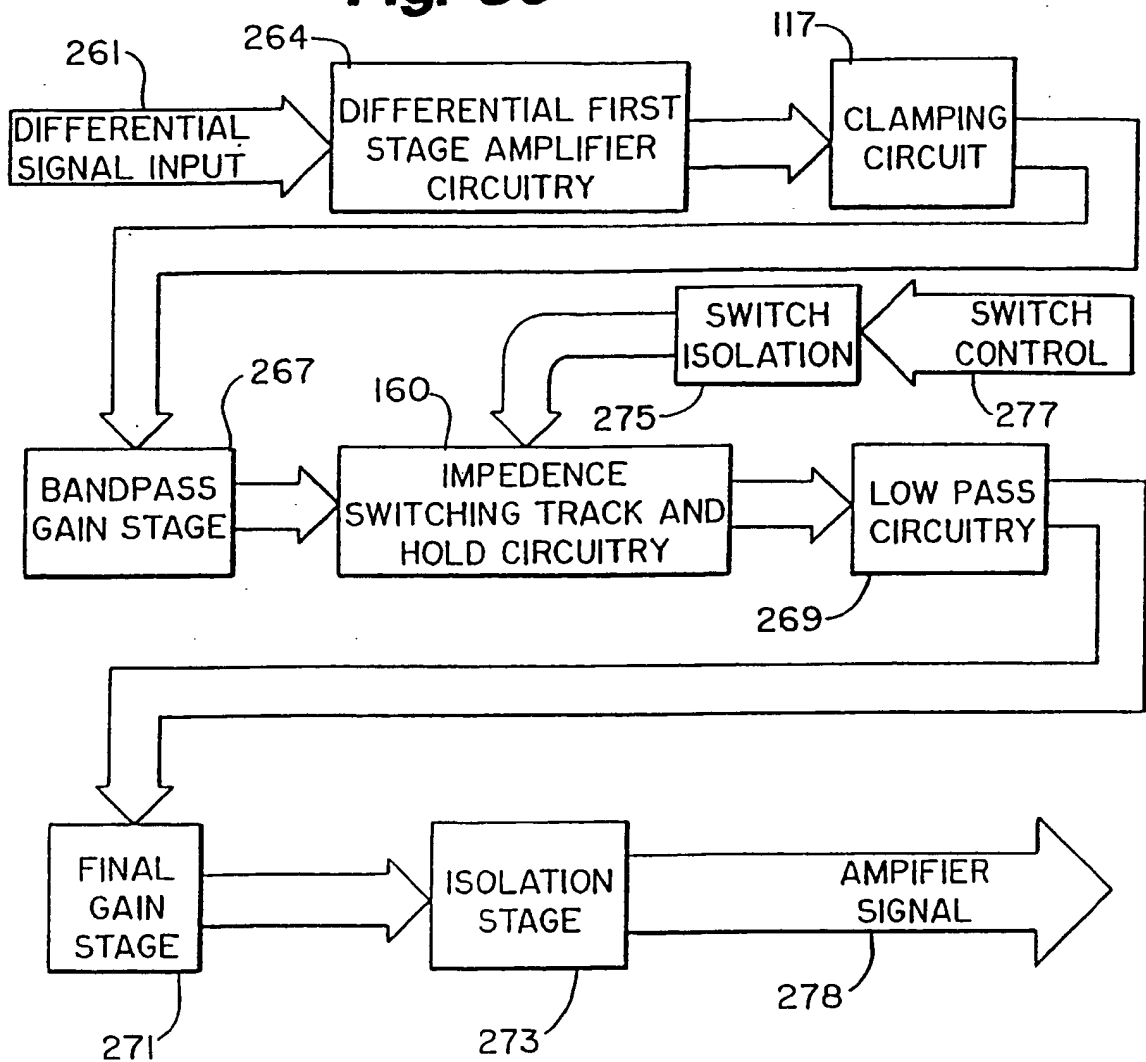


Fig. 40

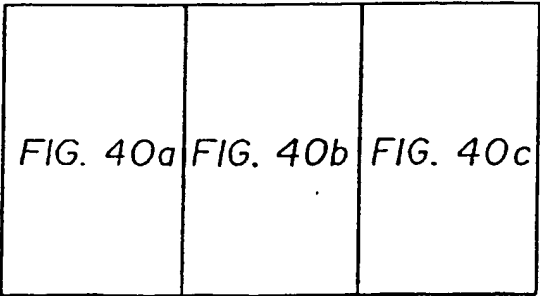


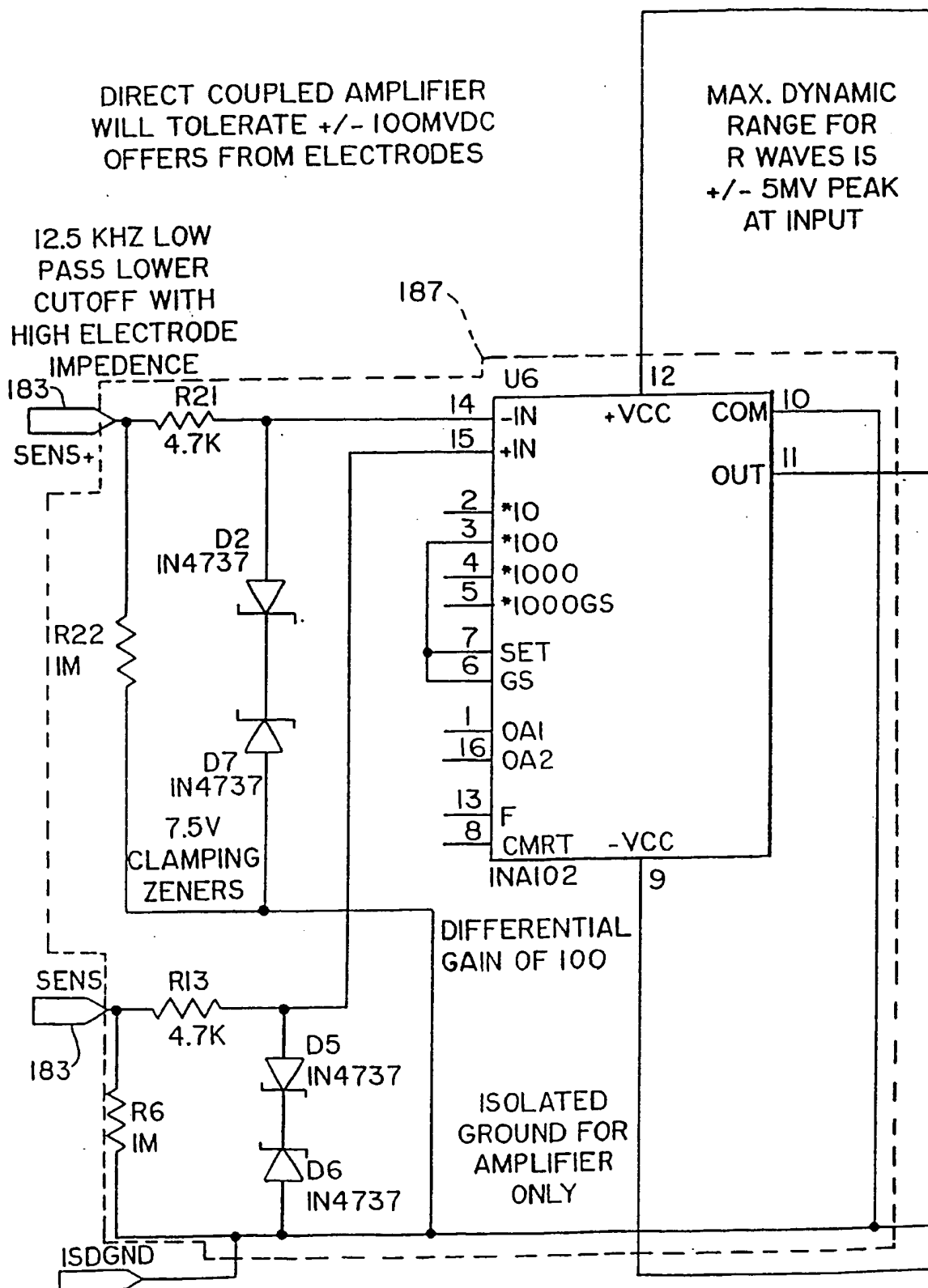
Fig. 40a

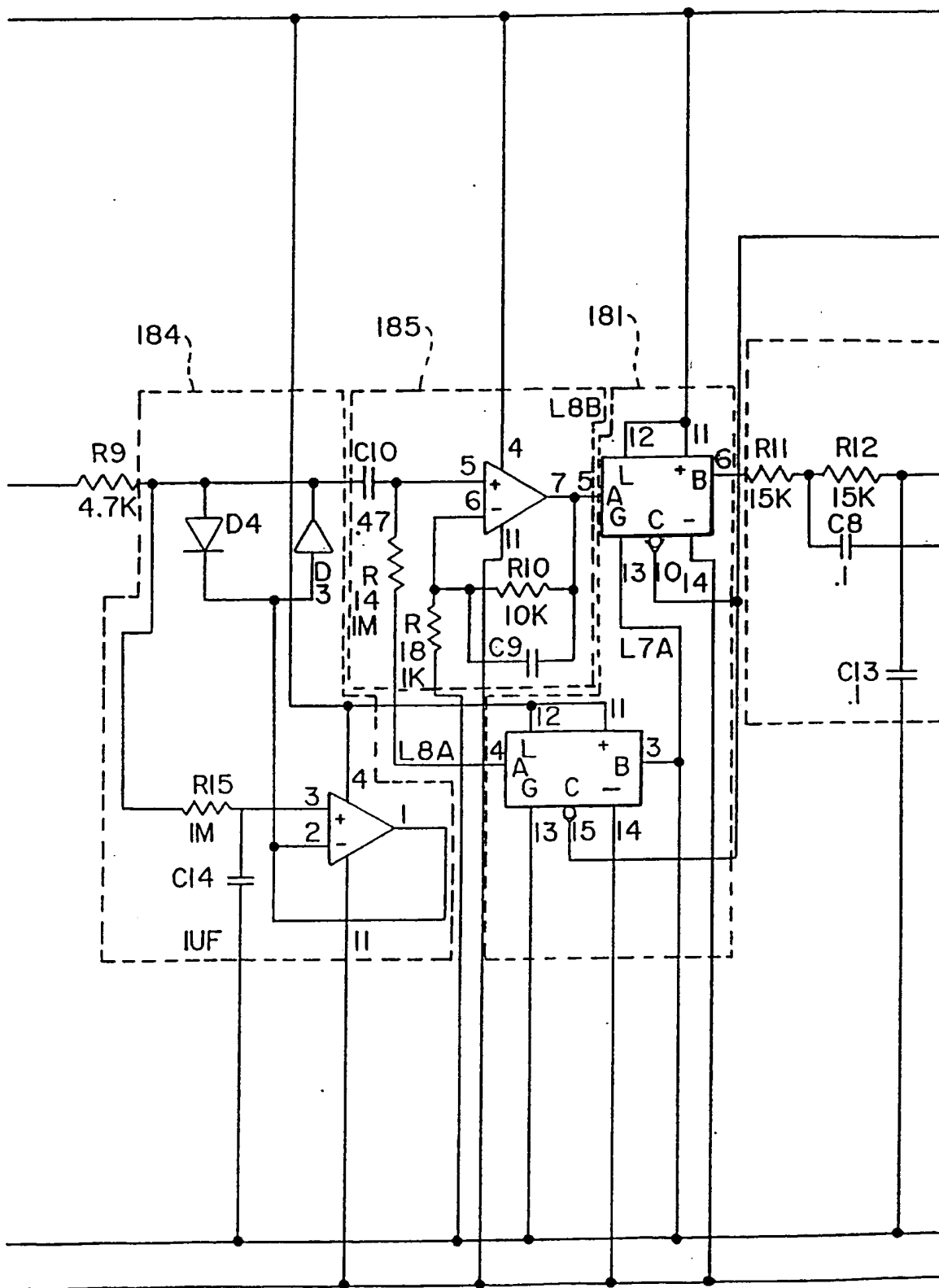
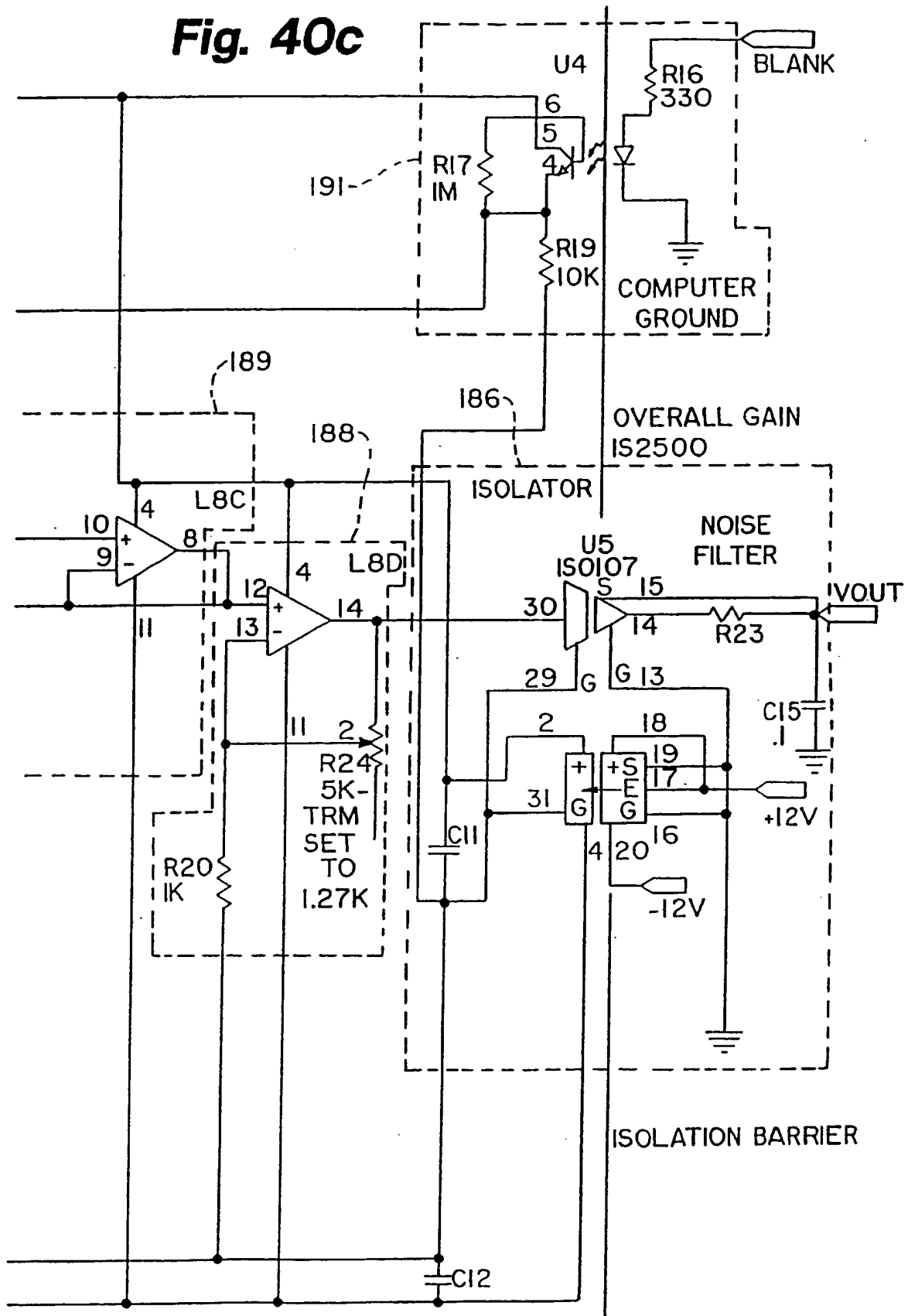
Fig. 40b

Fig. 40c

30/85

Fig. 41

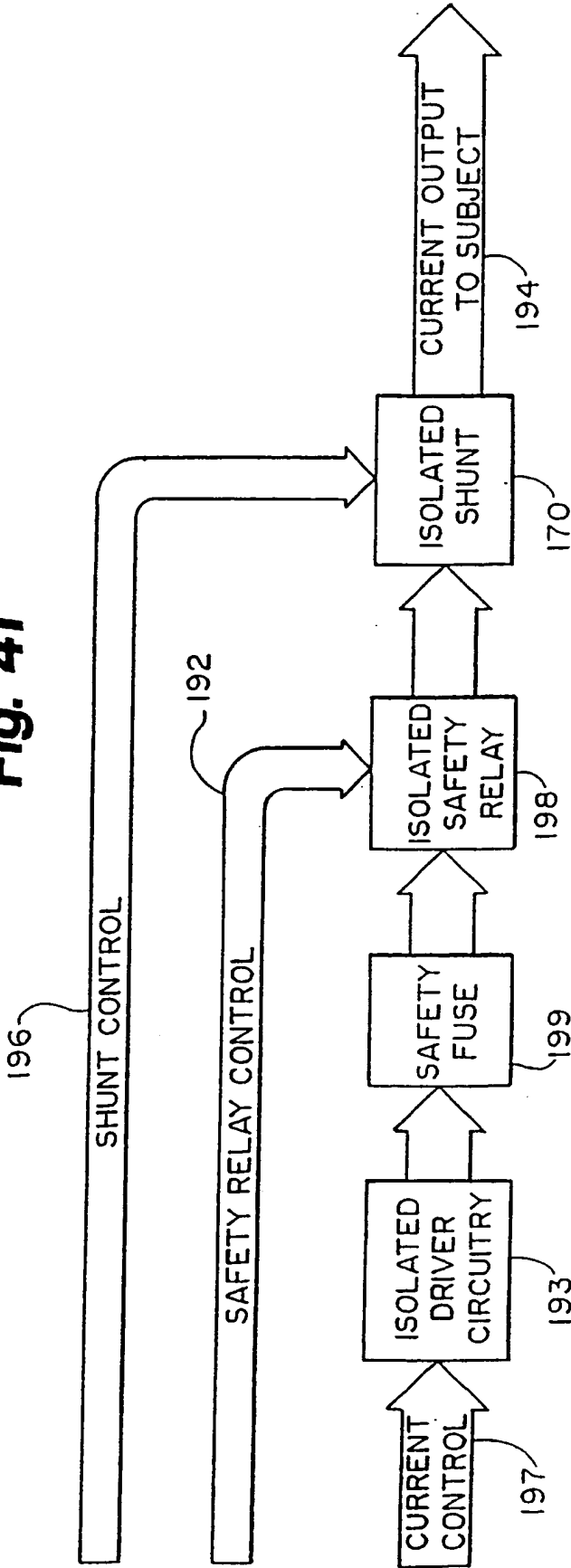
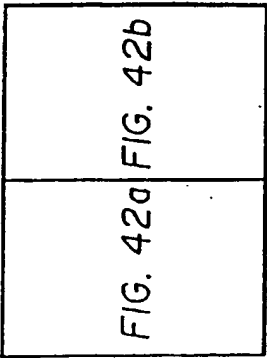
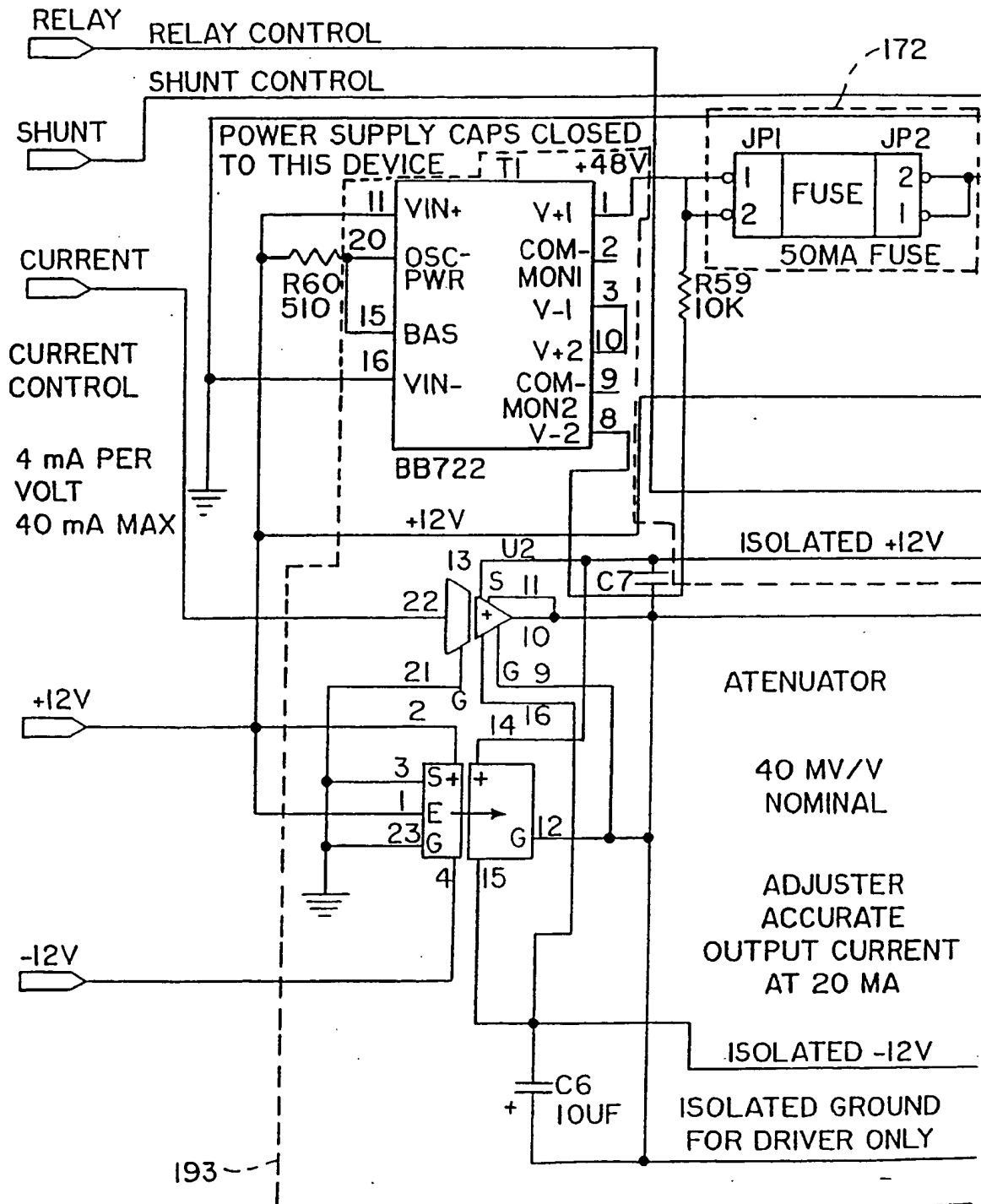


Fig. 42



31/85

Fig. 42a



32/85

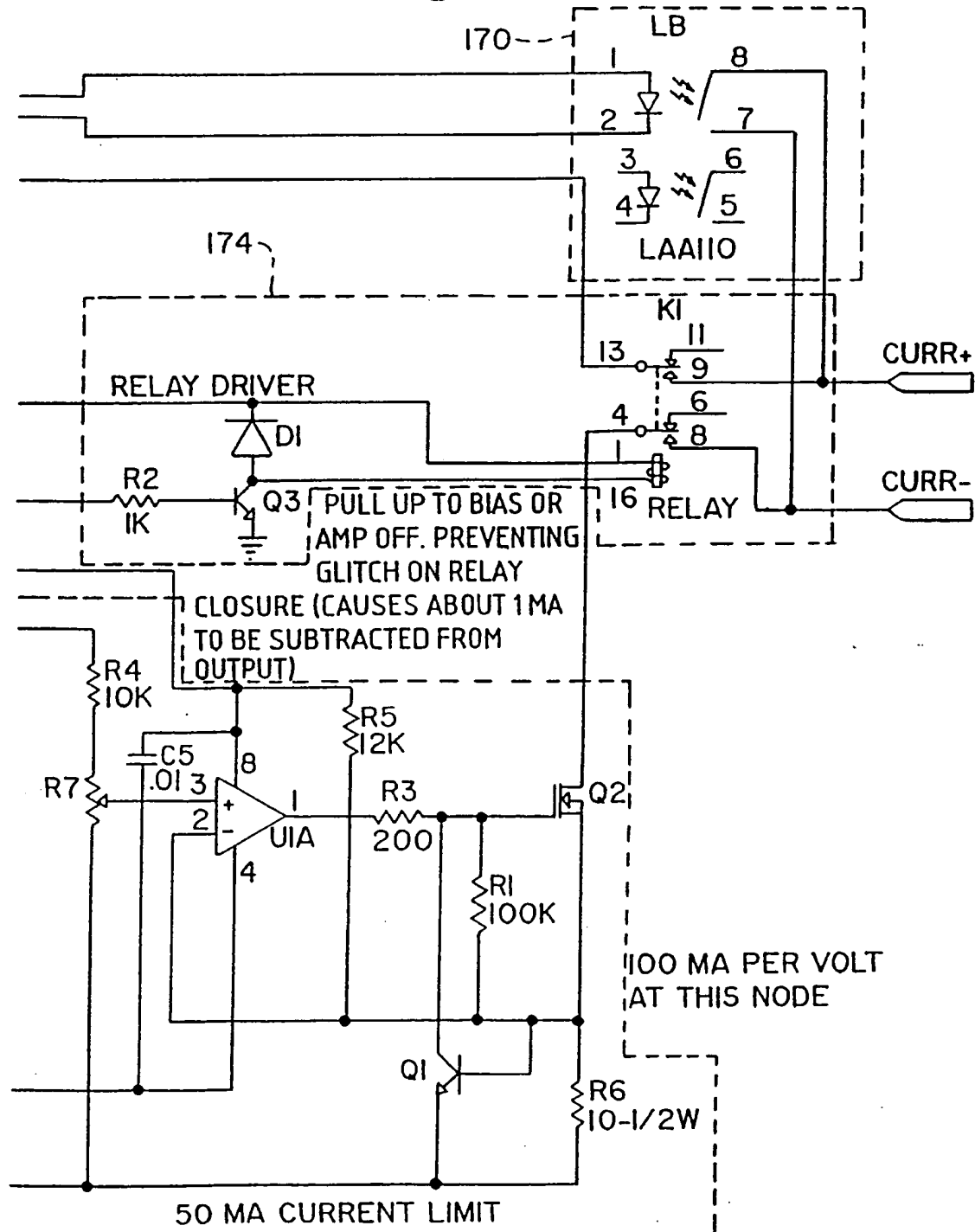
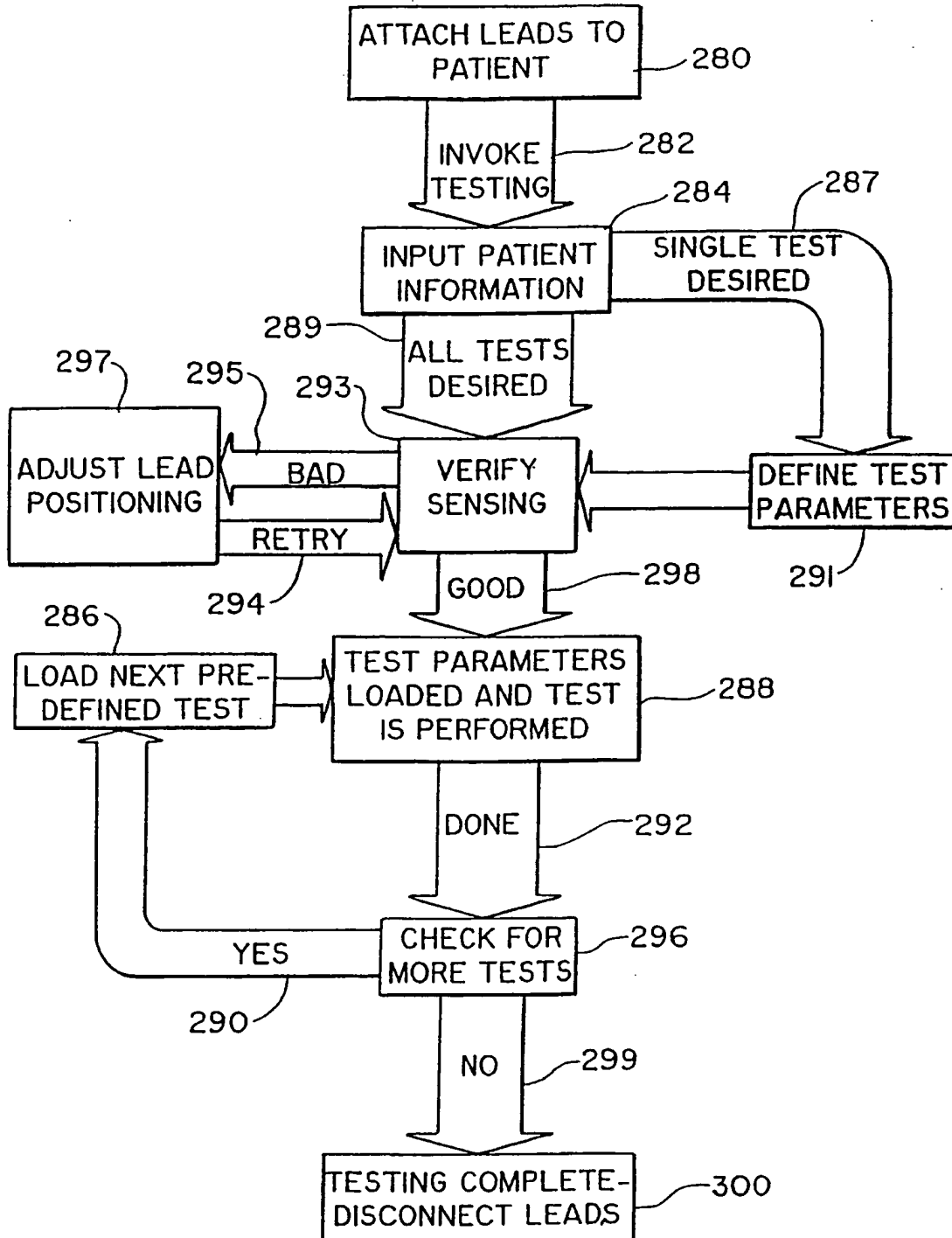
Fig. 42b

Fig. 43

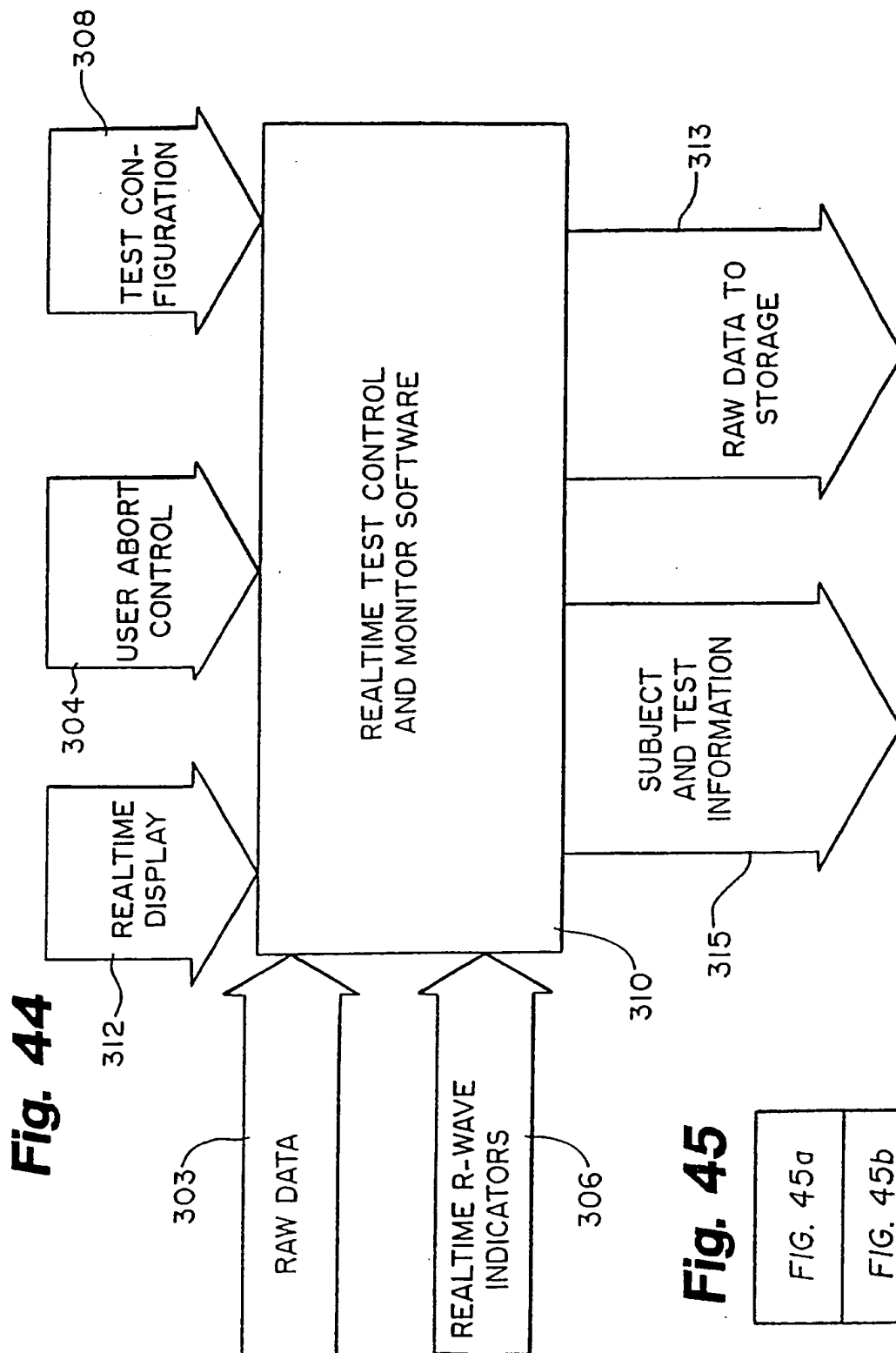
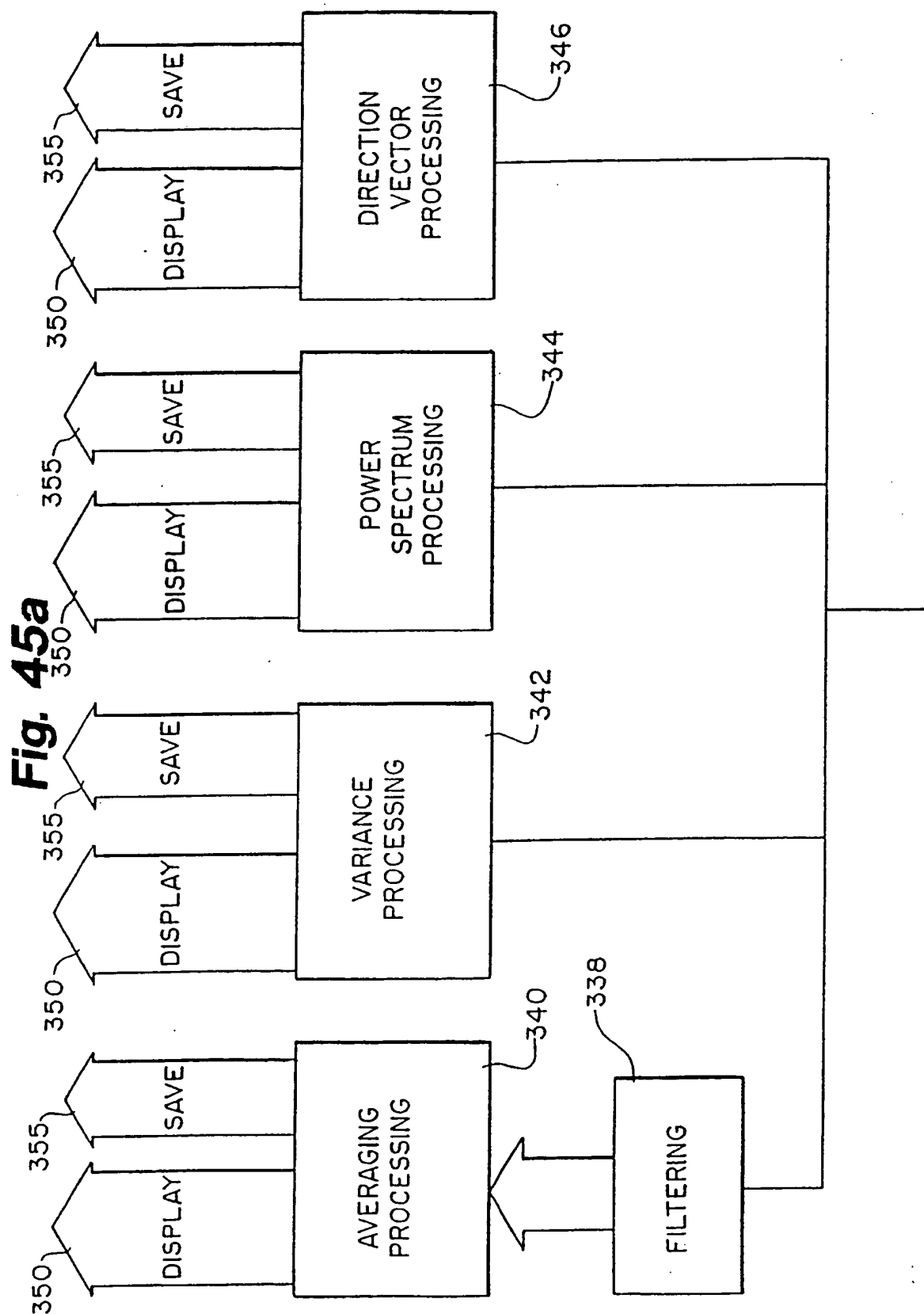


Fig. 45

FIG. 45a
FIG. 45b



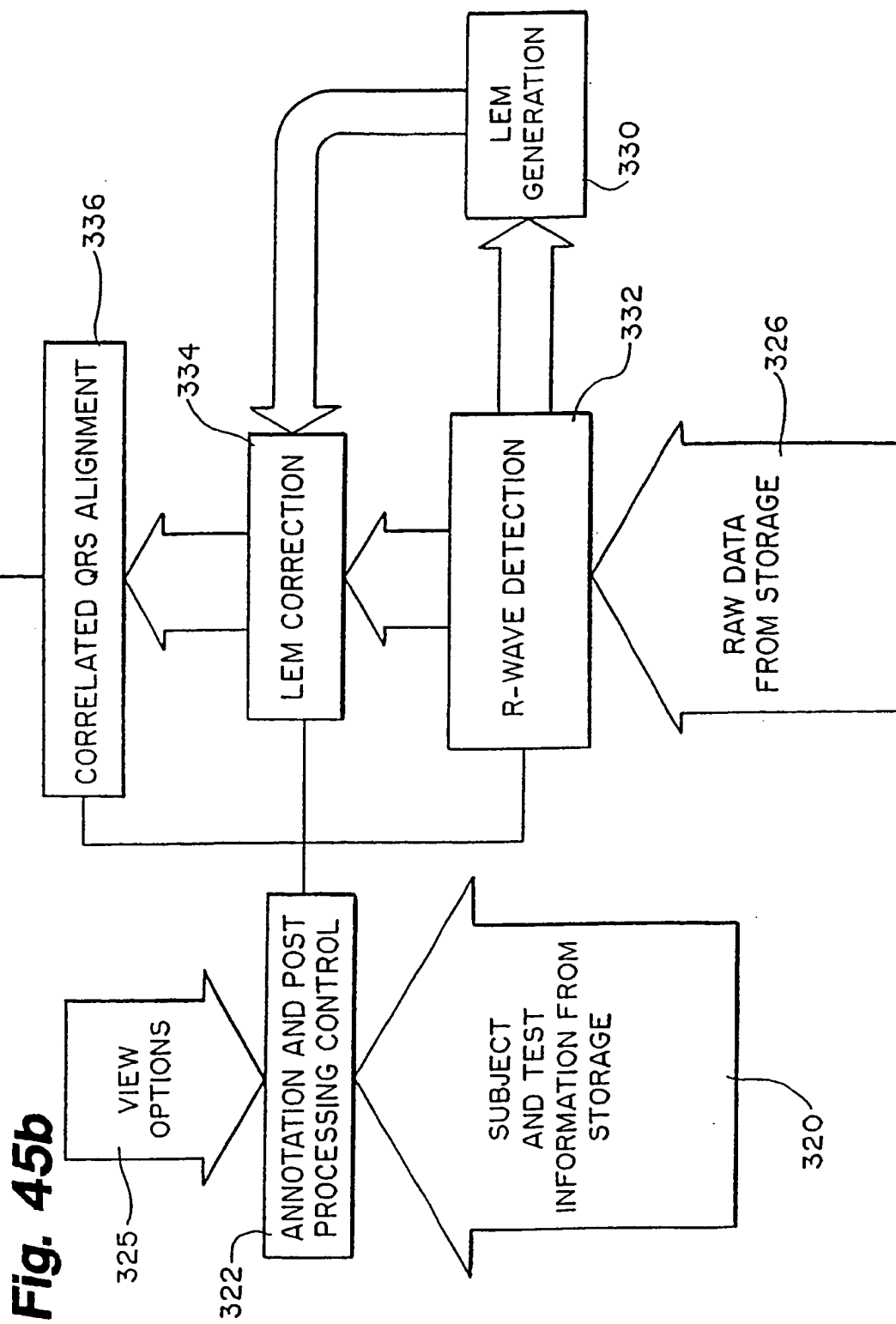
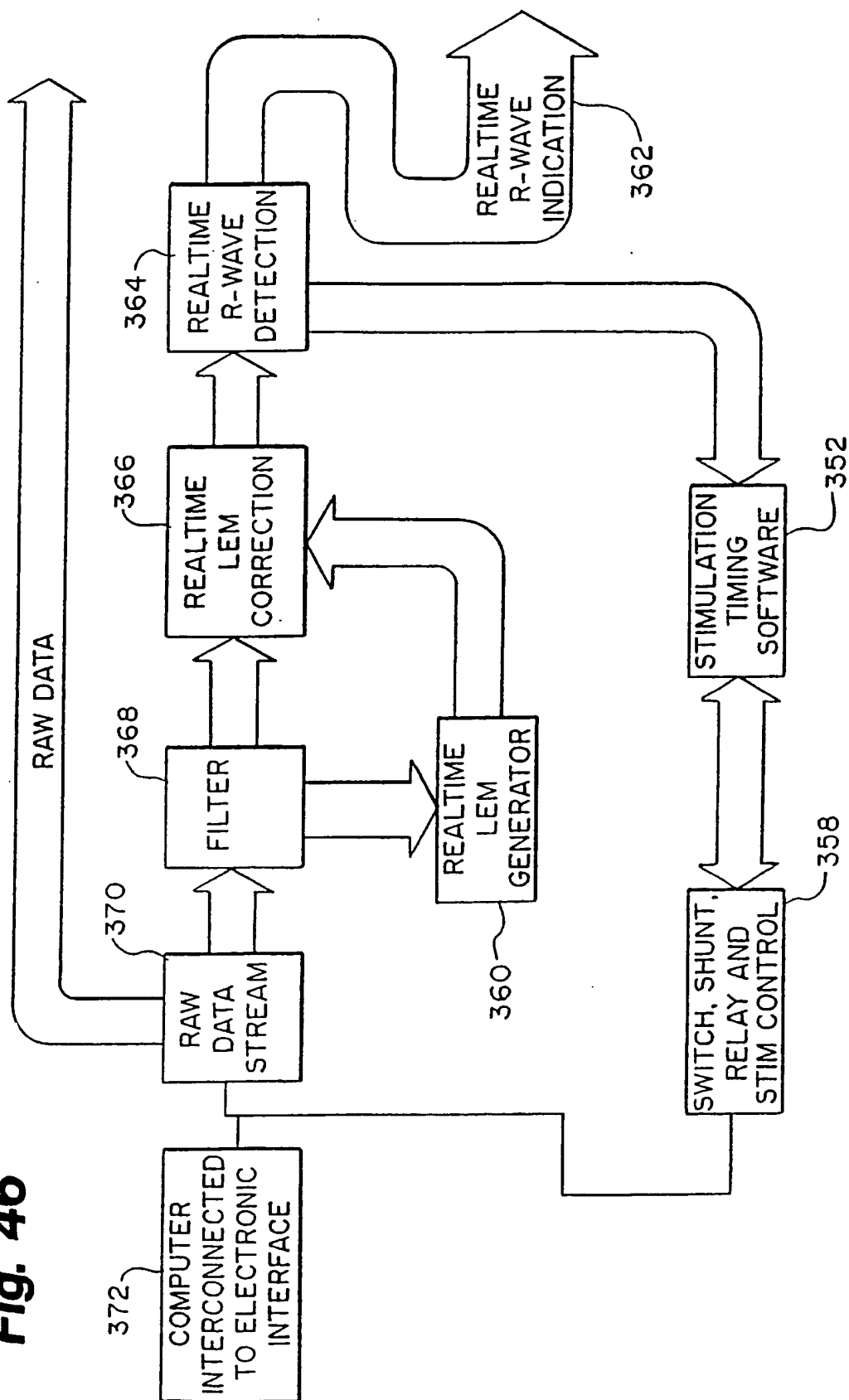


Fig. 46



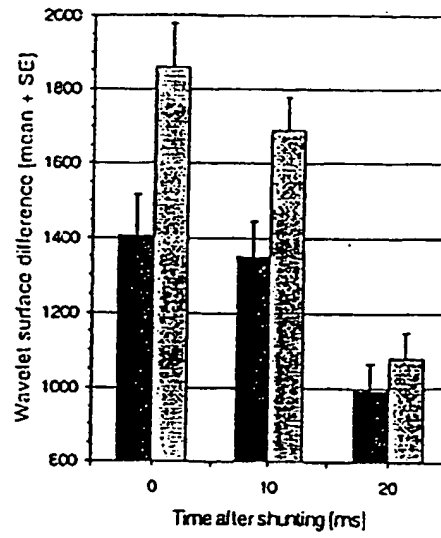


Fig. 47

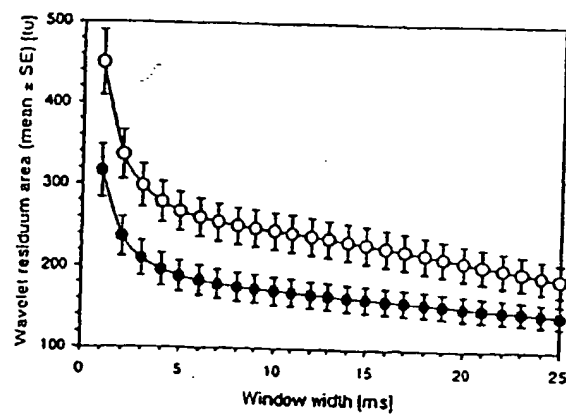


Fig. 48

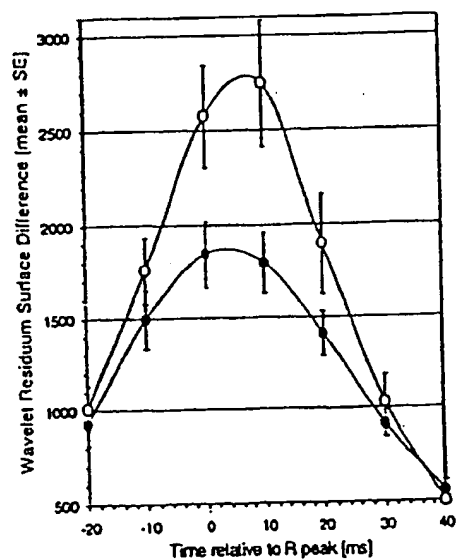


Fig. 49

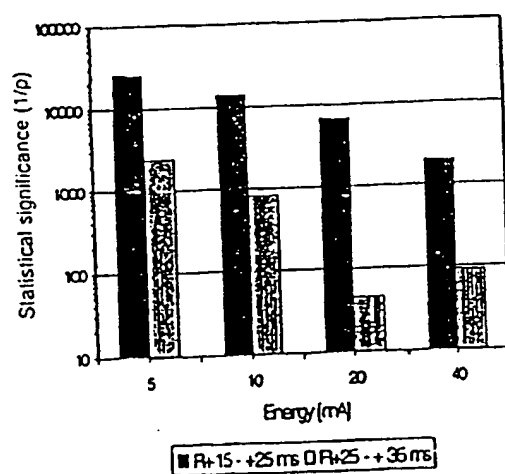


Fig. 50

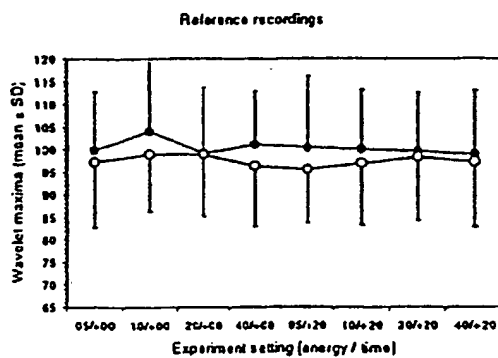


Fig. 51

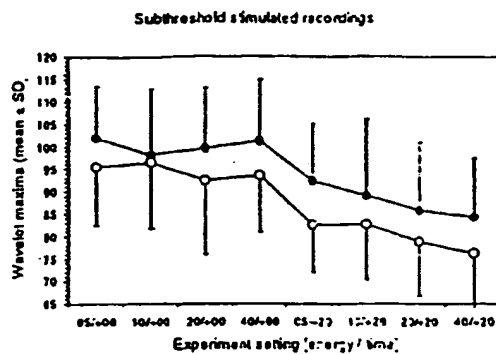


Fig. 52

4/1/85

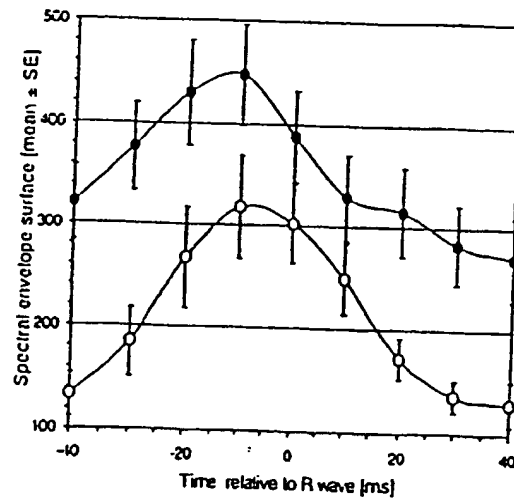


Fig. 53

Table 2
Interdependence of time-domain and wavelet decomposition indices

		IQRS	LAS	RMS	WCL	WMC	WSA	WRL
			r	r	r	r	r	r
IQRS			0.632	-0.683	0.540	0.454	0.457	-0.418
LAS	p <	10^{-3}		-0.880	0.308	0.296	0.208	-0.302
RMS	p <	10^{-3}	10^{-3}		-0.276	-0.267	-0.209	0.277
WCL	p <	10^{-3}	10^{-3}	10^{-3}		0.886	0.686	-0.826
WMC	p <	10^{-3}	10^{-3}	10^{-3}	10^{-3}		0.629	-0.733
WSA	p <	10^{-3}	10^{-3}	10^{-3}	10^{-3}	10^{-3}		-0.520
WRL	p <	10^{-3}	10^{-3}	10^{-3}	10^{-3}	10^{-3}	10^{-3}	

Table presents correlation coefficient between individual time-domain and wavelet analysis indices. The values of correlation coefficient are shown above the diagonal, the corresponding p-values are displayed below.

Fig. 54

43/85

Table 3
Comparison of Signal-averaged ECG Indices
in Patients With and Without Follow-up Events

EVENT	INDEX	PATIENTS		p ^{***}
		Event positive	Event negative	
Cardiac mortality	tQRS	101.25±26.54	96.77±29.22	0.21
	RMS ₄₀	18.50±15.08	15.98±12.64	0.60
	LAS	55.56±75.05	63.57±85.06	0.32
	WCL	155.66±29.45	146.13±22.42	7.48×10 ⁻³
	WMC	244.91±67.00	223.50±56.51	1.03×10 ⁻²
	WSA	4654.2±663.62	4398.2±607.51	6.13×10 ⁻³
	WRL	0.691±0.0822	0.730±0.084	1.79×10 ⁻²
Potentially arrhythmic death	tQRS	99.00±26.74	96.95±29.18	0.56
	RMS ₄₀	20.95±16.27	15.93±12.61	0.28
	LAS	62.33±90.04	63.14±84.30	0.48
	WCL	158.10±34.34	146.23±22.31	2.64×10 ⁻²
	WMC	248.29±76.48	223.81±56.29	3.69×10 ⁻²
	WSA	4642.6±767.24	4404.0±605.16	8.42×10 ⁻²
	WRL	0.690±0.085	0.729±0.0841	4.34×10 ⁻²
Sudden cardiac death	tQRS	98.05±27.91	96.99±29.13	0.88
	RMS ₄₀	22.23±16.52	15.91±12.60	0.15
	LAS	64.11±94.39	63.07±84.16	0.45
	WCL	158.95±35.85	146.25±22.28	3.72×10 ⁻²
	WMC	248.68±79.86	223.88±56.23	6.13×10 ⁻²
	WSA	4615.4±785.53	4405.9±605.55	0.16
	WRL	0.690±0.087	0.729±0.084	5.42×10 ⁻³
Ventricular tachycardia	tQRS	117.84±37.10	96.29±28.49	1.74×10 ⁻³
	RMS ₄₀	10.36±9.38	16.33±12.86	1.83×10 ⁻²
	LAS	124.74±151.13	60.90±80.27	4.29×10 ⁻³
	WCL	175.74±45.02	145.65±21.08	3.84×10 ⁻³
	WMC	291.53±98.23	222.35±53.86	2.85×10 ⁻⁵
	WSA	4783.8±1092.2	4399.9±585.3	3.47×10 ⁻²
	WRL	0.660±0.087	0.730±0.083	1.10×10 ⁻¹
Arrhythmic events	tQRS	97.71±25.48	97.00±29.25	0.62
	RMS ₄₀	19.98±15.64	15.95±12.63	0.35
	LAS	59.79±84.52	63.26±84.53	0.52
	WCL	156.29±32.81	146.25±22.35	3.43×10 ⁻²
	WMC	245.88±72.50	223.78±56.41	2.92×10 ⁻²
	WSA	4616.1±751.7	4403.9±605.2	8.44×10 ⁻²
	WRL	0.700±0.089	0.729±0.084	0.10
Arrhythmic fatalities	tQRS	96.77±26.38	97.04±29.20	0.91
	RMS ₄₀	21.00±15.89	15.92±12.62	0.21
	LAS	61.09±88.07	63.19±84.38	0.49
	WCL	156.86±34.08	146.26±22.32	4.80×10 ⁻²
	WMC	246.00±75.24	223.85±56.35	4.80×10 ⁻²
	WSA	4590.2±765.54	4405.7±605.6	0.16
	WRL	0.701±0.091	0.729±0.084	0.13

Fig. 55

44/85

Table 4
Association of Positive SAECG Findings with Follow-up Events

EVENT	CRITERION														
	TD ⁺			TD			WA _{all}			WA _{simplest}			WA _{simplest2}		
	tp	tn	p=	tp	tn	p=	tp	tn	p=	tp	tn	p=	tp	tn	p=
CM	18	222	1.00	17	321	0.10	10	412	0.18	14	387	0.04	11	402	0.13
PAI	11	226	0.66	10	325	0.50	7	420	0.18	9	393	0.13	7	409	0.29
SCD	10	227	0.81	8	325	0.81	6	421	0.26	8	394	0.12	6	410	0.41
VT	15	232	0.06	13	330	0.01	11	426	4.2×10^{-4}	11	397	3.2×10^{-3}	11	415	9.7×10^{-4}
PAIC	13	225	0.83	11	323	0.52	8	418	0.20	10	391	0.10	8	407	0.22
ARF	12	226	0.83	9	323	0.83	7	419	0.28	9	392	0.14	7	408	0.31

Fig. 56

Table 5
Comparison of Positive Predictive Accuracy of Predicting Follow-up Events

EVENT	Sen [%]	PPA [%]		Discordance		p=
		TD	WD	TD+	WD+	
Cardiac mortality	25	10.53	25.00	15	59	2.55×10^{-3}
	40	9.56	13.54	37	77	2.27×10^{-4}
	50	8.37	11.69	61	112	1.30×10^{-4}
	60	8.26	11.41	59	109	1.41×10^{-4}
	75	7.12	10.91	38	155	5.74×10^{-18}
	80	6.28	10.88	15	232	3.64×10^{-31}
Potentially arrhythmic death	25	6.49	21.88	13	62	8.40×10^{-9}
	40	6.30	14.29	18	89	1.78×10^{-12}
	50	5.53	8.77	42	125	9.05×10^{-11}
	60	5.06	7.65	56	132	2.95×10^{-4}
	75	4.15	6.87	29	182	2.75×10^{-28}
	80	4.00	6.62	18	209	2.03×10^{-42}
Sudden cardiac death	25	6.49	20.00	9	61	1.28×10^{-18}
	40	4.71	8.51	34	129	3.15×10^{-14}
	50	4.71	7.90	47	124	3.38×10^{-9}
	60	4.40	7.38	53	154	1.29×10^{-12}
	75	3.63	6.83	20	201	8.61×10^{-39}
	80	3.57	5.84	8	276	6.30×10^{-71}
Ventricular tachycardia	25	21.74	31.25	15	22	0.32
	40	14.29	22.22	26	51	5.37×10^{-3}
	50	12.82	16.67	41	59	8.86×10^{-2}
	60	11.83	11.96	62	63	1.00
	75	7.96	9.46	63	91	2.92×10^{-2}
	80	6.52	8.67	60	117	2.20×10^{-5}
Arrhythmic event	25	6.43	21.88	7	111	3.38×10^{-25}
	40	6.15	10.64	33	116	5.92×10^{-12}
	50	6.03	9.40	61	115	5.71×10^{-5}
	60	5.51	9.40	48	153	5.72×10^{-14}
	75	4.66	7.66	29	180	8.20×10^{-21}
	80	4.55	7.20	18	212	3.24×10^{-43}
Arrhythmic fatalities	25	6.12	18.75	11	77	2.40×10^{-13}
	40	5.24	9.57	34	129	3.15×10^{-14}
	50	4.96	8.73	52	129	9.75×10^{-9}
	60	4.73	8.73	23	187	3.95×10^{-33}
	75	4.15	6.81	29	180	8.20×10^{-24}
	80	4.14	6.36	12	230	1.91×10^{-53}

Fig. 57

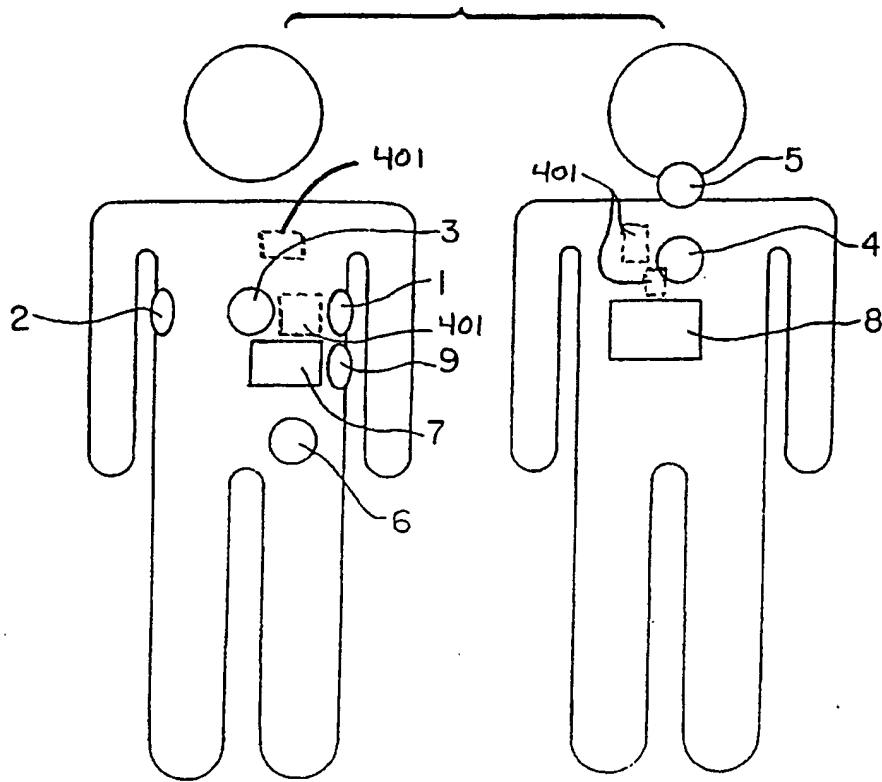


Fig. 58

47/85

Stamp	Subject	Reason
980930101037	EEL:1-552-388	3
981001101428	HCG:2-601-377	3
981001112933	JDB:5-225-099	3
981007094605	GFB:5-183-555	3
981007123334	AHL:3-788-070	3
981009110519	odv:2-177-526	3
981015140518	cmo:1768075-4	1
981015141116	cmo:1768075-4	1
981015141707	cmo:1768075-4	1
981015142252	cmo:1768075-4	1
981015143043	cmo:1768075-4	1
981015143642	cmo:1768075-4	1
981015150826	dea:1899945-0	3
981015161514	JMD:1413932-5	2
981015162049	JMD:1413932-5	2
981015162625	JMD:1413932-5	2
981015163211	JMD:1413932-5	2
981015164636	JMD:1413932-5	2
981022103401	GSA:4-025-353	3
981022120039	EOS:1-571-066	3
981022142532	GJZ:5-124-965	3
981026093649	JMO:1-205-859	3
981026105436	CRM:2-888-528	3
981026133306	Barron, Jesse j.:	3
981026152052	med:136-116-21	3
981028134601	can:185-88-683	3
981028150513	dee:158-4698-5	3
981106101803	LAK:2-597-563	3
981119103852	OE:	3
981119145005	HL:	1
981119150050	HL:	1
981119151053	HL:	1
981119152201	HL:	1
981119153404	HL:	1
981119154337	HL:	1
981119155621	HL:	1
981119160738	HL:	1
981119161901	HL:	1
981119162825	HL:	1
981119163910	HL:	1
981119165040	HL:	1
981125131046	OF:	1
981125131911	OF:	1
981127120552	BO:	1
981127121326	BO:	1
981127122124	BO:	1
981127122952	BO:	1
981127123753	BO:	1
981127124626	BO:	1
981127125510	BO:	1
981127130405	BO:	1
981127131256	BO:	1
981127132157	BO:	1
981127133053	BO:	1
981127133946	BO:	1

Fig. 59A

48/85

Stamp	Subject	Reason
981201134146	KE:	2
981201135133	KE:	2
981201135920	KE:	2
981201140710	KE:	2
981201141511	KE:	2
981201142346	KE:	2
981201143216	KE:	2
981201144058	KE:	2
981201144933	KE:	2
981201145810	KE:	2
981201150637	KE:	2
981201151515	KE:	2
981204121331	AJ:	2
981204122233	AJ:	2
981204123125	AJ:	2
981204124031	AJ:	2
981204124924	AJ:	2
981204125807	AJ:	2
981204130713	AJ:	2
981204131656	AJ:	2
981204132640	AJ:	2
981204133619	AJ:	2
981204134549	AJ:	2
981204135529	AJ:	2
981207082610	IV:	1
981207083302	IV:	1
981207083941	IV:	1
981207084616	IV:	1
981207085255	IV:	1
981207085945	IV:	1
981207090629	IV:	1
981207091309	IV:	1
981207092003	IV:	1
981207092659	IV:	1
981207093353	IV:	1
981207094041	IV:	1
981207142900	KH:	1
981207143336	KH:	1
981207143829	KH:	1
981207144324	KH:	1
981211102018	lgs:5-202-329	3
981211130958	wgn:5-275-563	2
981211131806	wgn:5-275-563	2
981211132618	wgn:5-275-563	2
981211133434	wgn:5-275-563	2
981211135037	wgn:5-275-563	2
981211135912	wgn:5-275-563	2
981217101203	mhh:2-769-149	3
981218141112	rwk:3-051-401	3
981229113055	GLH:2-968-205	3
981230100404	CrS:2-939-848	3
990114122754	KM:	3
990120131943	HE:	2
990120132838	HE:	2
990120133730	HE:	2

Fig. 59B

Stamp	Subject	Reason
990120134620	HE:	2
990120135456	HE:	2
990120140405	HE:	2
990120141317	HE:	2
990120142240	HE:	2
990120143148	HE:	2
990120144051	HE:	2
990120144944	HE:	2
990120145901	HE:	2
990121134832	DAL:181-530-82	2
990121135600	DAL:181-530-82	2
990121140325	DAL:181-530-82	2
990121141035	DAL:181-530-82	2
990121141906	DAL:181-530-82	2
990121142622	DAL:181-530-82	2
990121160243	DRM:193-057-07	2
990121161136	DRM:193-057-07	2
990121162231	DRM:193-057-07	2
990121163105	DRM:193-057-07	2
990121164300	DRM:193-057-07	2
990121164644	DRM:193-057-07	2
990121165641	DRM:193-057-07	2
990125104638	mdl:1-120-002	3
990126114501	rfd:3-523-621	3
990128120653	cel:2-150-607	3
990128144107	hja:5-288-070	3

Fig. 59C

50/85

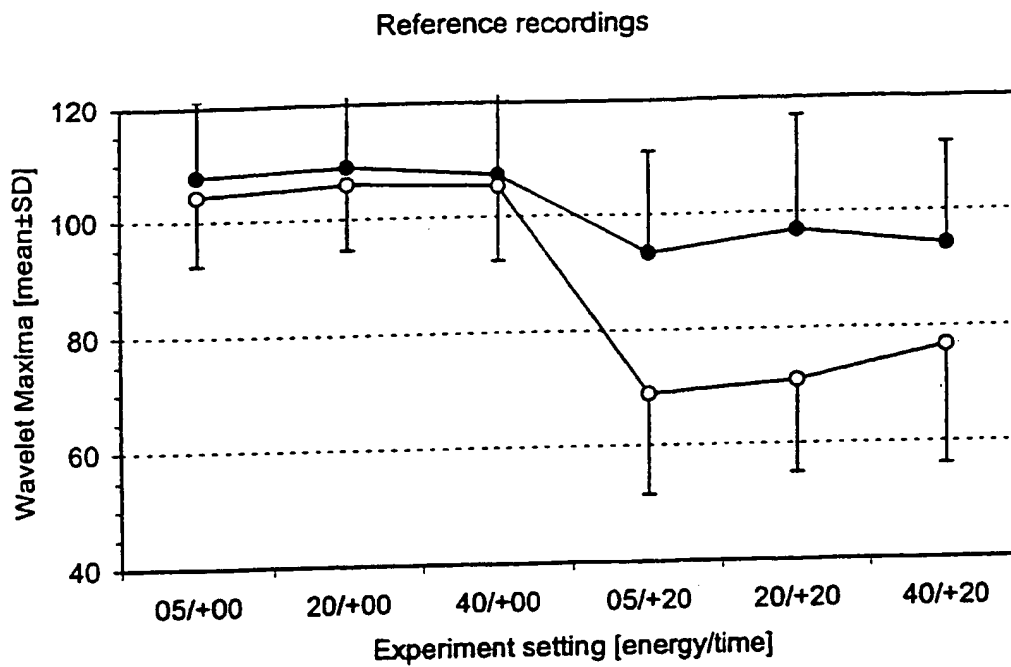


Fig. 60A

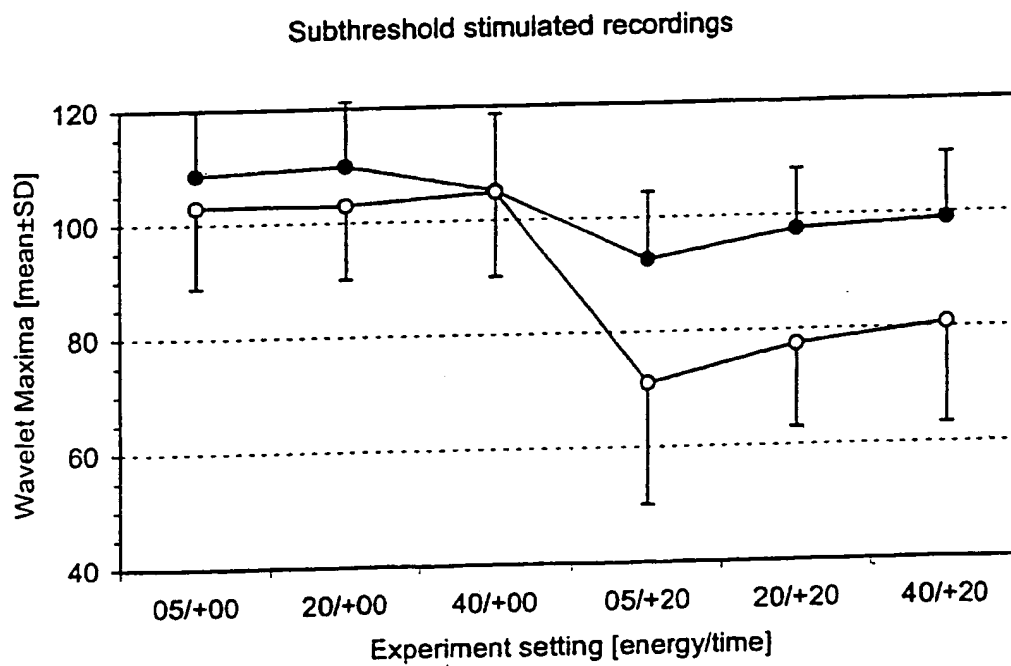


Fig. 60B

5/1/85

Stimulation 0 mA, position 0 ms

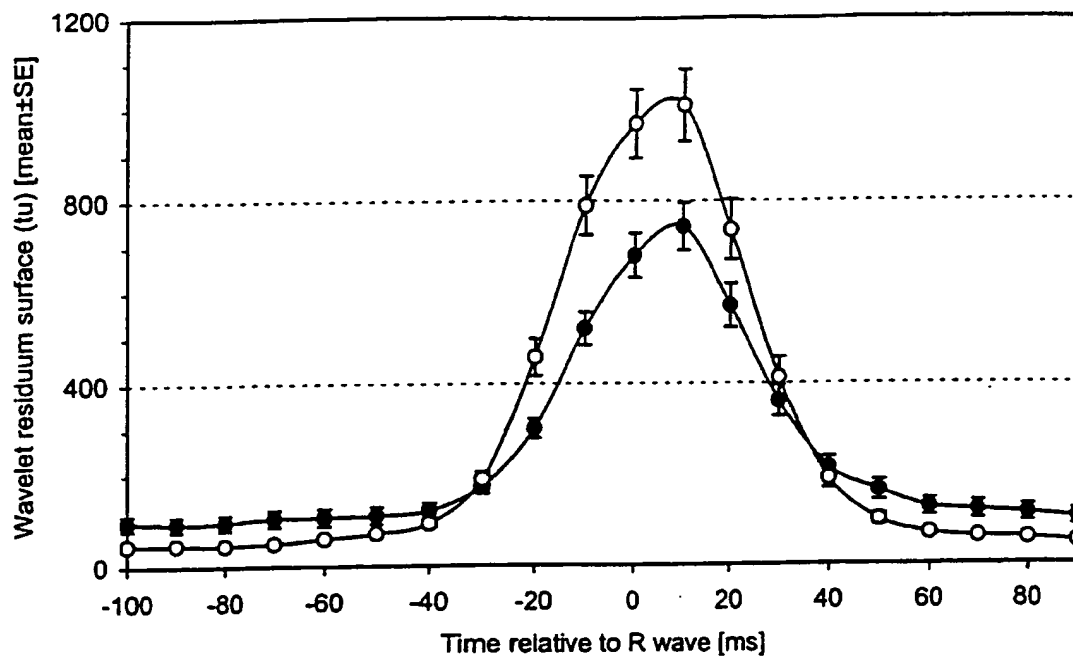


Fig. 61 A

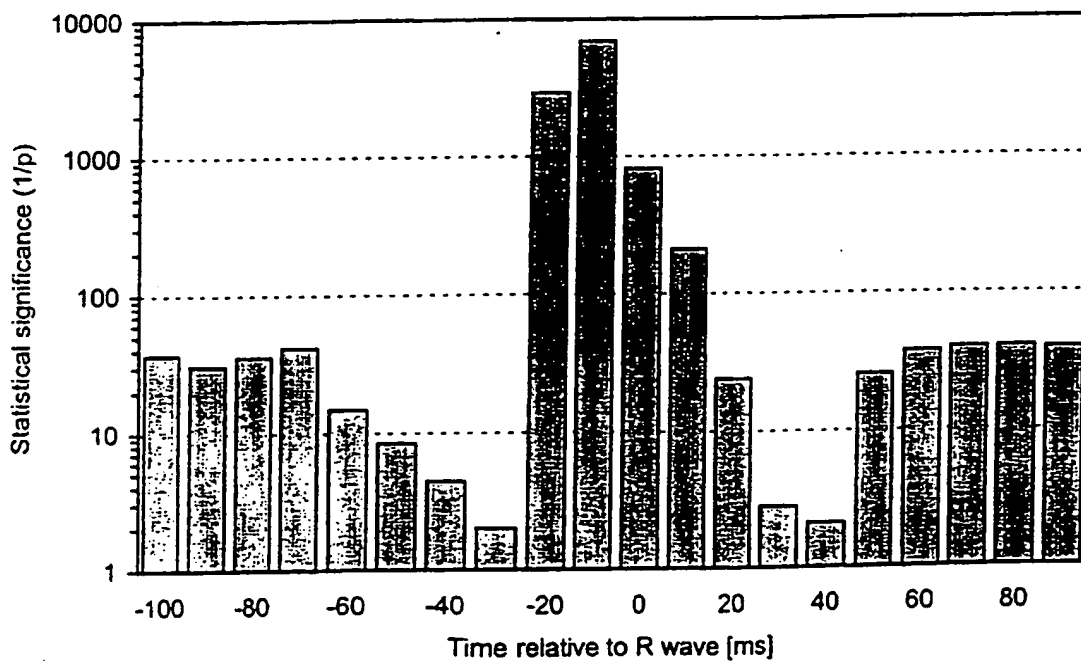


Fig. 61 B

Stimulation 5 mA, position 0 ms

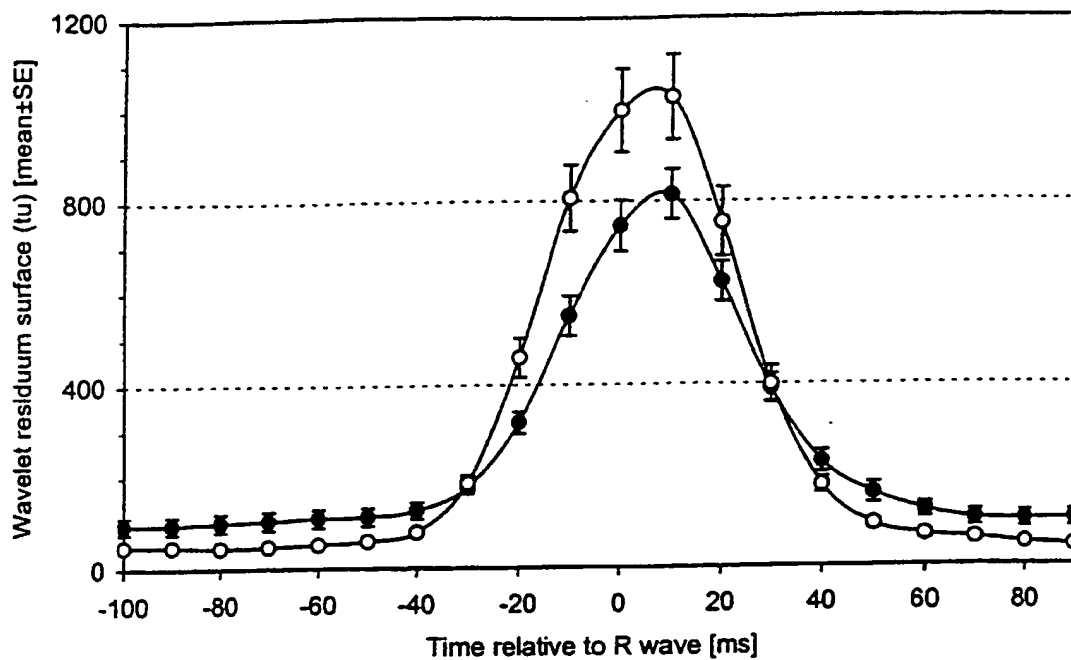


Fig. 62C

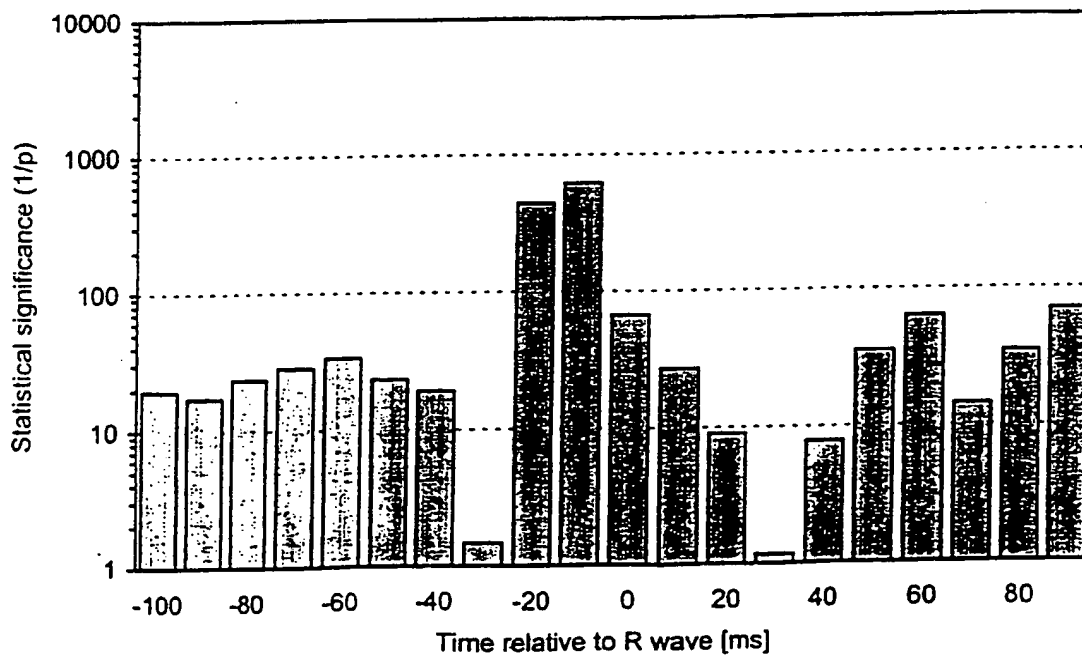


Fig. 62D

Stimulation 20 mA, position 0 ms

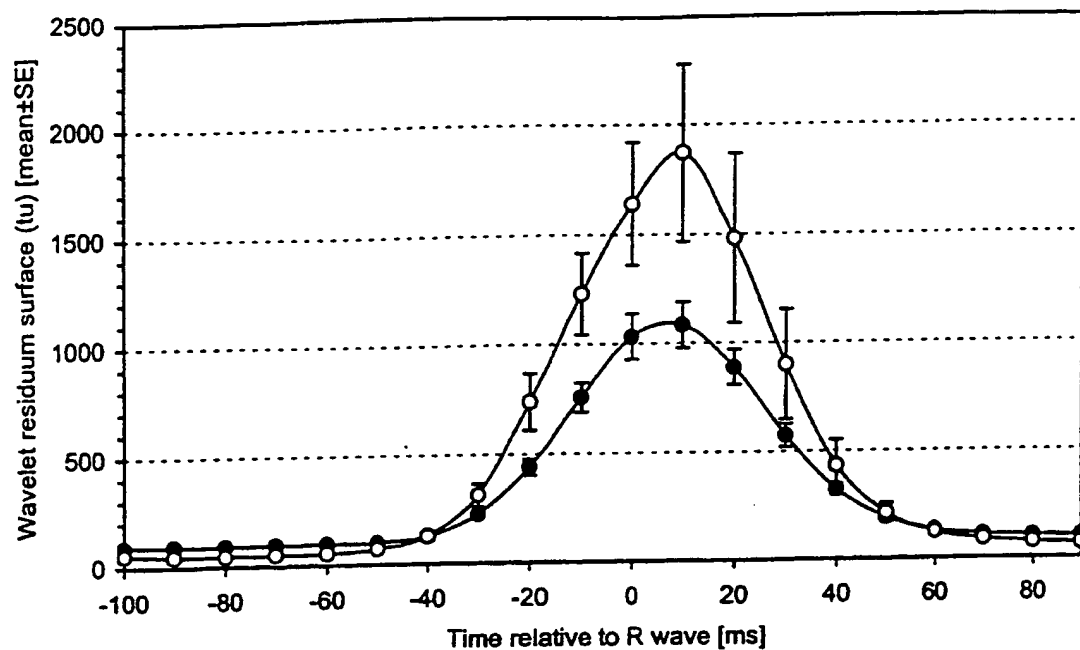


Fig. 62E

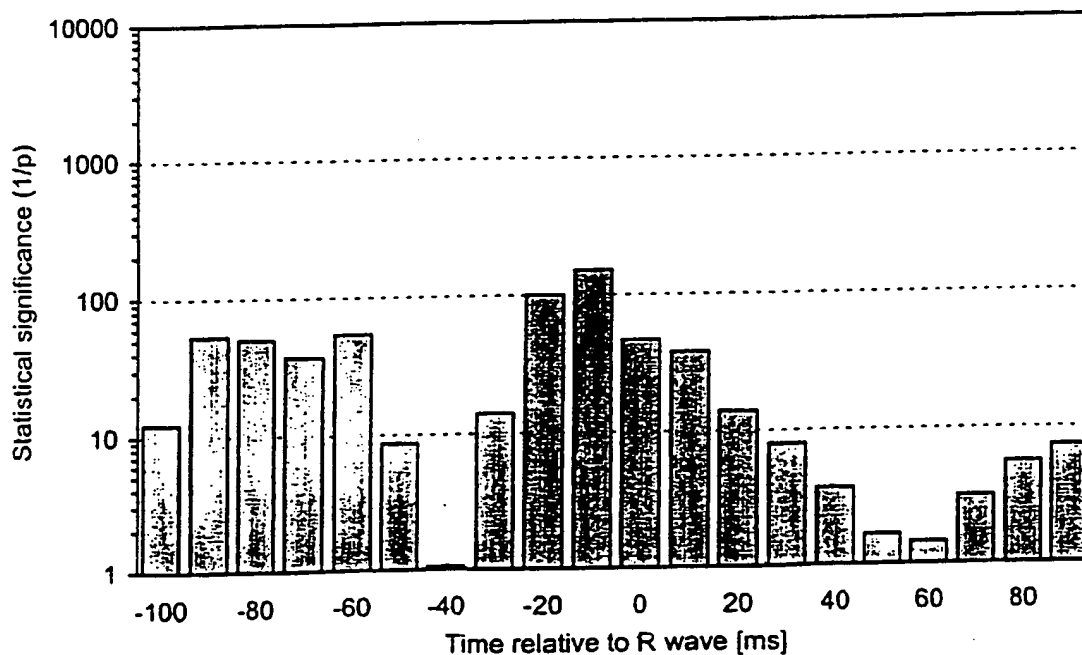


Fig. 62F

56/85

Stimulation position 0 ms after R wave

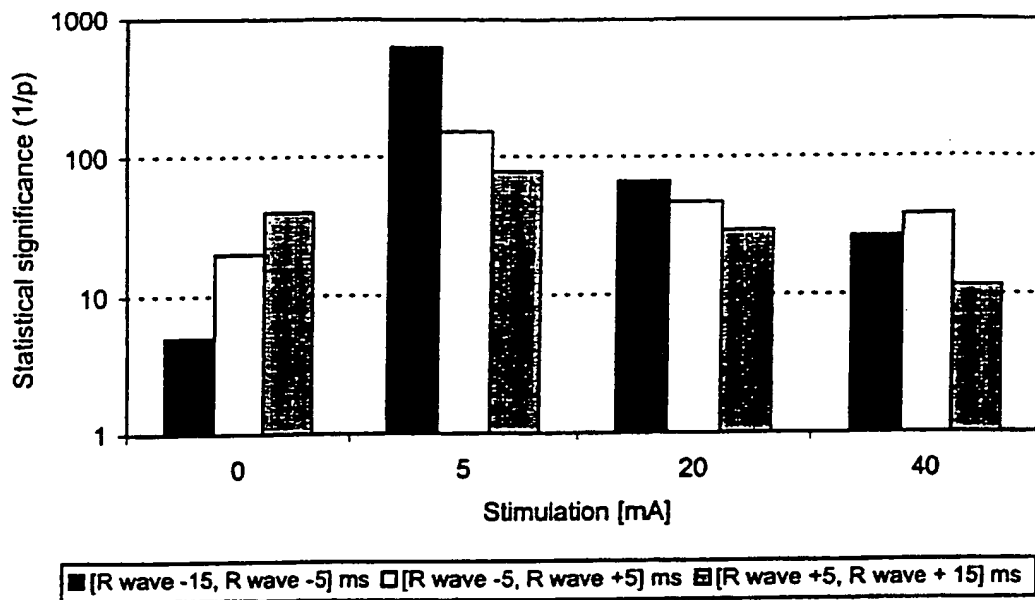


Fig. 63A

Stimulation position 20 ms after R wave

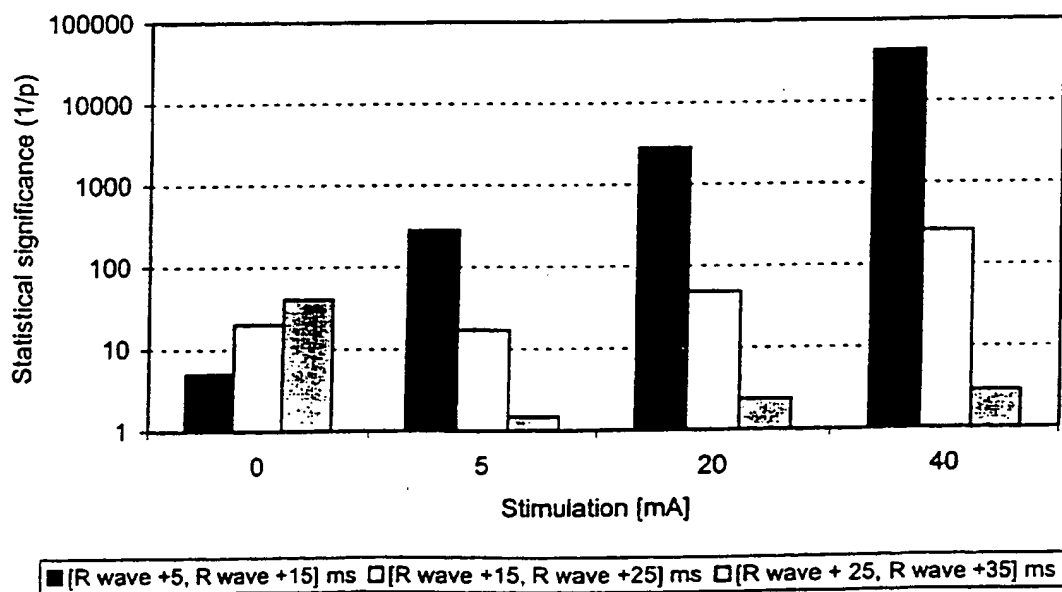


Fig. 63B

Comparison of windows symmetric around R wave
([R- α to R+ α])

Stimulation 0 mA, position 0 ms

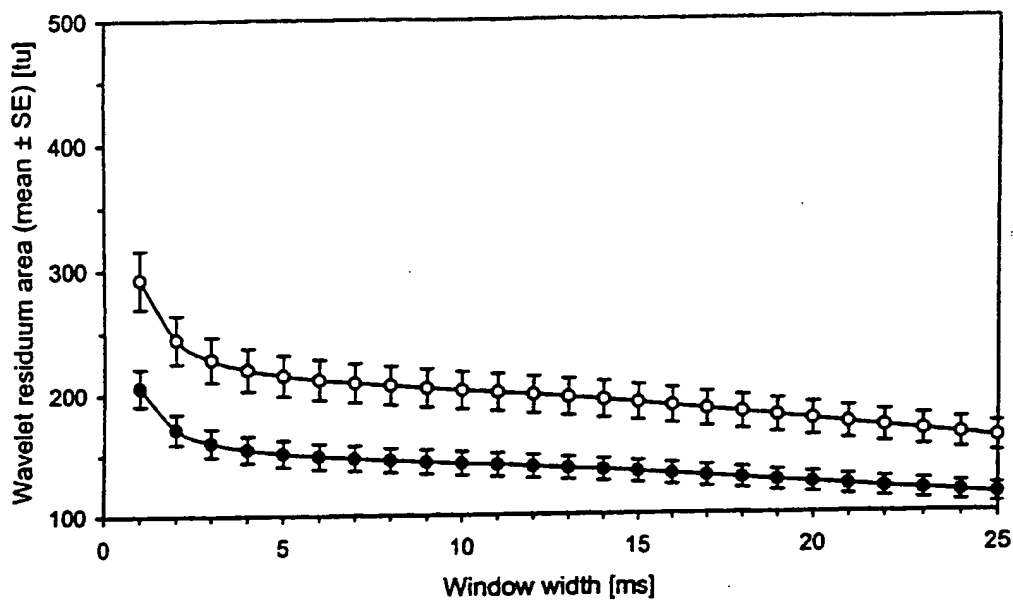


Fig. 64A

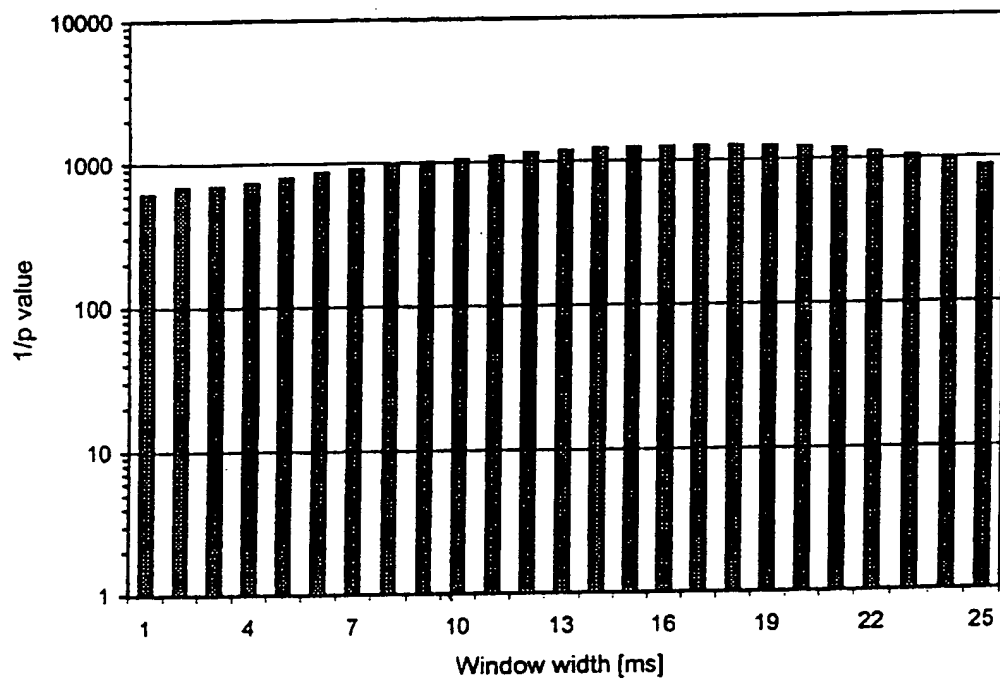


Fig. 64B

Comparison of windows symmetric around R wave
([R- α to R+ α])

Stimulation 5 mA, position 0 ms

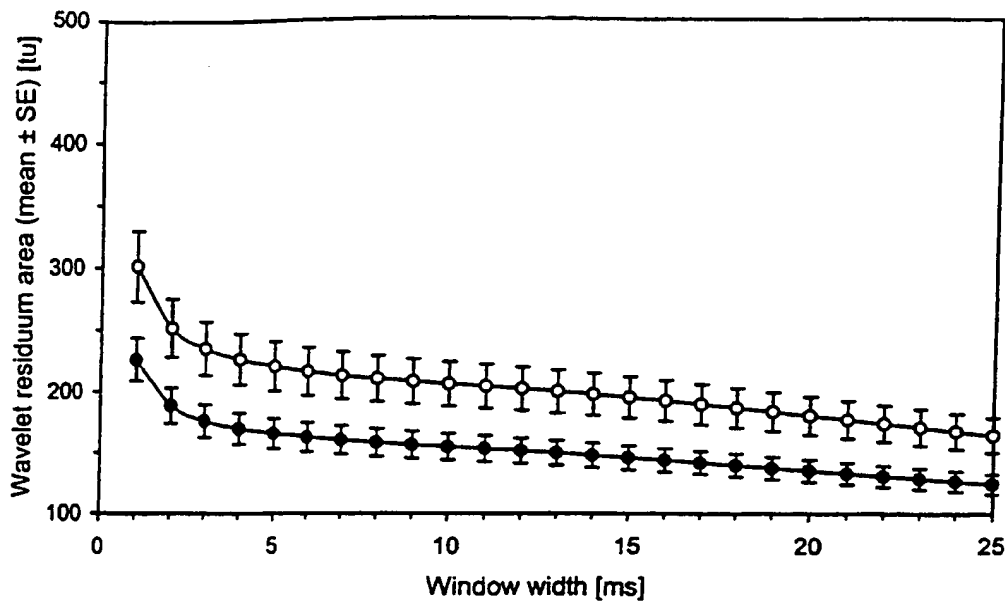


Fig. 64C

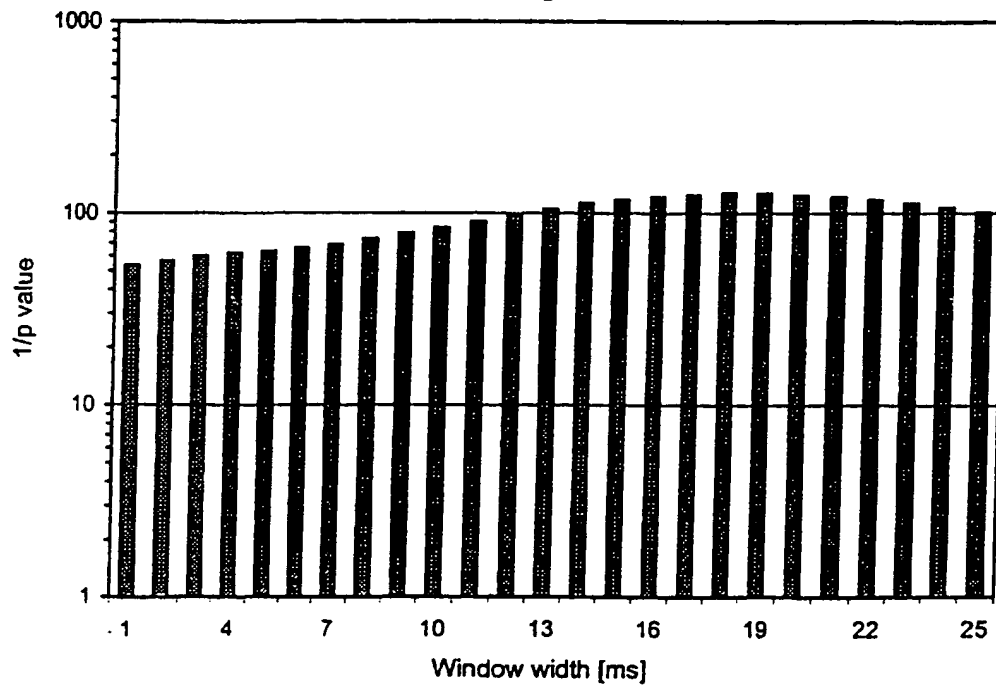


Fig. 64D

Comparison of windows symmetric around R wave
([R- α to R+ α])

Stimulation 20 mA, position 0 ms

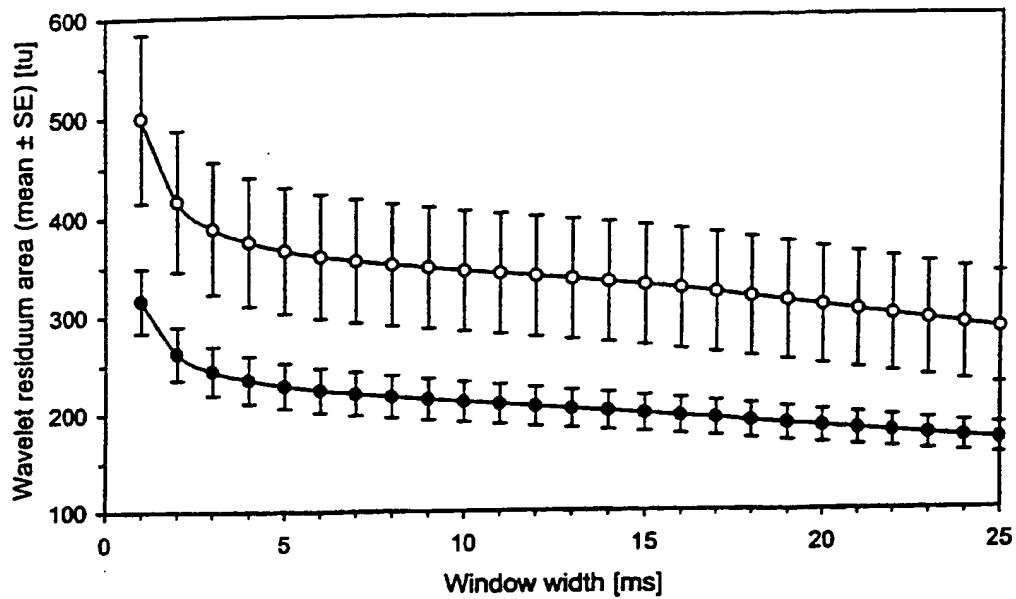


Fig. 64E

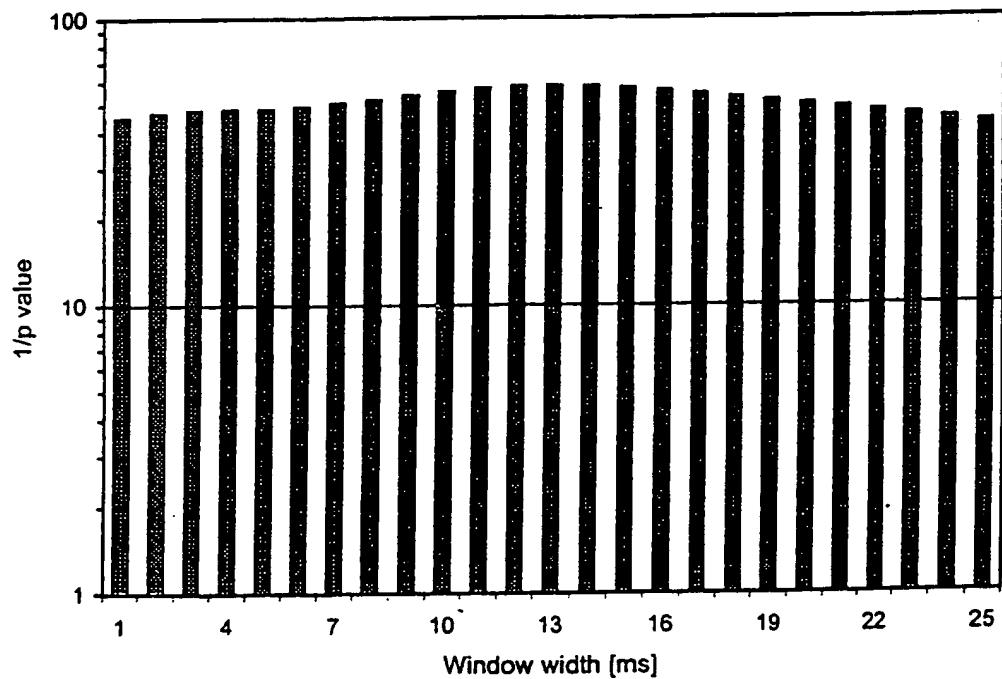


Fig. 64F

Comparison of asymmetric windows starting from the R wave ([R to R+ α])

Stimulation 0 mA, position 0 ms

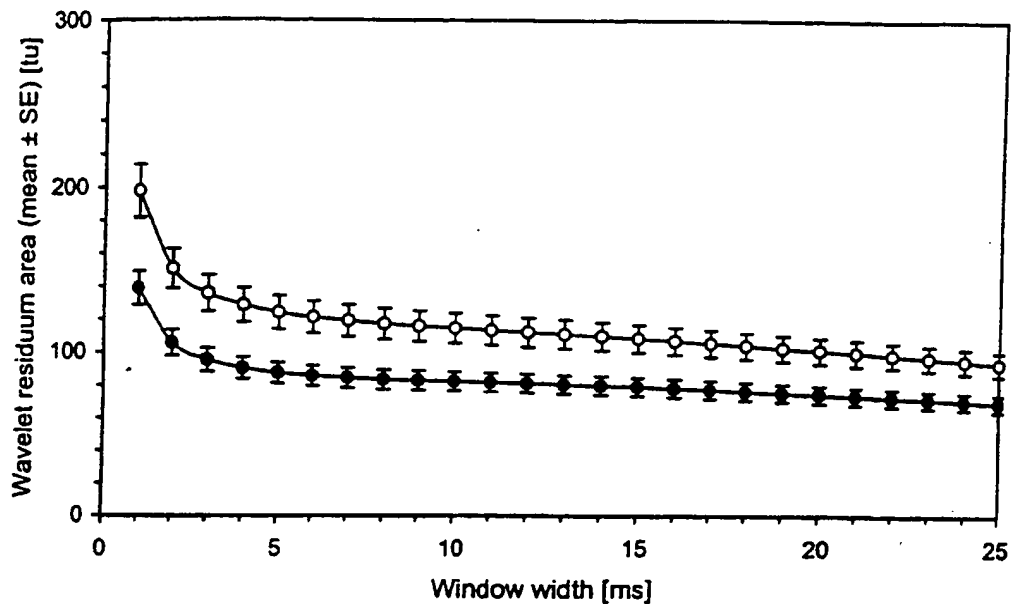


Fig. 65A

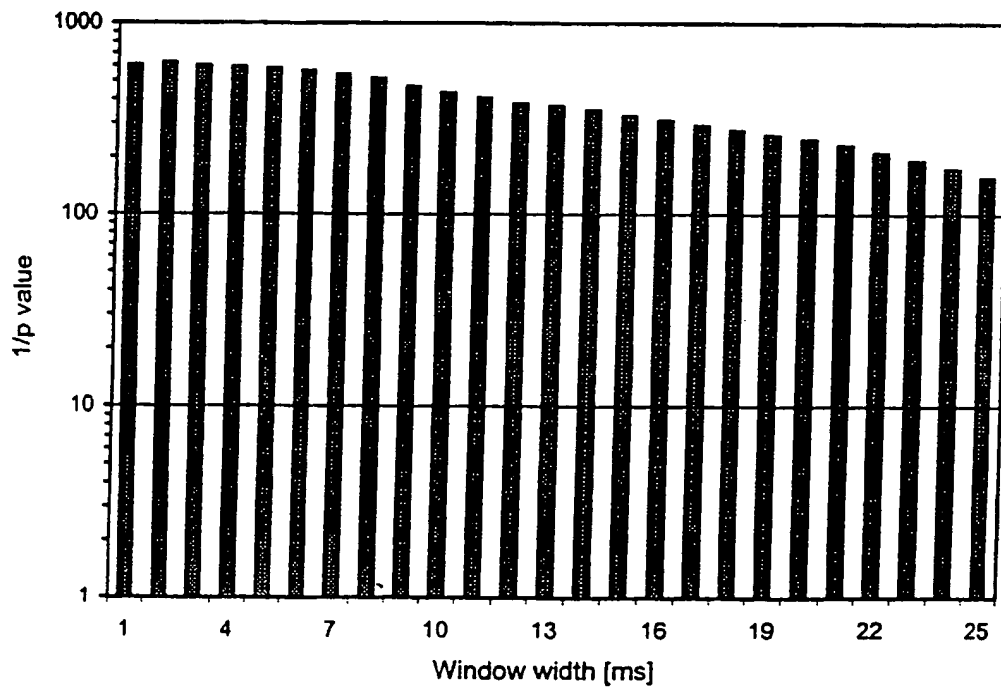


Fig. 65B

Comparison of asymmetric windows starting from the R wave
([R to R+ α])

Stimulation 5 mA, position 0 ms

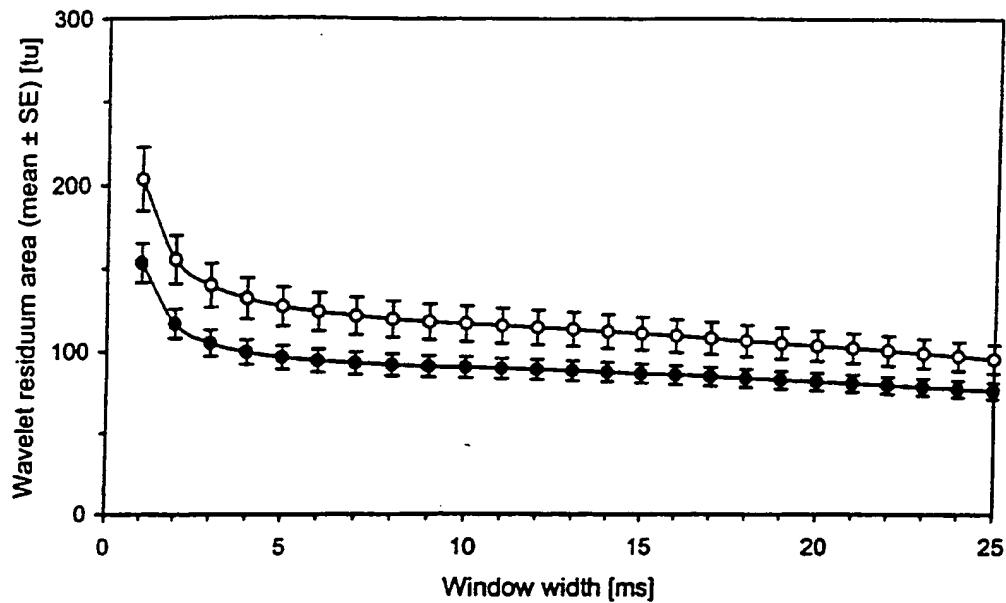


Fig. 65C

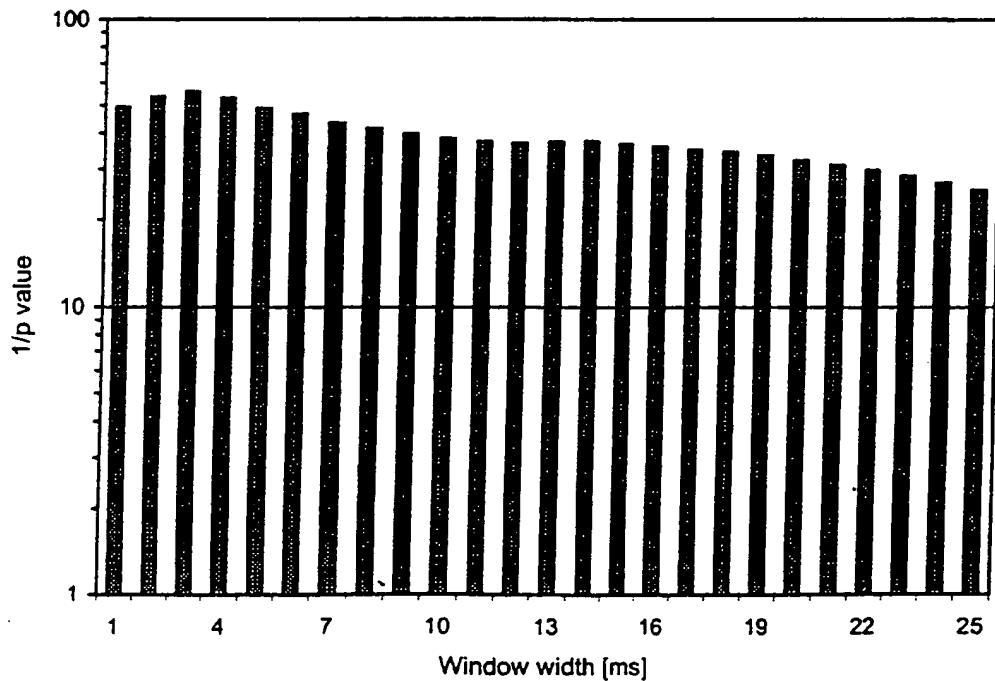


Fig. 65D

Comparison of asymmetric windows starting from the R wave
([R to R+ α])

Stimulation 20 mA, position 0 ms

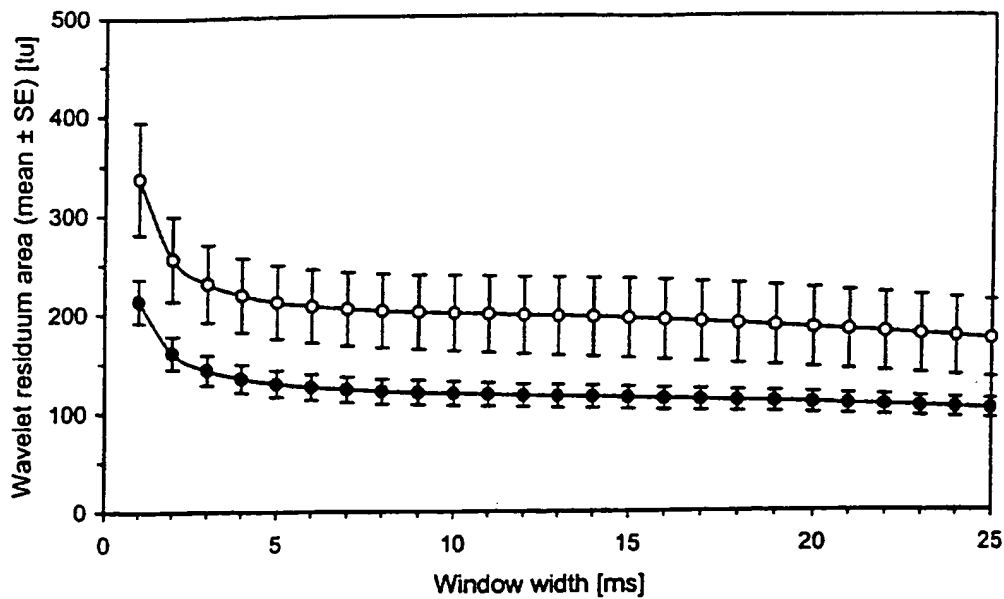


Fig. 65E

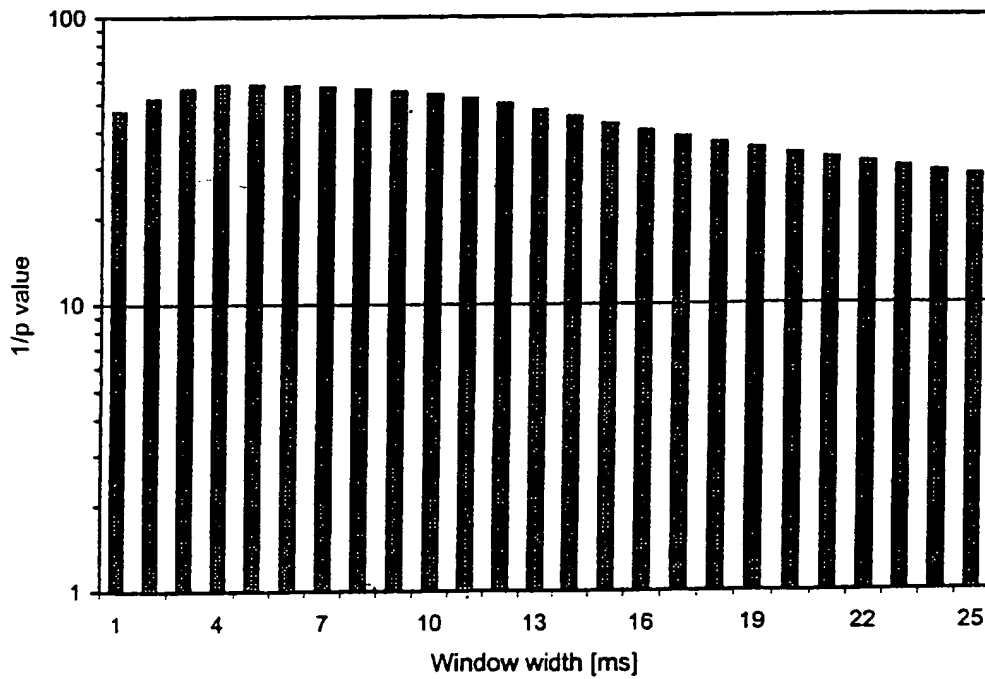


Fig. 65F

Upper cross-section

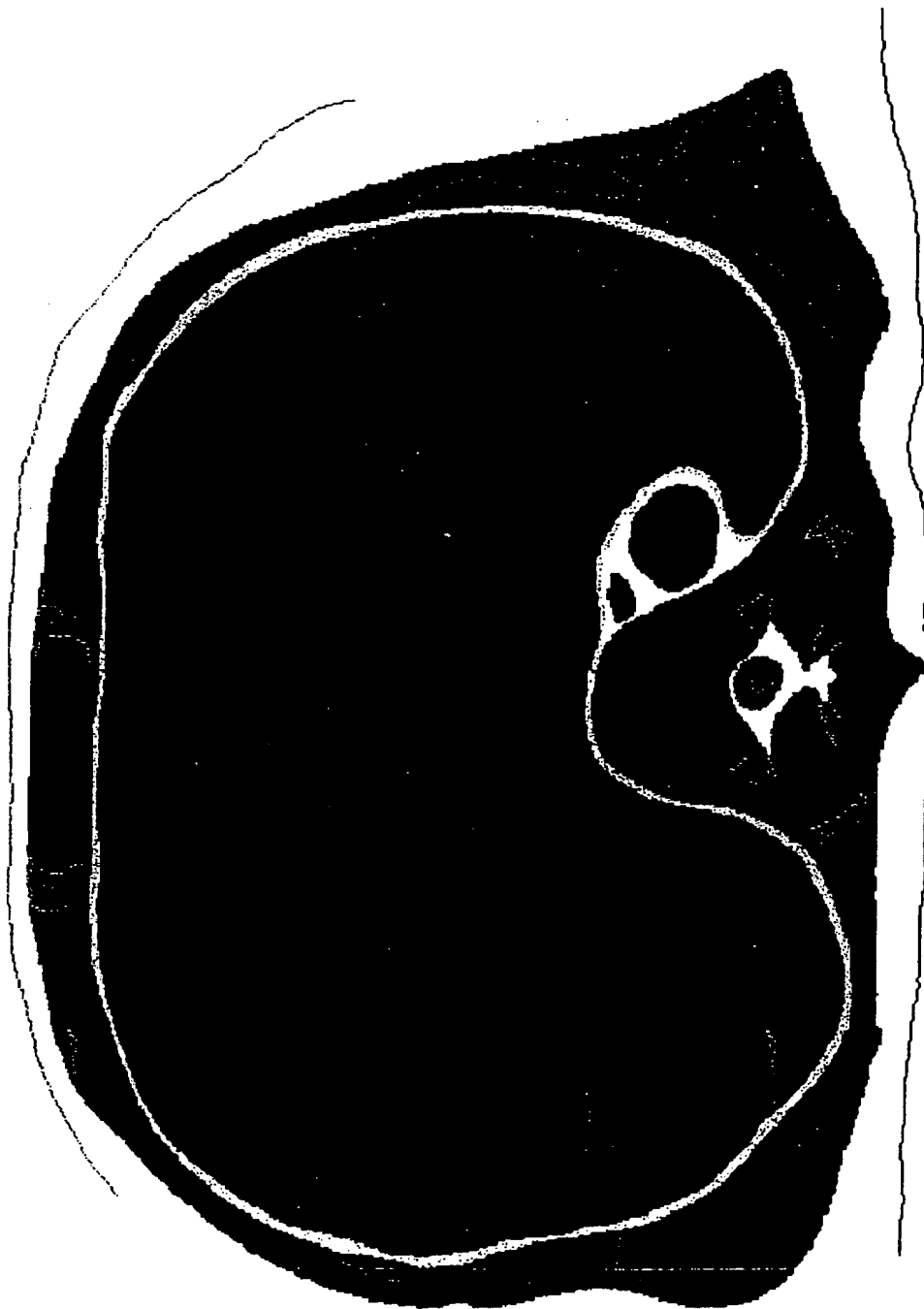


Fig. 66A

Middle cross-section

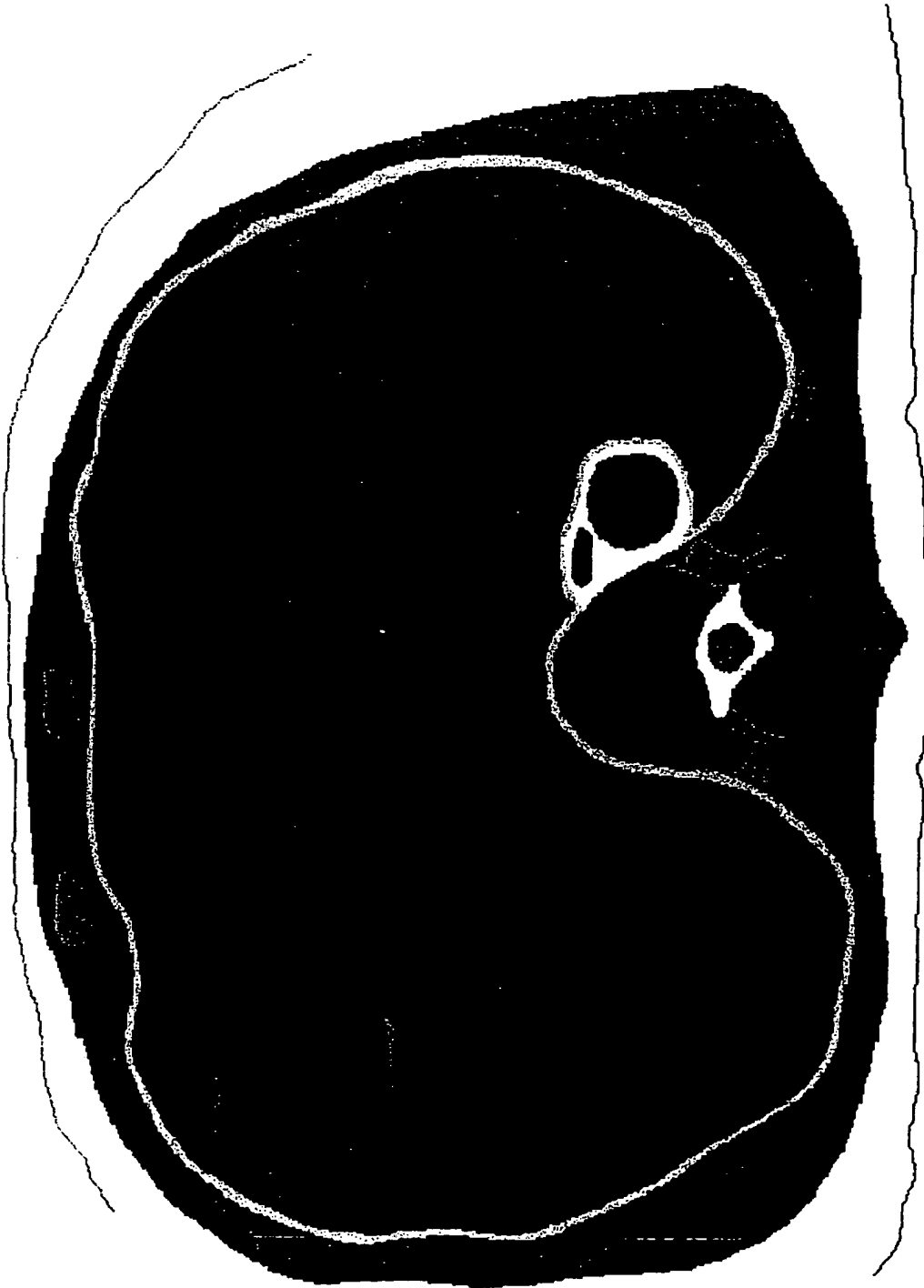


Fig. 66B

Lower cross-section

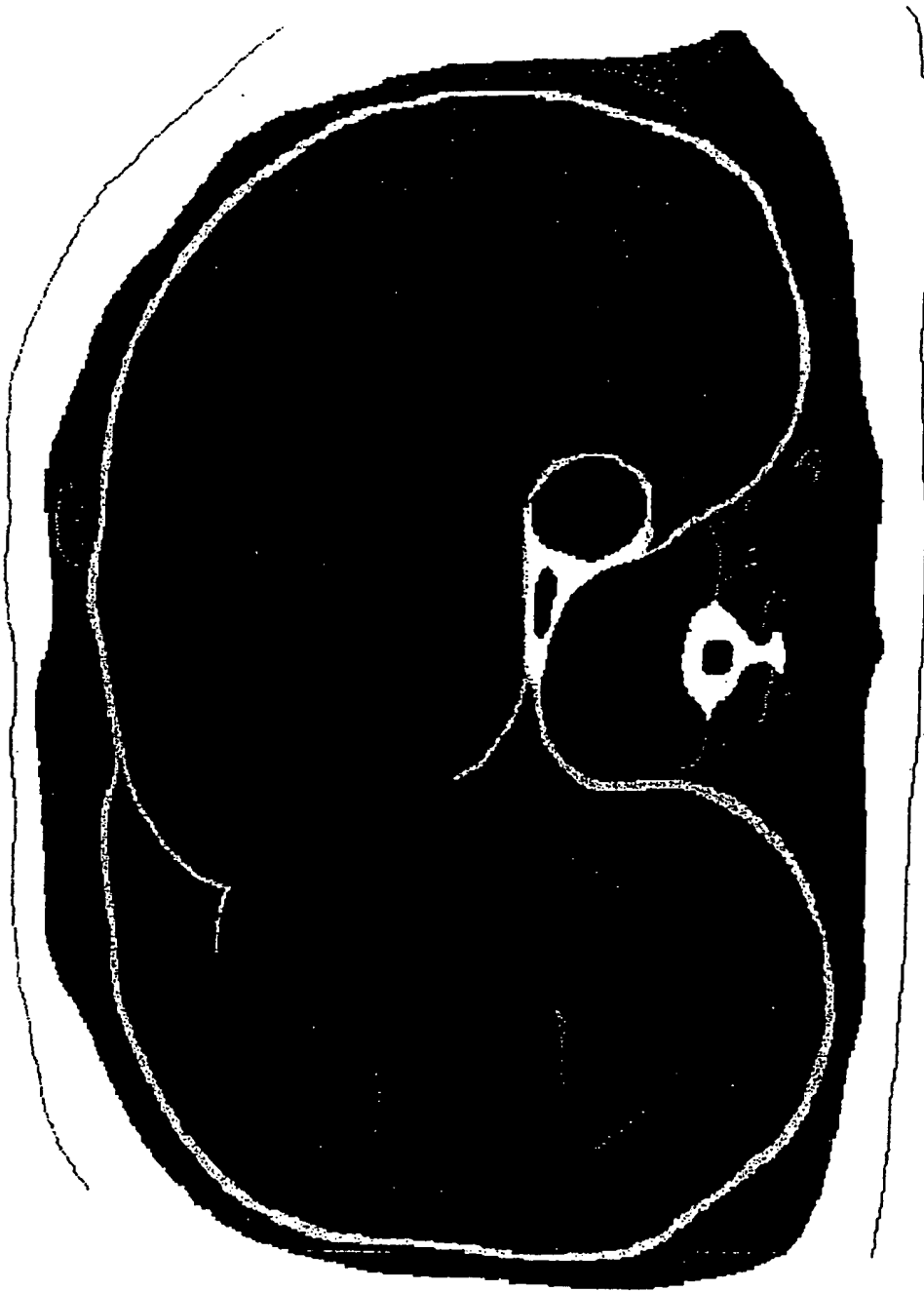


Fig. 6bC

64/
85

Middle cross-section

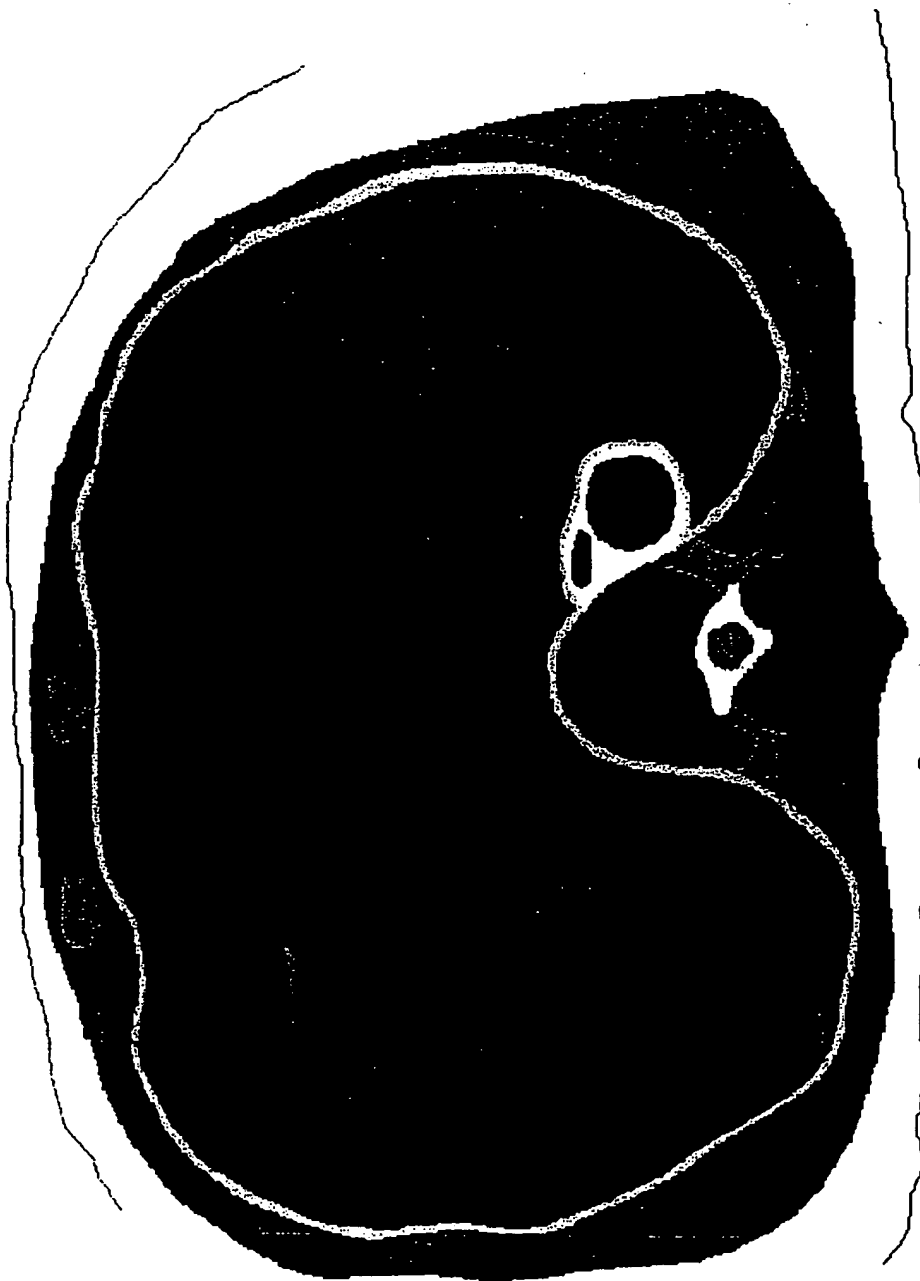


Fig. 66D

Upper cross-section

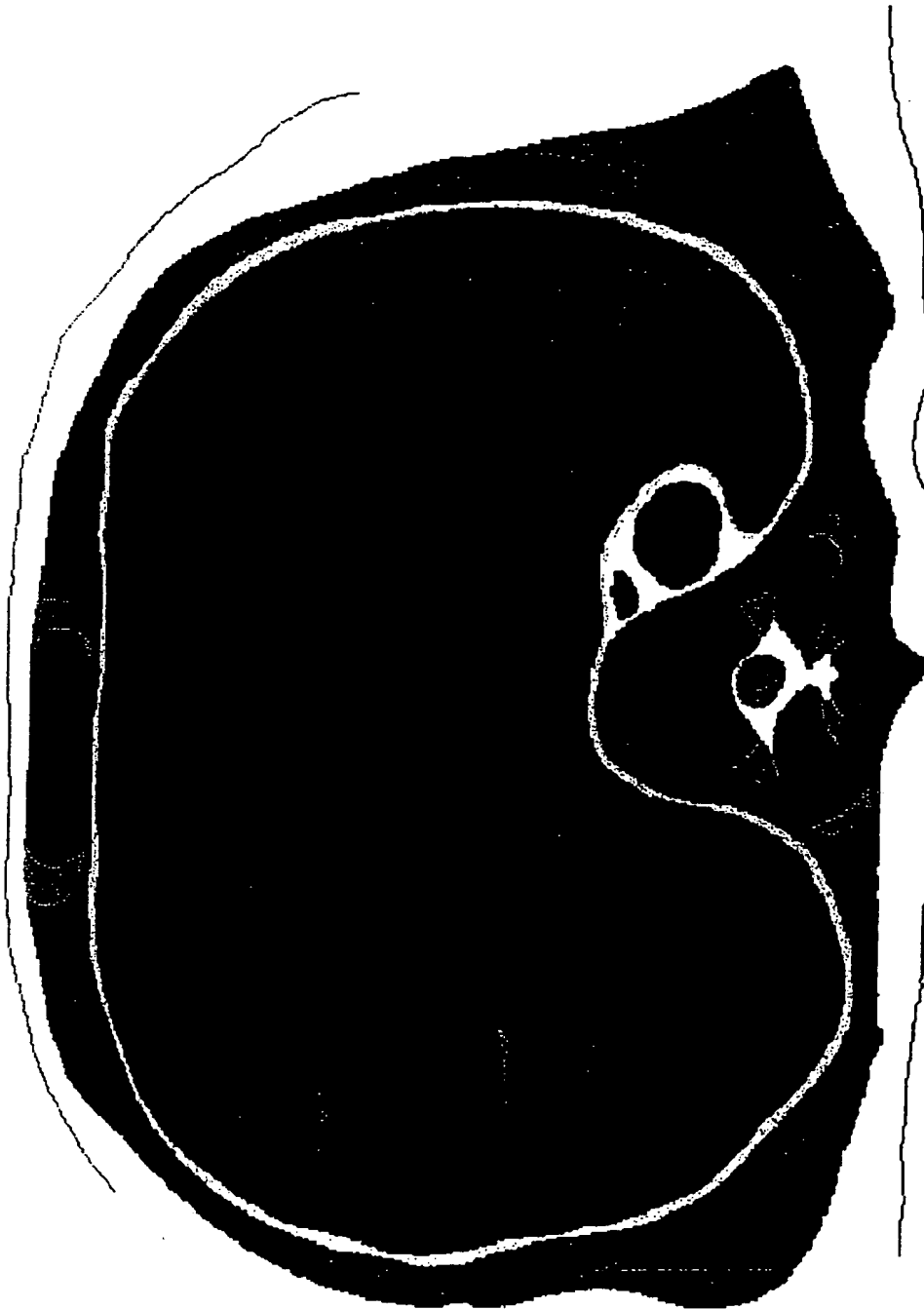


Fig. 66E

Tissue	Resistance
atrial myocardium	4.00
blood	1.50
bone	150.00
cartilage	70.00
fat	20.00
liver	4.50
lungs	12.00
muscle	7.00
oesophagus	6.00
pleura	2.00
spinal chord	3.00
ventricular myocardium	4.00

Fig. 67

Electrode	Segment 1	Segment 2	Segment 3	Segment 4	Segment 5
1	000 — 059				
2	000 — 089				
3	000 — 119				
4	000 — 149				
5	000 — 179				
6	000 — 209				
7	000 — 239				
8	000 — 039	060 — 099			
9	000 — 039	080 — 119			
10	000 — 039	100 — 139			
11	000 — 039	120 — 159			
12	000 — 059	080 — 119			
13	000 — 059	100 — 159			
14	000 — 059	120 — 189			
15	000 — 059	140 — 199			
16	000 — 079	100 — 179			
17	000 — 079	120 — 199			
18	000 — 079	140 — 219			
19	000 — 079	160 — 239			
20	000 — 099	120 — 219			
21	000 — 099	140 — 239			
22	000 — 039	060 — 099	120 — 159		
23	000 — 039	080 — 119	160 — 199		
24	000 — 039	100 — 139	200 — 239		
25	000 — 059	080 — 119	140 — 209		
26	000 — 069	090 — 159	180 — 239		
27	000 — 029	060 — 089	120 — 149	180 — 209	
28	000 — 029	070 — 099	140 — 169	210 — 239	
29	000 — 039	060 — 099	120 — 159	180 — 219	
30	000 — 029	050 — 079	100 — 129	150 — 179	200 — 229

Fig. 66

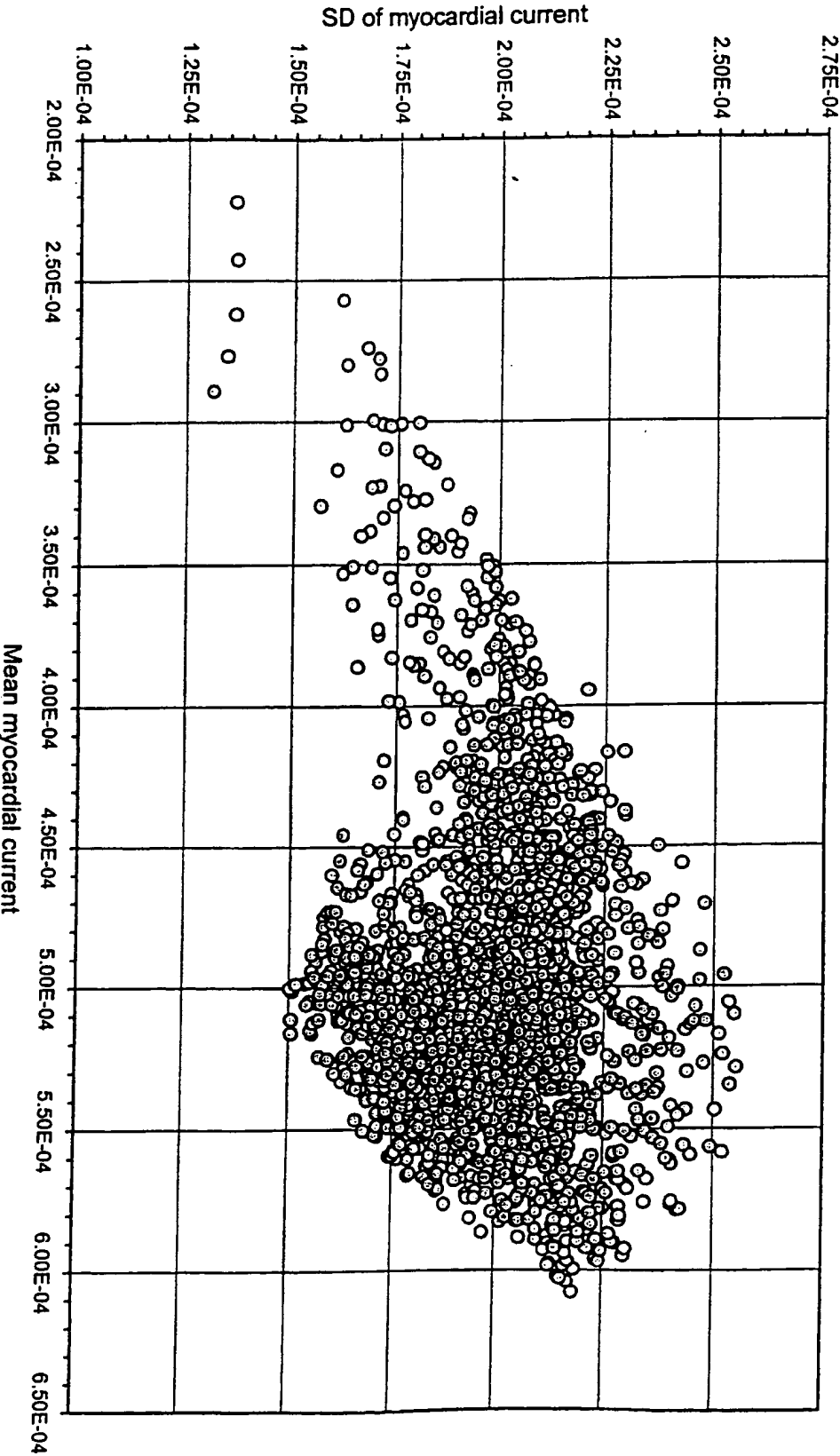


FIG. 69A

69/85

Fig. 69B

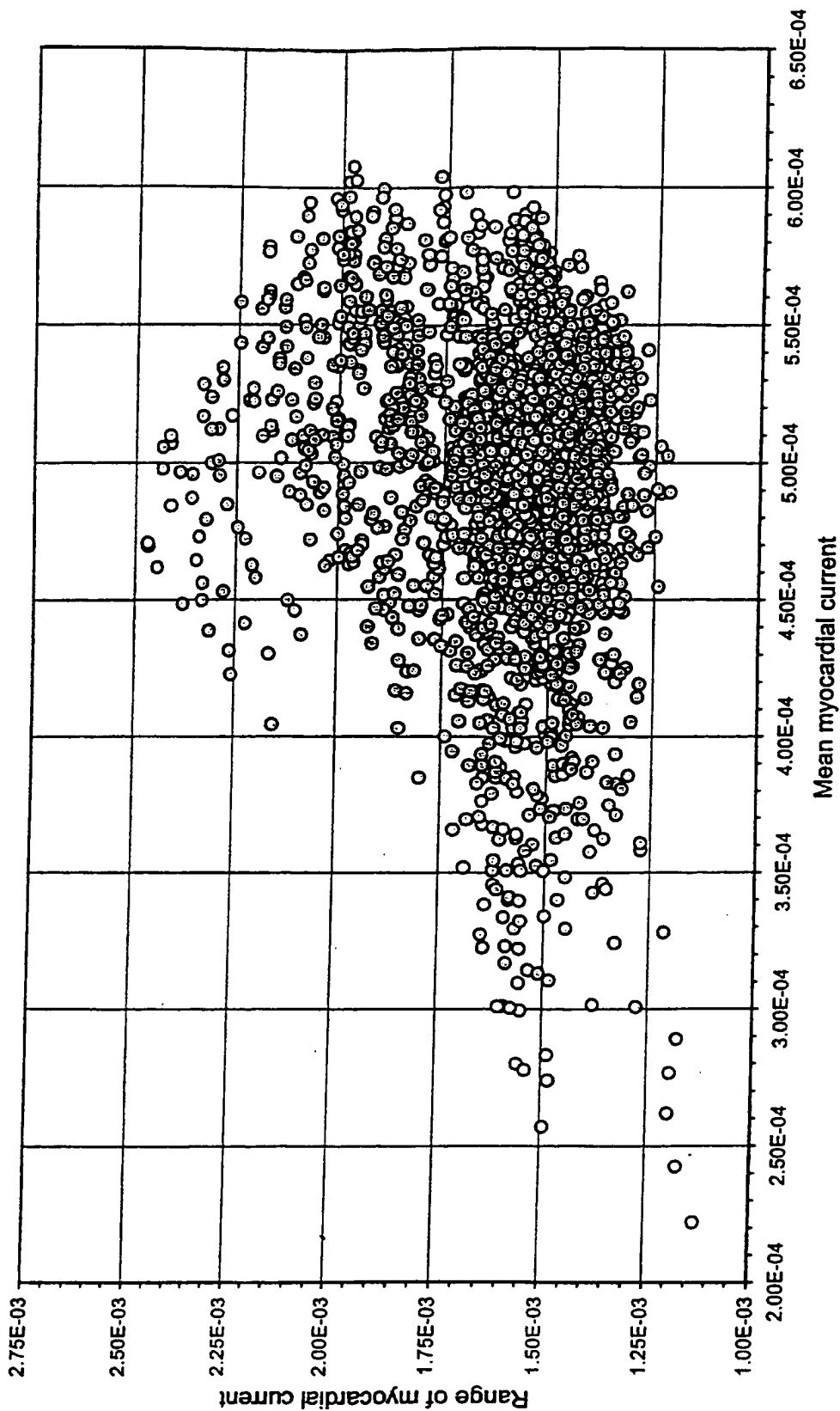
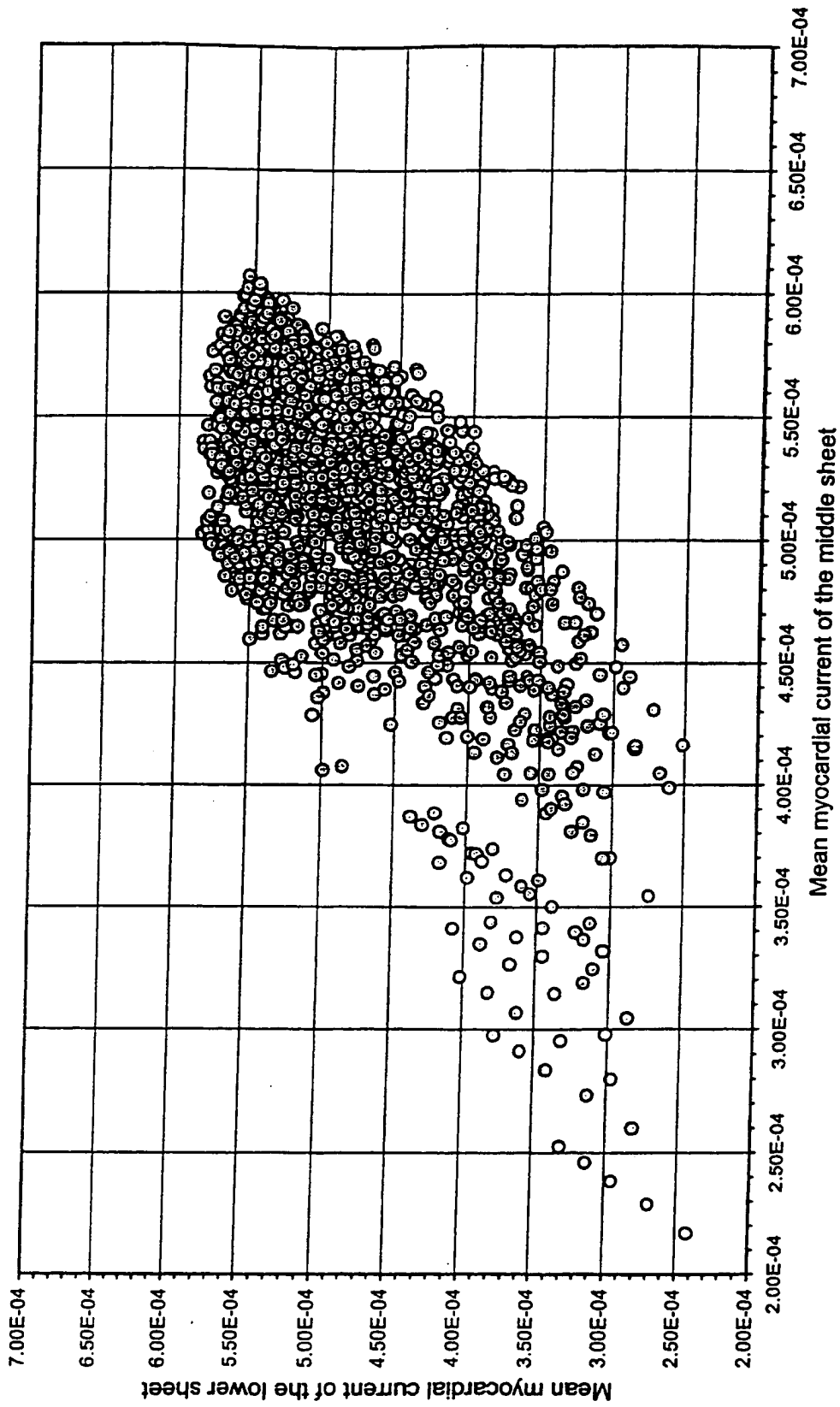


Fig. 69C



71/85

Fig. 69D

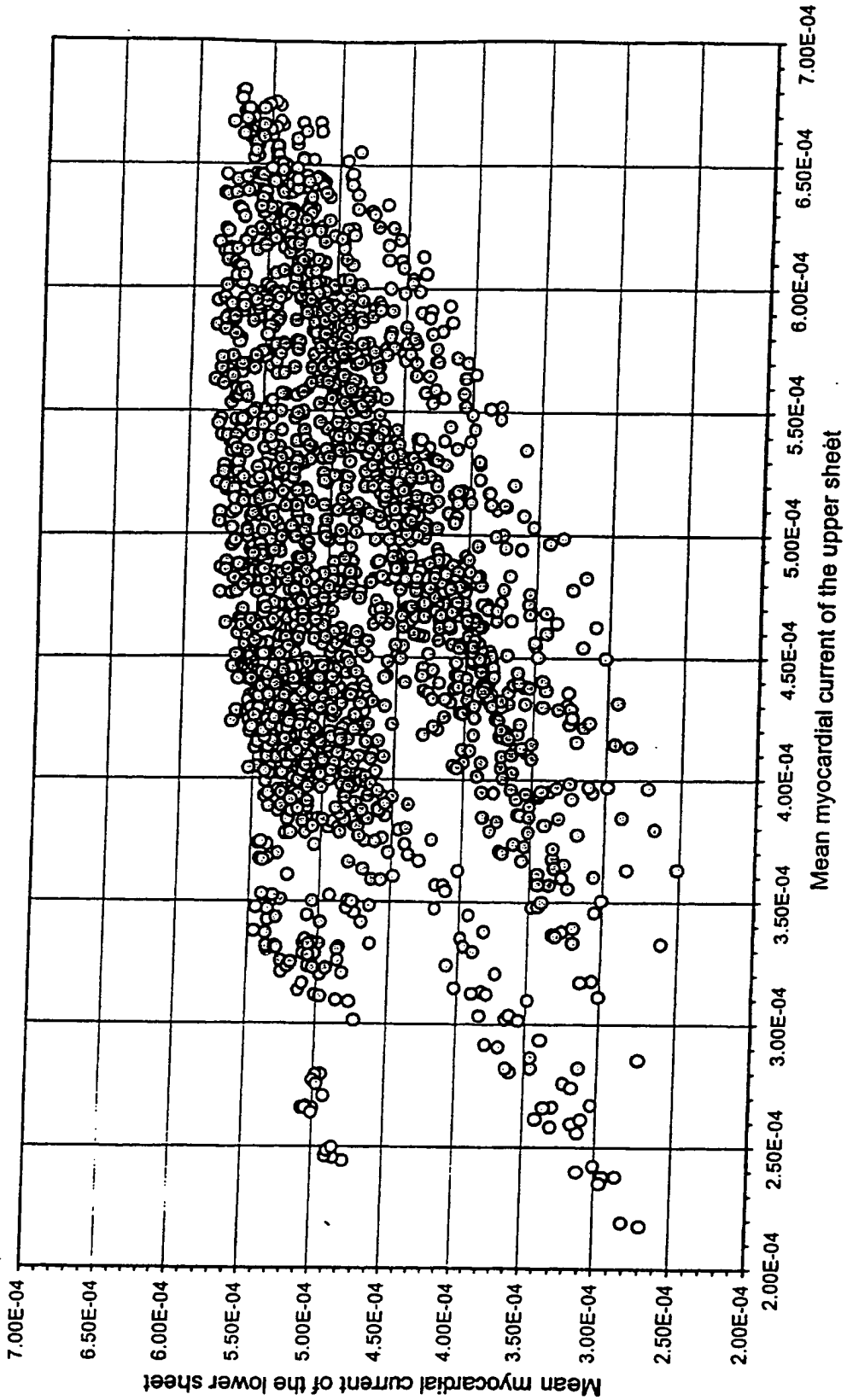
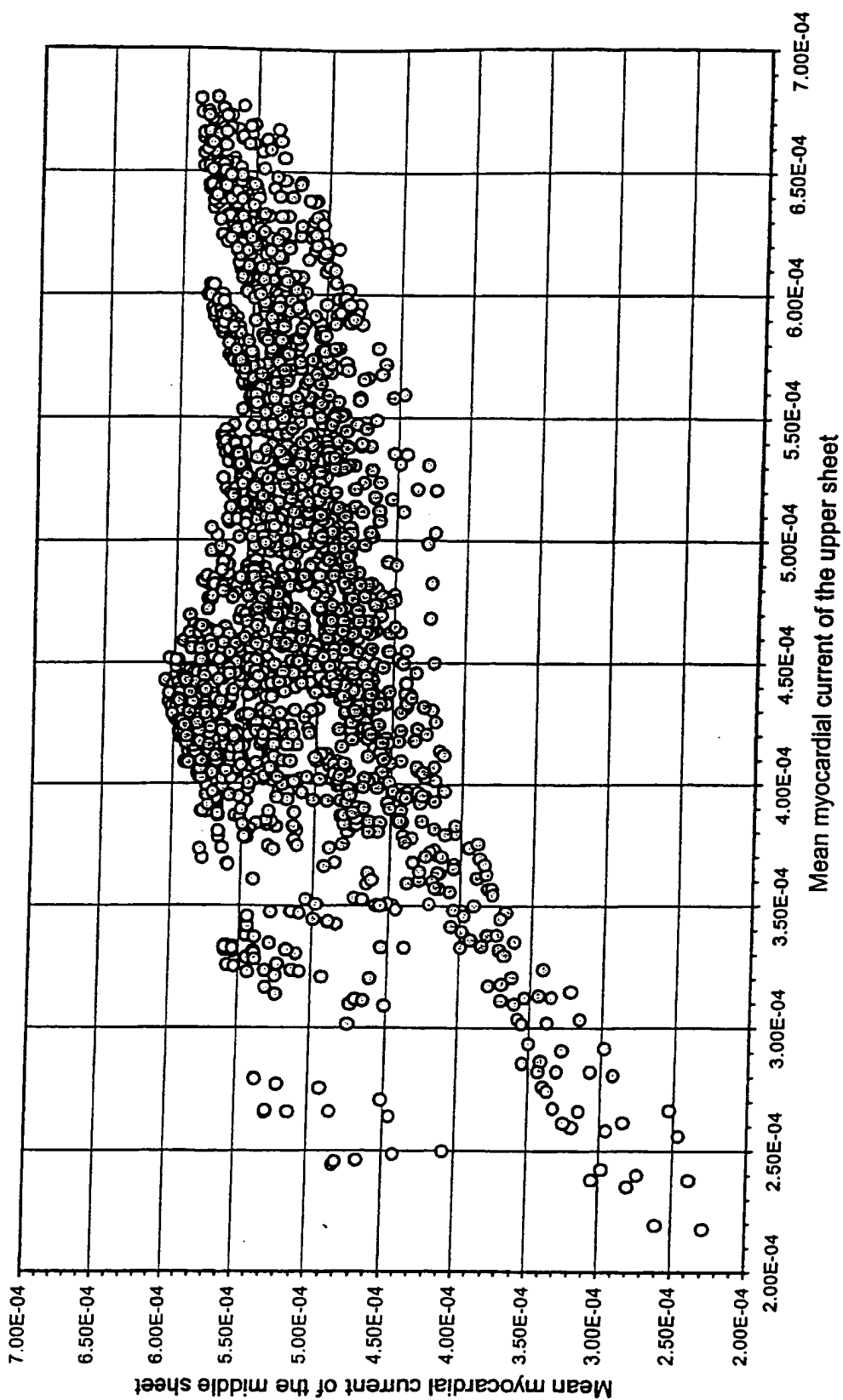
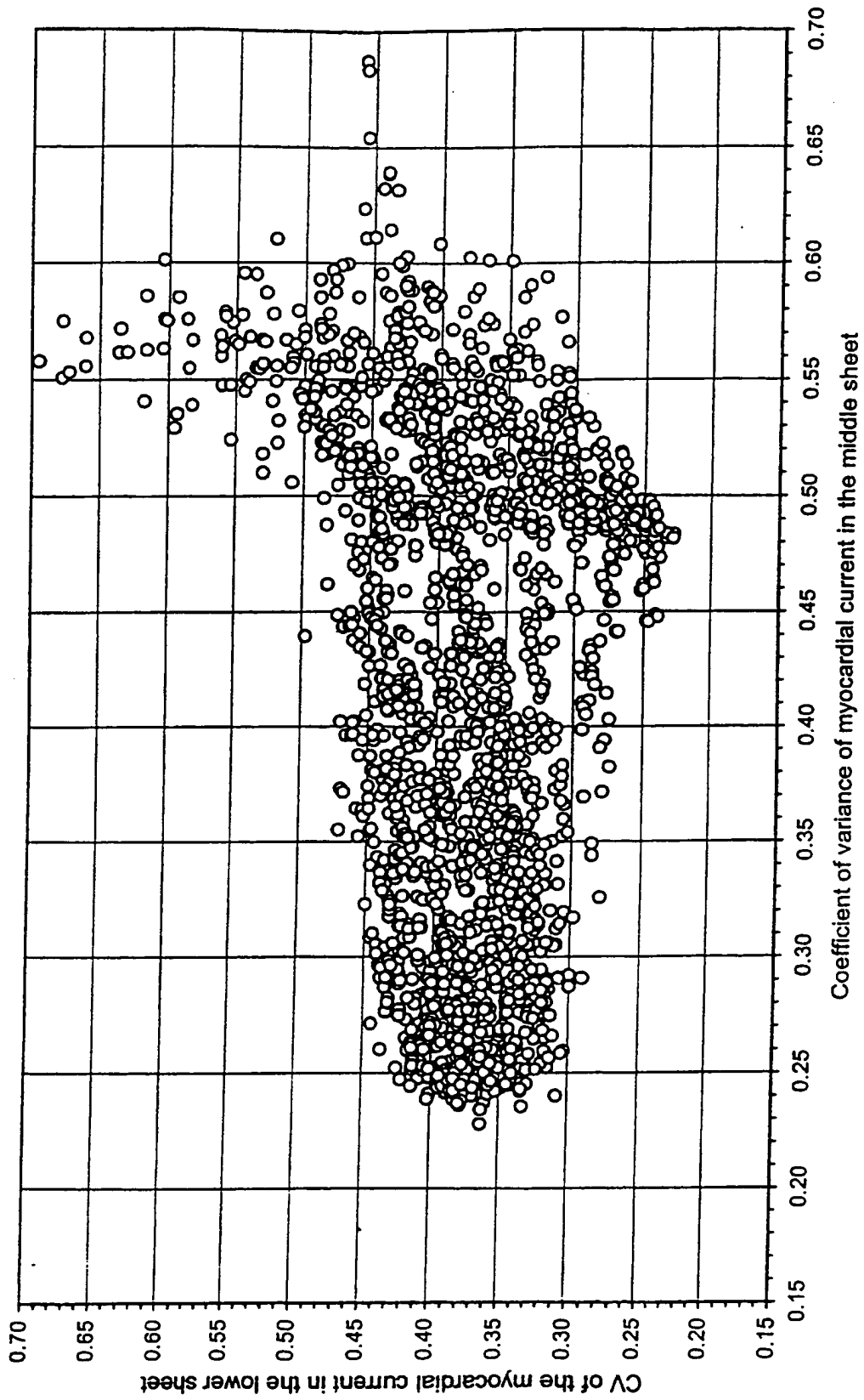


Fig. 6⁹E



73/85

Fig. 69F



74/85

Fig. 696

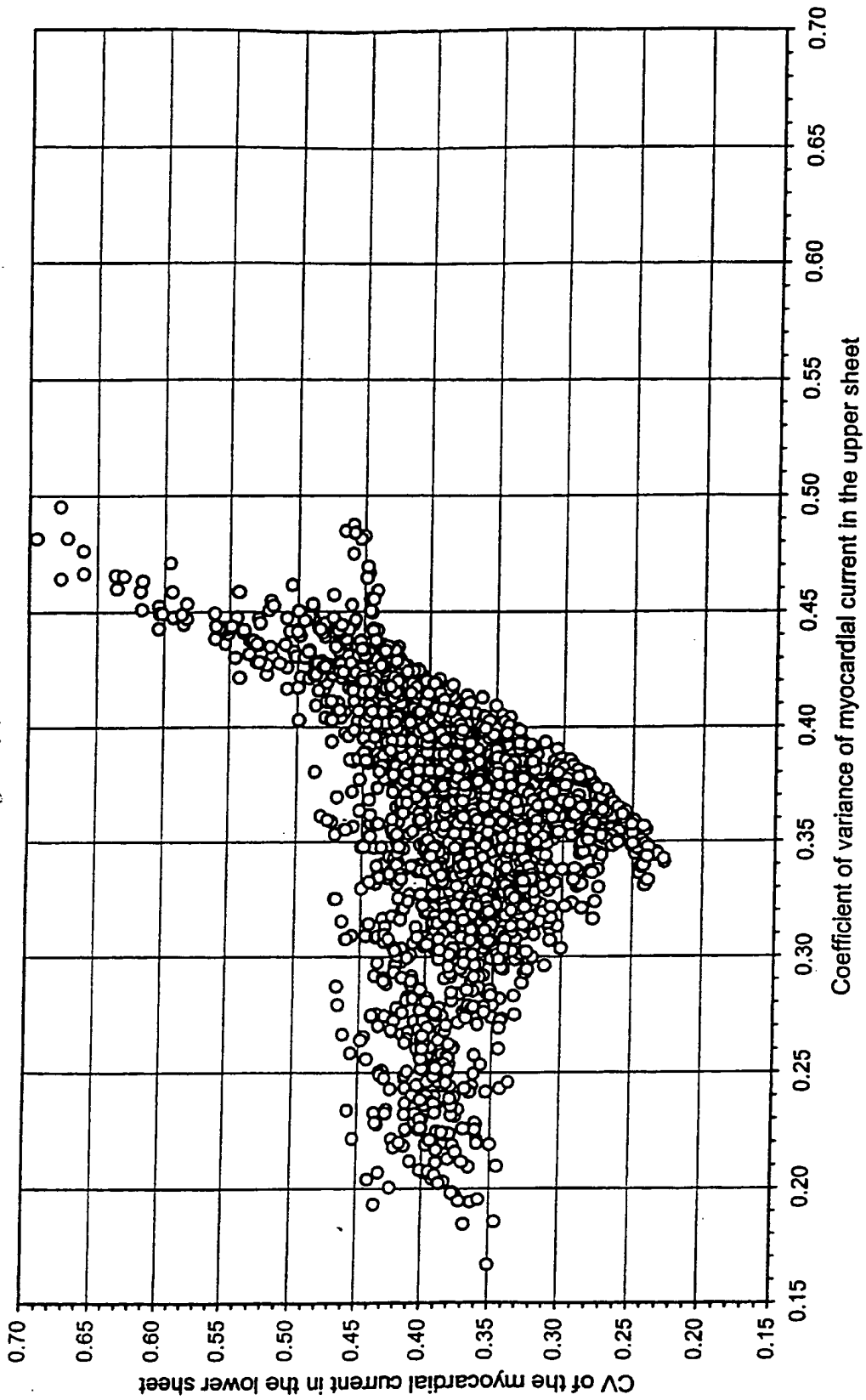
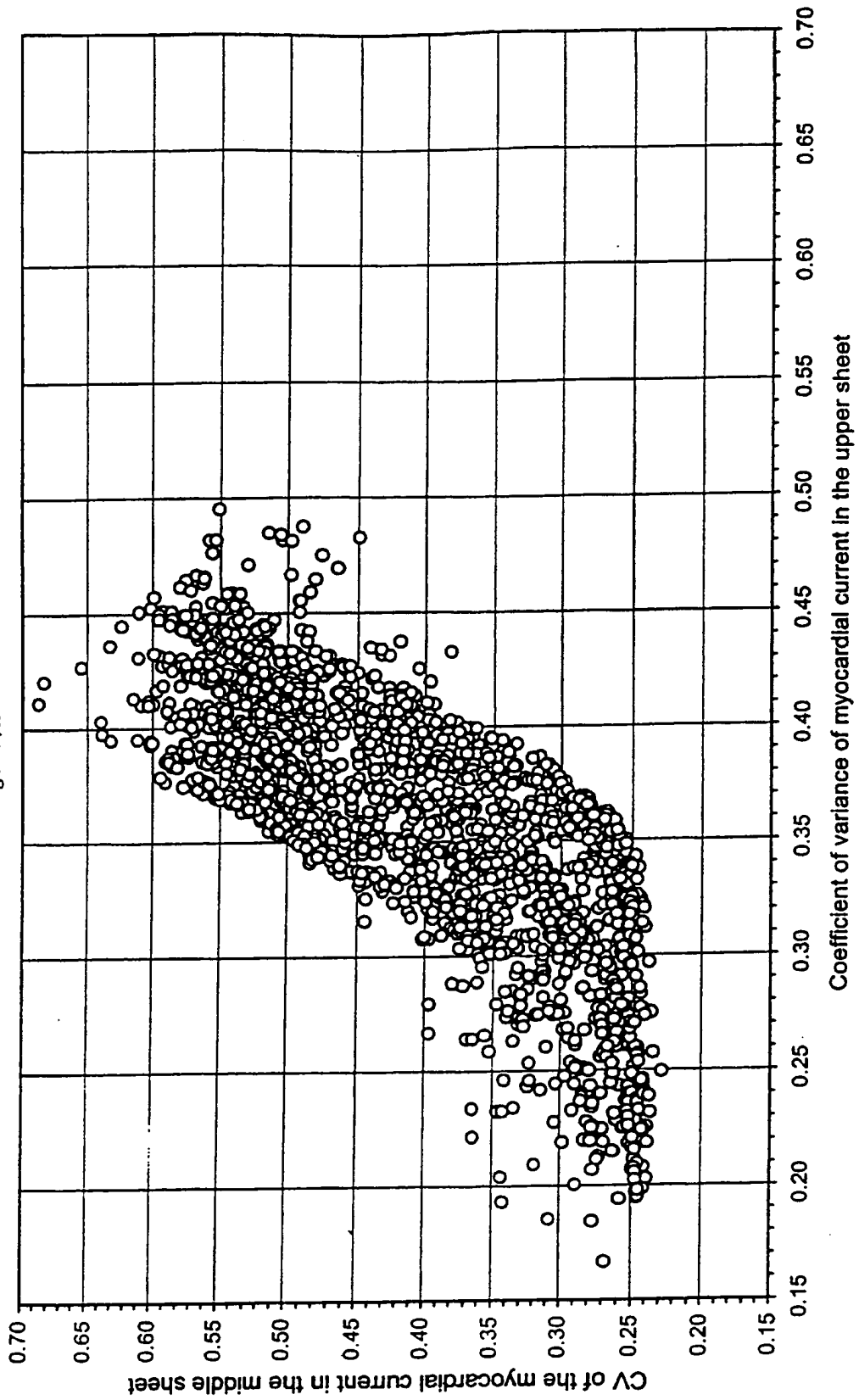


Fig. 69H



76/85

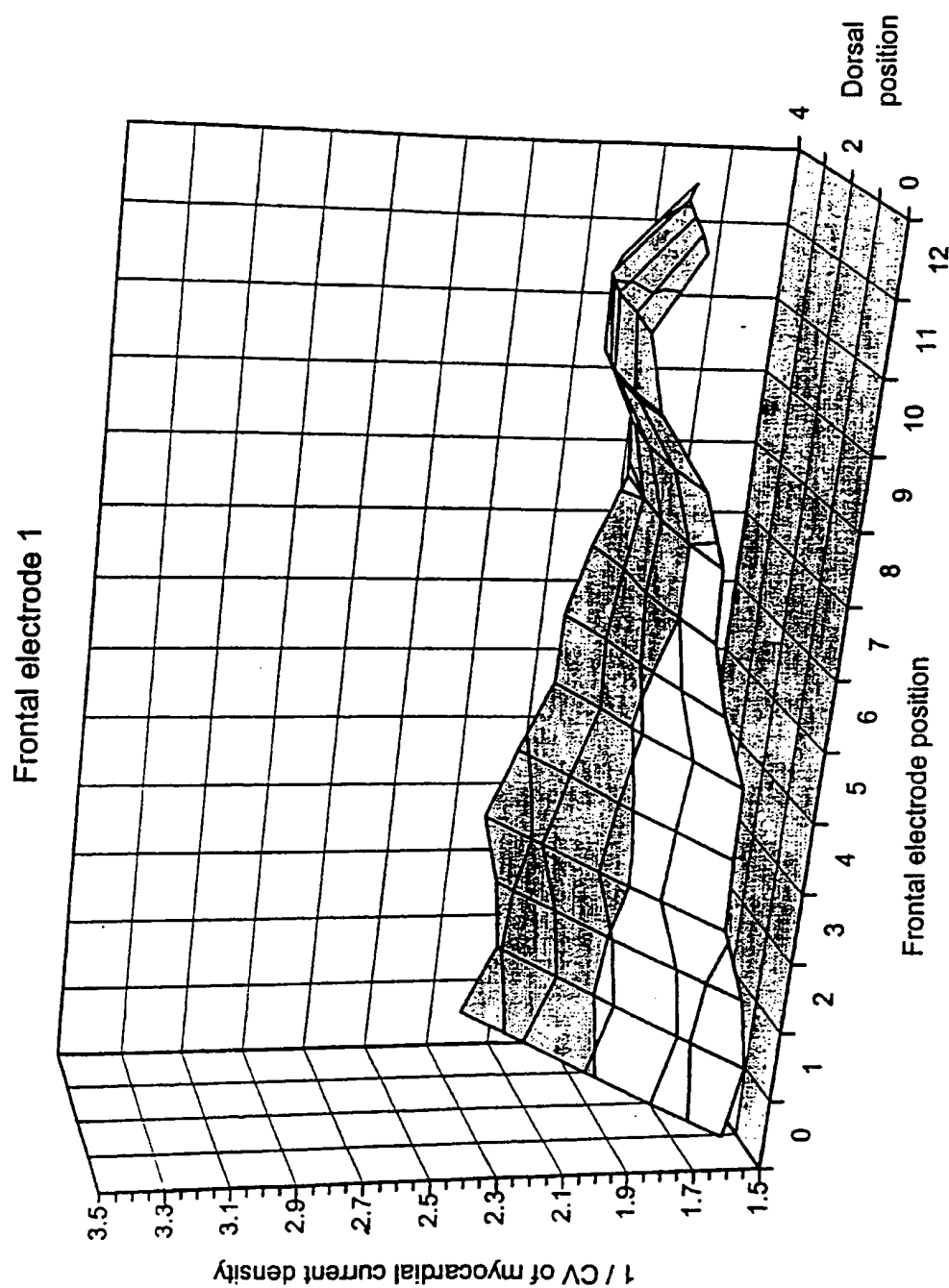


Fig. 70A

77/85

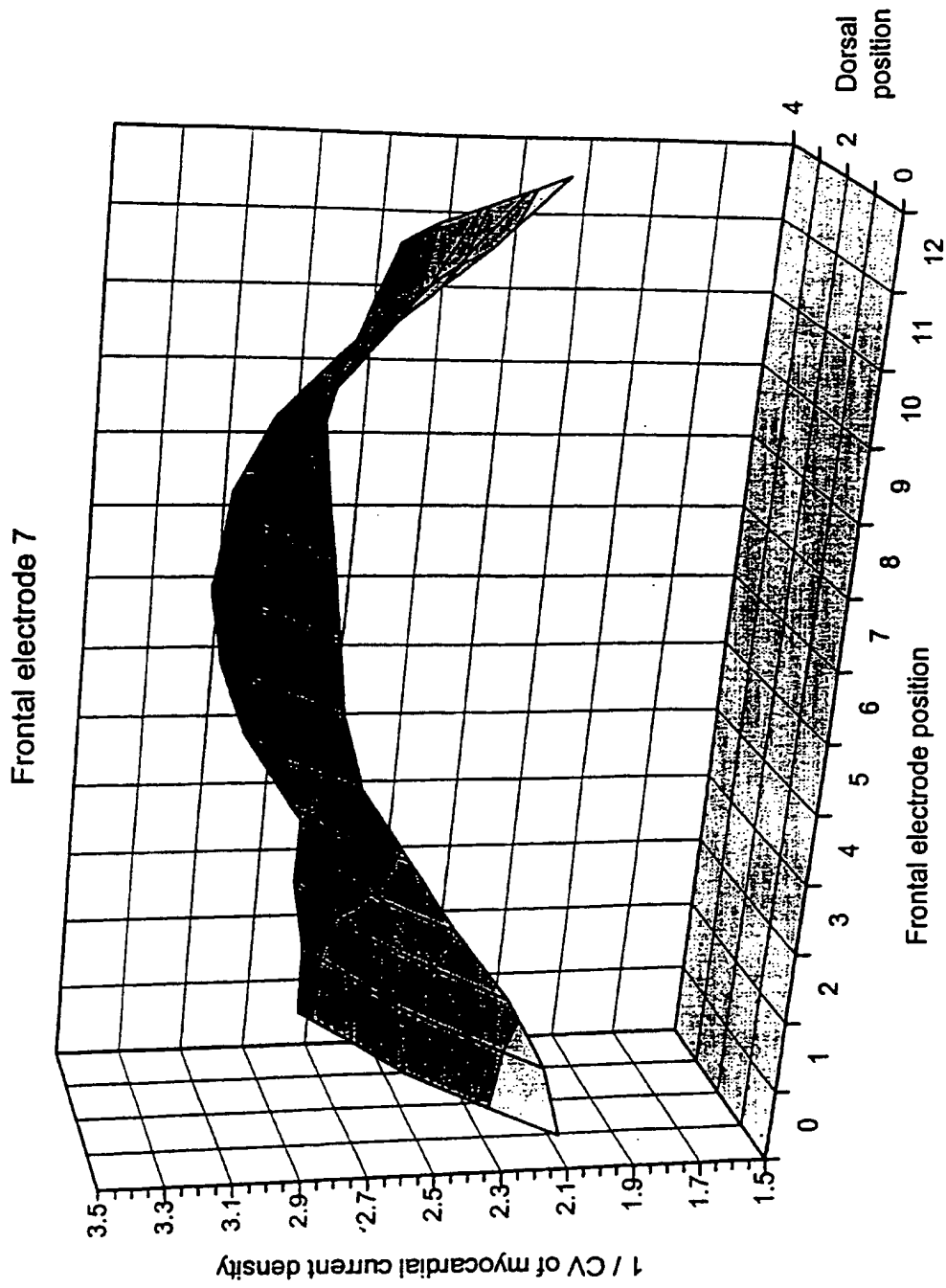


Fig. 70 B

78/85

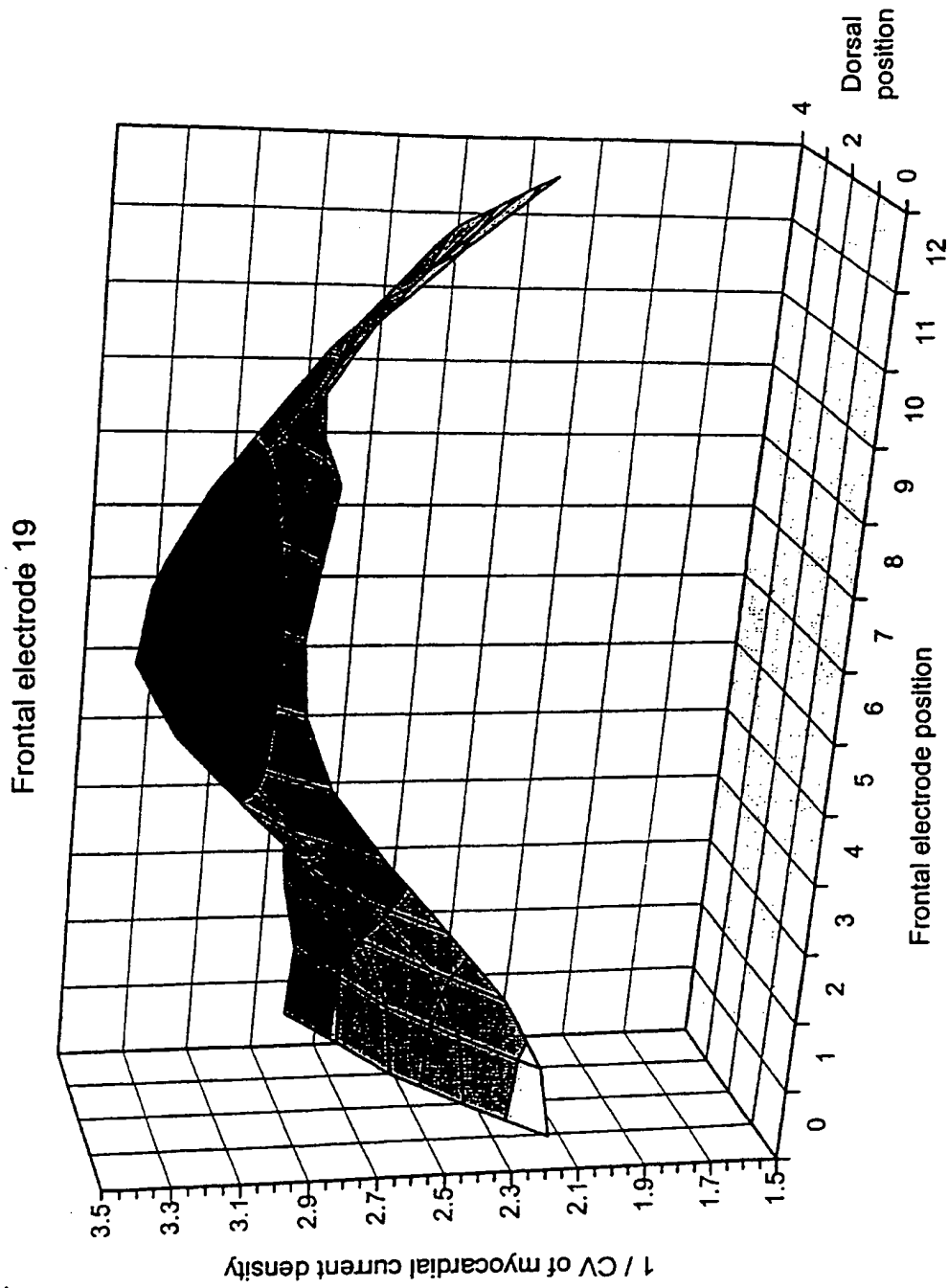


Fig. 10C

79/85

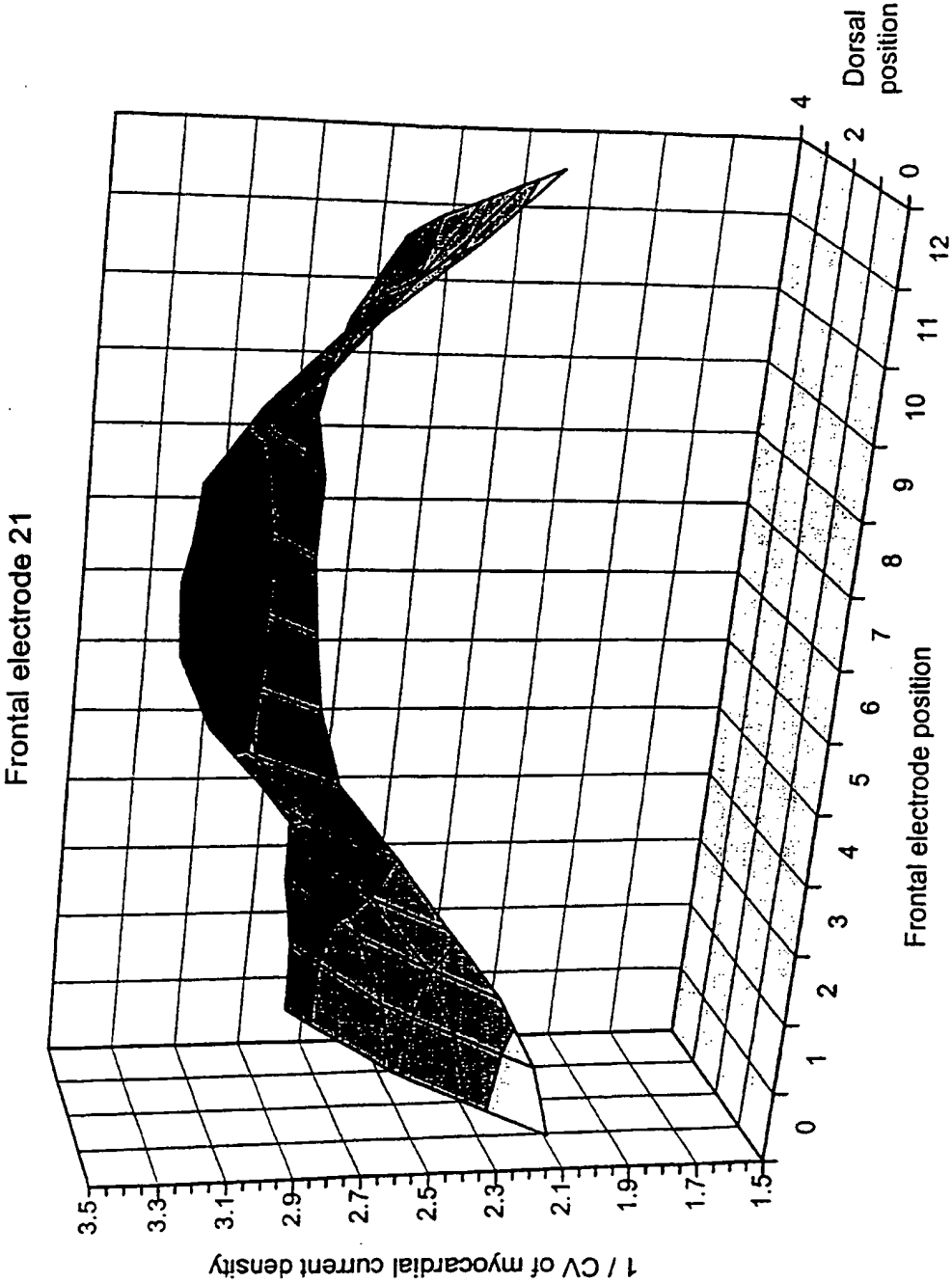


Fig. 70 D

80/85

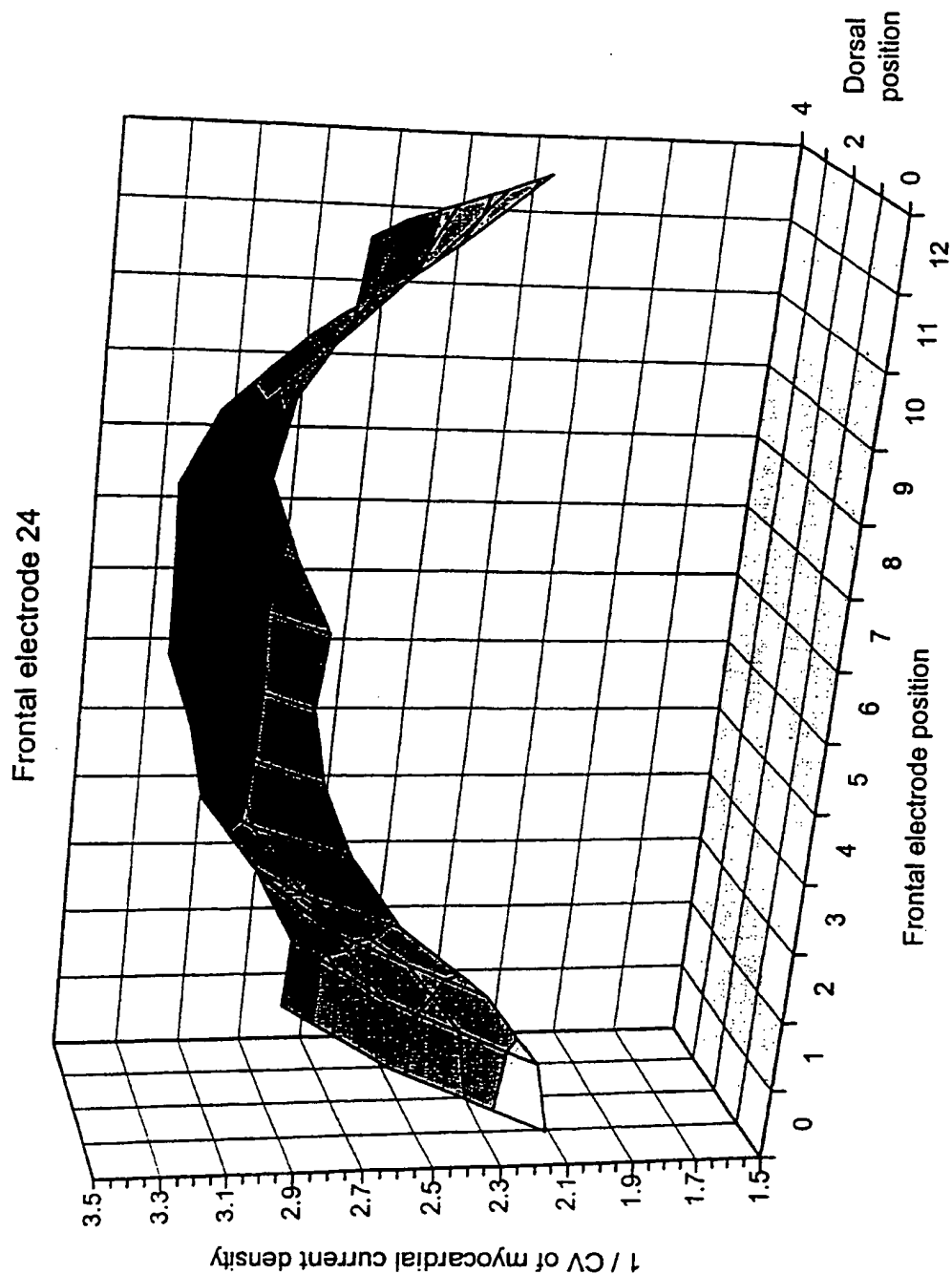


Fig. 70E

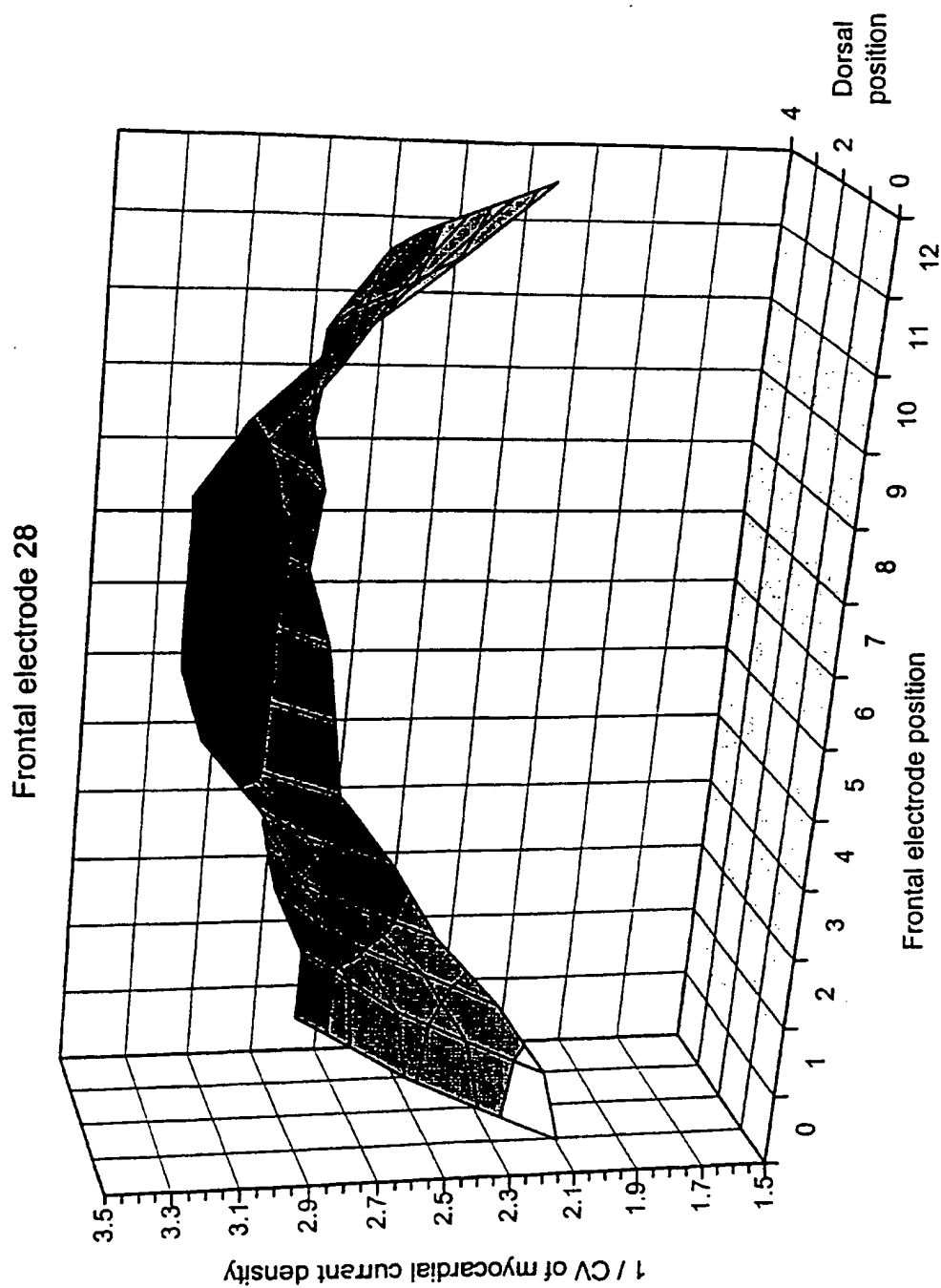


Fig. 10F

82/85

Frontal electrode 30

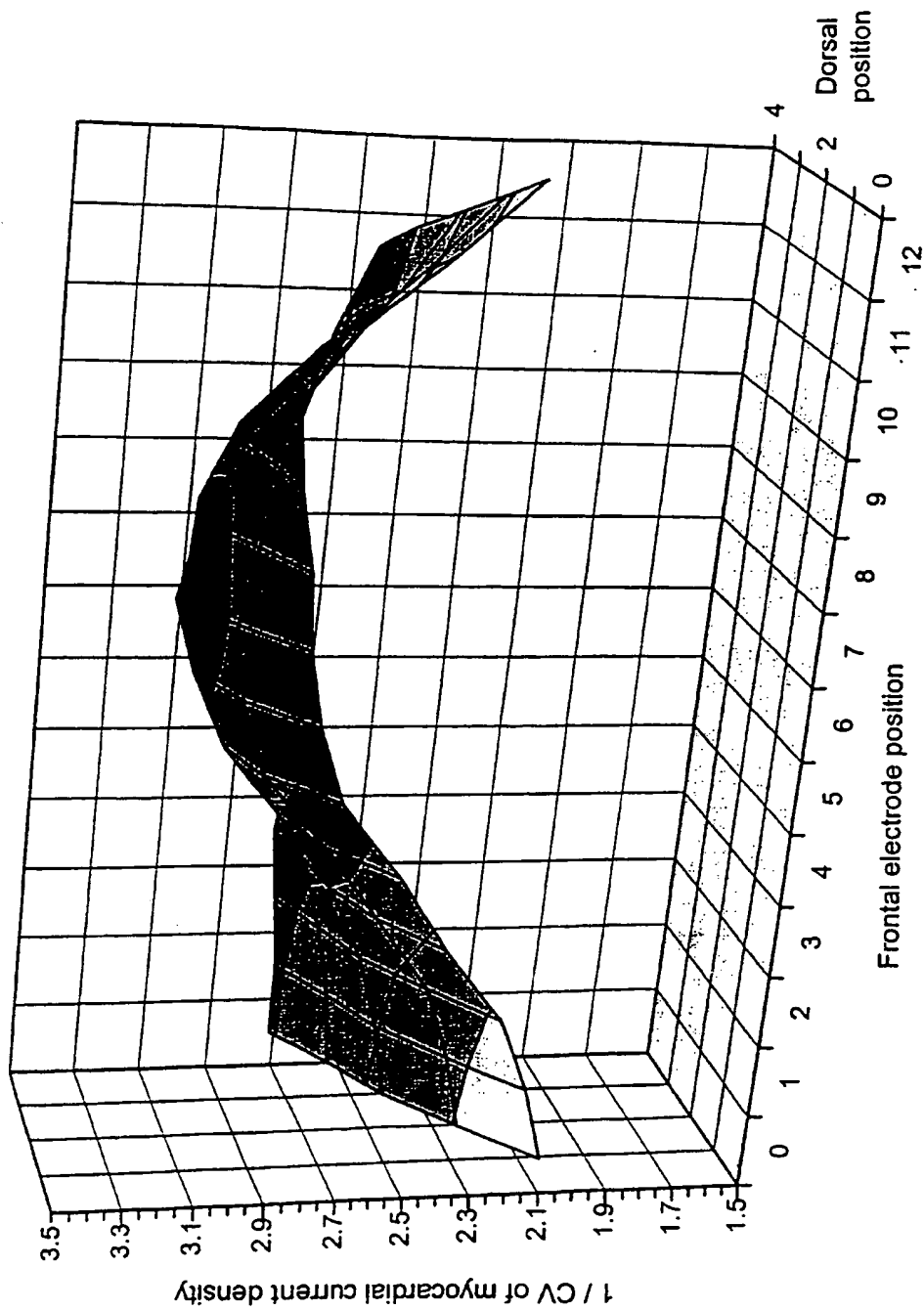


Fig. 70G

83/85

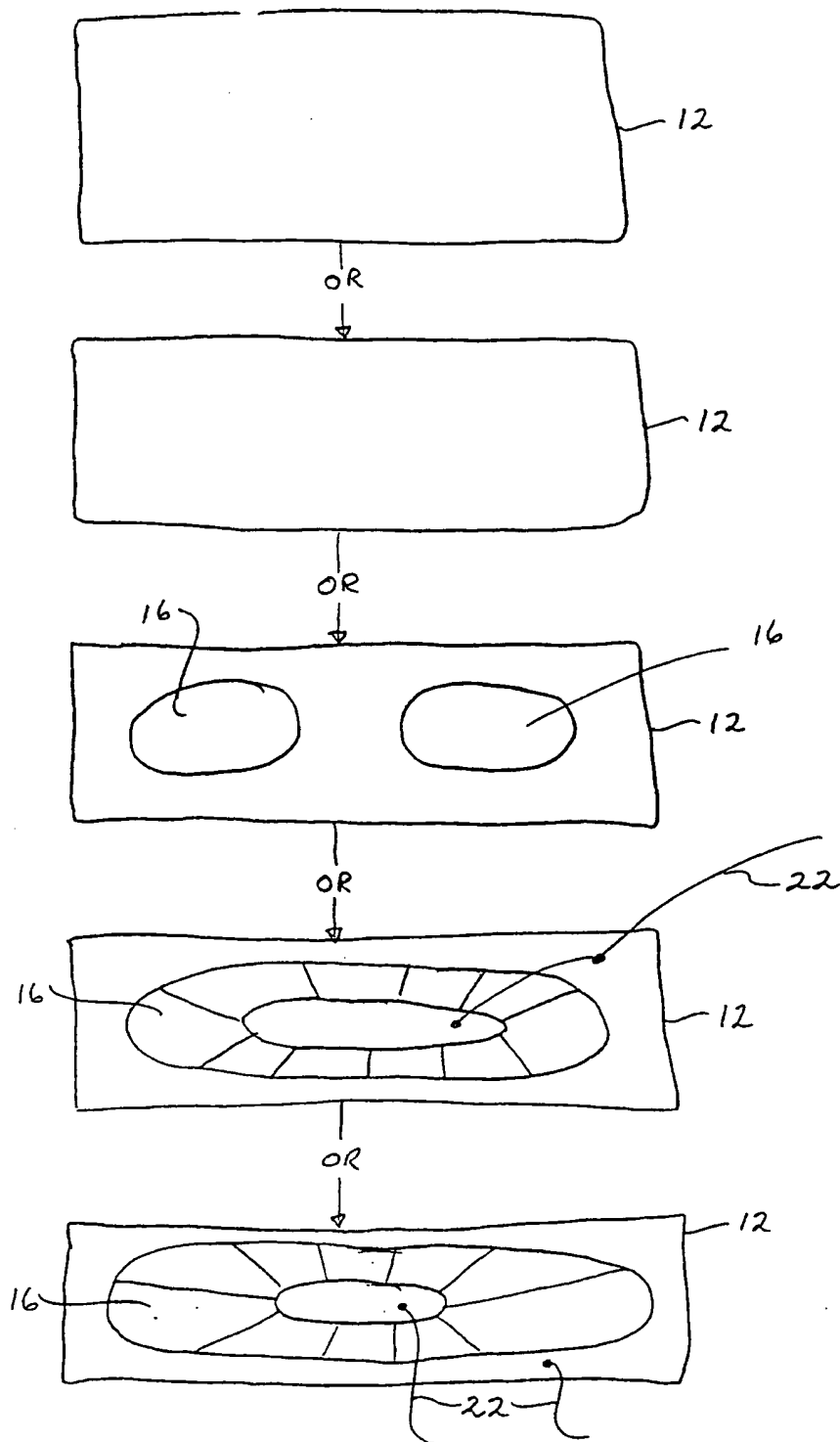


Fig. 71

84/85

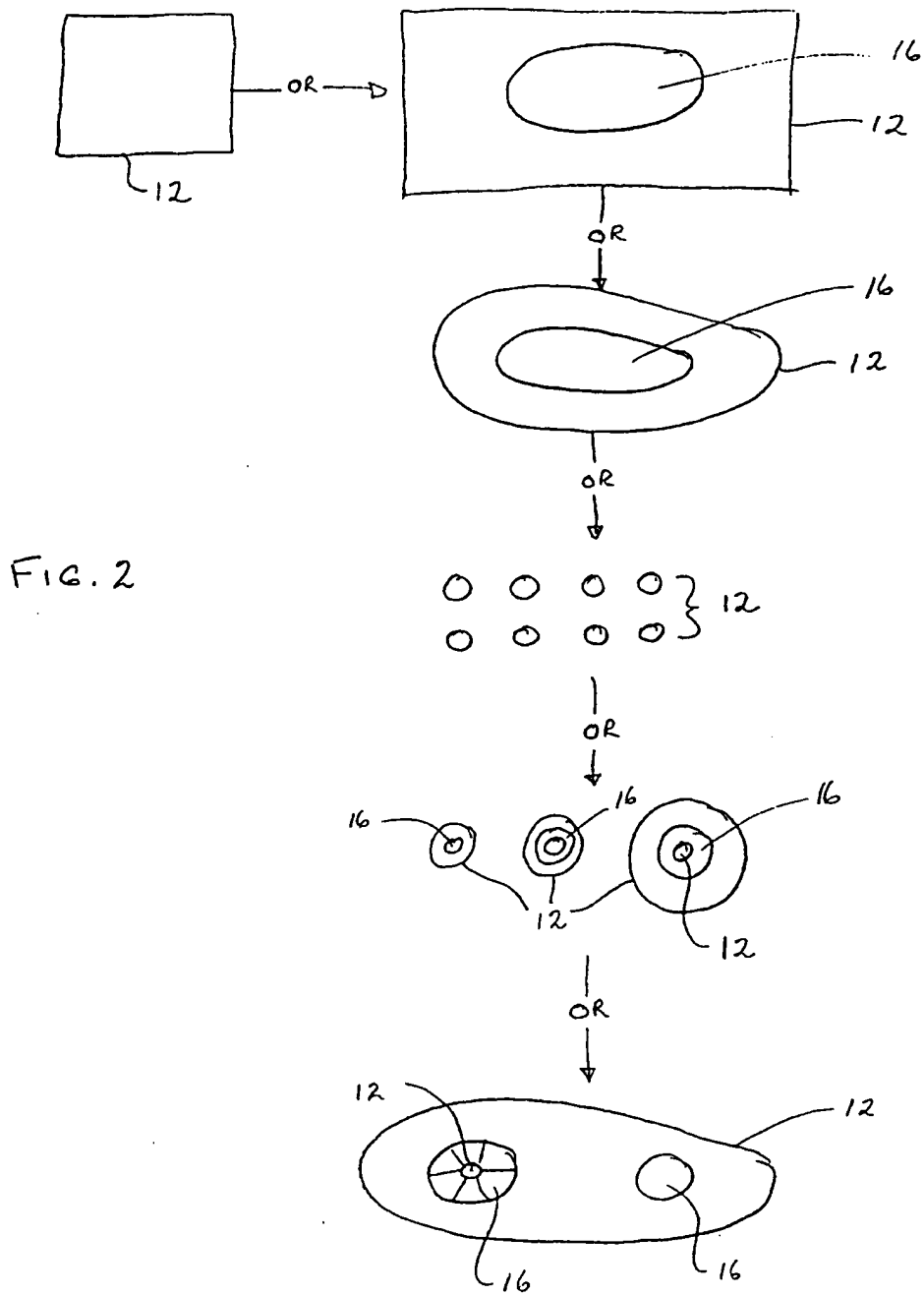


Fig. 72

95/85

FIG. 3

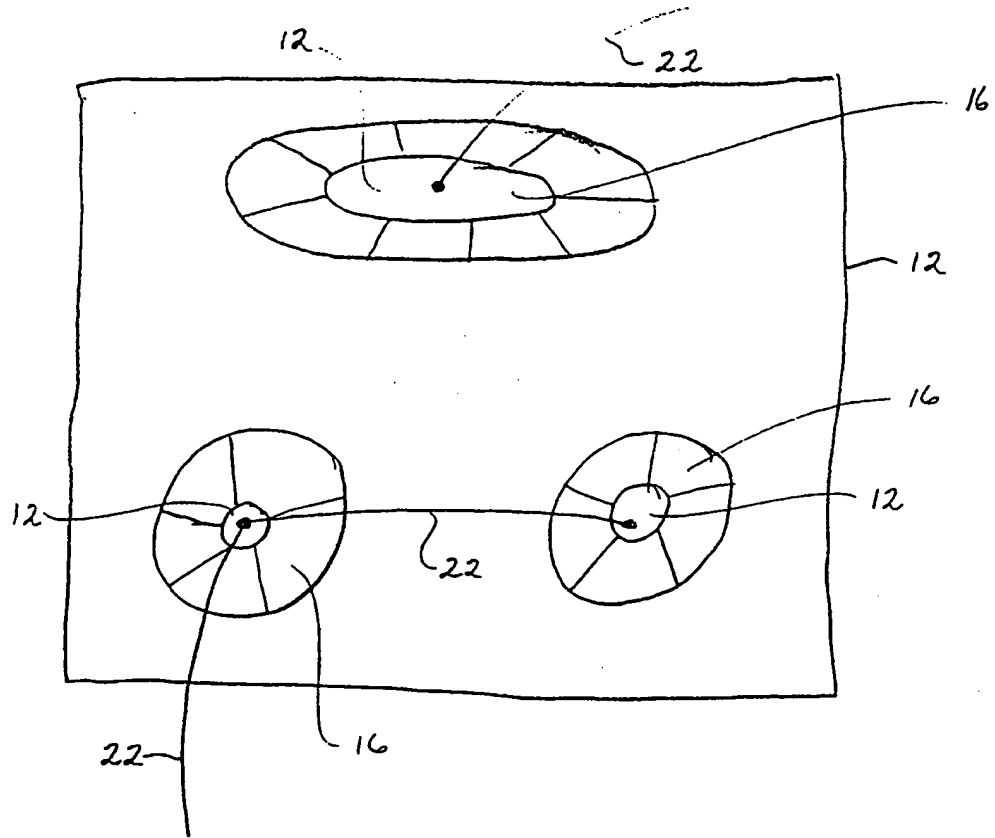


Fig. 70

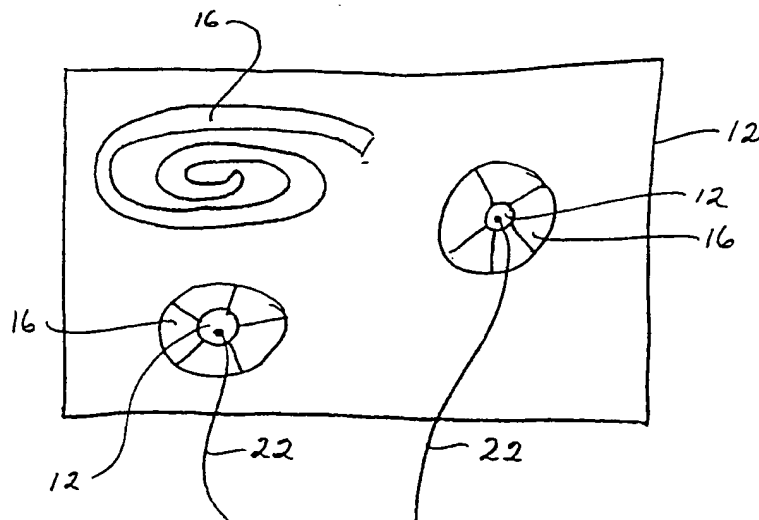


FIG. 4

Fig. 73

INTERNATIONAL SEARCH REPORT

International Application No.

PCT/US 00/15965

A. CLASSIFICATION OF SUBJECT MATTER

IPC 7 A61B5/0472

According to International Patent Classification (IPC) or to both national classification and IPC

B. FIELDS SEARCHED

Minimum documentation searched (classification system followed by classification symbols)

IPC 7 A61B

Documentation searched other than minimum documentation to the extent that such documents are included in the fields searched

Electronic data base consulted during the international search (name of data base and, where practical, search terms used)

EPO-Internal

C. DOCUMENTS CONSIDERED TO BE RELEVANT

Category *	Citation of document, with indication, where appropriate, of the relevant passages	Relevant to claim No.
X	WO 99 05964 A (HARBINGER MEDICAL INC) 11 February 1999 (1999-02-11) claims 1,56	24-28, 31-35
X	US 5 117 834 A (KROLL MARK W ET AL) 2 June 1992 (1992-06-02) abstract	24-28, 31-35
X	GB 2 301 037 A (SIEMENS AG) 27 November 1996 (1996-11-27) abstract	24-28, 31-35

☐ Further documents are listed in the continuation of box C.

Patent family members are listed in annex.

* Special categories of cited documents :

"A" document defining the general state of the art which is not considered to be of particular relevance

"E" earlier document but published on or after the international filing date

"L" document which may throw doubts on priority claim(s) or which is cited to establish the publication date of another citation or other special reason (as specified)

"O" document referring to an oral disclosure, use, exhibition or other means

"P" document published prior to the international filing date but later than the priority date claimed

"T" later document published after the international filing date or priority date and not in conflict with the application but cited to understand the principle or theory underlying the invention

"X" document of particular relevance; the claimed invention cannot be considered novel or cannot be considered to involve an inventive step when the document is taken alone

"Y" document of particular relevance; the claimed invention cannot be considered to involve an inventive step when the document is combined with one or more other such documents, such combination being obvious to a person skilled in the art.

"&" document member of the same patent family

Date of the actual completion of the international search

9 October 2000

Date of mailing of the international search report

17/10/2000

Name and mailing address of the ISA

European Patent Office, P.B. 5818 Patentlaan 2
NL - 2280 HV Rijswijk
Tel. (+31-70) 340-2040, Tx. 31 651 epo nl,
Fax: (+31-70) 340-3016

Authorized officer

Martelli, L

INTERNATIONAL SEARCH REPORT

Information on patent family members

International Application No

PCT/US 00/15965

Patent document cited in search report		Publication date	Patent family member(s)	Publication date
WO 9905964	A	11-02-1999	AU 8897298 A	22-02-1999
			EP 1003416 A	31-05-2000
			US 5951484 A	14-09-1999
US 5117834	A	02-06-1992	US 5351687 A	04-10-1994
GB 2301037	A	27-11-1996	DE 19519237 A	28-11-1996
			FR 2734467 A	29-11-1996
			JP 8322950 A	10-12-1996
			US 5692515 A	02-12-1997